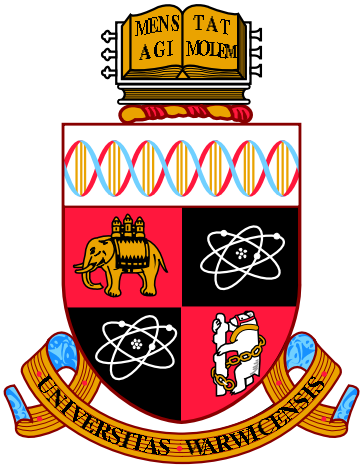

Essays on Commodity and Foreign Exchange Derivatives

by

Yujing Gong

Thesis

Submitted to the University of Warwick

for the degree of

Doctor of Philosophy

in Finance & Econometrics

Warwick Business School

December 2021

Contents

List of Tables

List of Figures

Acknowledgments

I would like to express sincere gratitude to my supervisors Arie Gozluklu, Gi Kim and Xing Jin for their guidance, support and patience. Arie and Gi stimulated my research interests in empirical finance after my previous supervisor Xing left Warwick. They give me inspiring comments to polish my thesis and unwavering encouragement to do research better. I am also grateful to Alex Ferreira for continuous support and advice. This thesis would not have been possible without them.

I would like to thank greatly the members of the Finance Group at Warwick Business School for their support, especially Sarah Qian Wang, Ilias Filippou, Roman Kozhan and Ganesh Viswanath Natraj for their helpful discussions and invaluable advice during my upgrade and annual review across my PhD study. I would also want to express my gratitude to my two examiners, Alexandros Kostakis and Sarah Qian Wang, for their valuable inputs and comments. I would also like to thank Alex Ferko, Christopher Jones (WFA discussant), Esen Onur, Michel Robe, Pradeep Yadav and Vikas Raman as well as participants at the CFTC Seminar, the 2020 WFA annual meeting, 2020 AFA Poster Session, and WBS Finance Brown Bag Seminar for helpful comments and suggestions.

My gratitude also goes to my friends, Tingting Cheng, Jiaqi Zhao, Zhou Zhang, Bobo Zhang, Thao Nguyen, Siti Farida, Xiaohan Xue, Wei Xing, Alexandru Vasile and many others. Without whom, my PhD journey would not be as delightful as it has been.

I would like to take the opportunity to thank my family and my parents for their love and unlimited support. I wish I would have a chance to say thank you to my grandpa, who passed away in 2019. I believe he would be happy for me and I will forever be grateful for the values he instilled in me.

Declarations

I declare that the three essays contained in this thesis have not been submitted for a degree to any other university. Moreover, I declare that the Chapter 3 titled "Speculator Spreading Pressure and the Commodity Futures Risk Premium" is a collaboration work with my supervisors, Dr. Arie Gozluklu and Dr. Gi Kim. Chapter 4 titled "Option Prices and Risk-Corrected Probabilities of Binary Events" is written in co-authorship with my supervisor Dr. Arie Gozluklu and Dr. Alex Ferreira from Universidade de São Paulo.

Yujing Gong

December, 2021

Abstract

This thesis consists of three essays on commodity and foreign exchange derivatives. Chapter 2 proposes a comprehensive option pricing model to capture stylized features in the energy commodity market. We use the Brent crude oil as a showcase and show that its implied volatility exhibits seasonal pattern and the skewness of its return distributions is time-varying. The option pricing model we proposed in this paper is able to capture these stylized features. The estimation results show that the model pricing performance for the crude oil options is significantly improved by capturing the time-varying skewness of return distributions, while there is no significant improvement by capturing the seasonal pattern in volatility.

Chapter 3 investigates the impact of speculative trading on the commodity futures risk premium. We focus on speculators' spread positions, and study the asset pricing implications of *spreading pressure* on the cross-section of commodity futures returns. In an era of financialization of commodity markets, a long-short portfolio based on the spreading pressure signal carries a significant risk premium. We show that spreading pressure reflects speculators' expectations about the change in the shape of the futures term structure, which is linked to commodity index investment. The spreading pressure factor can be explained by economic fundamentals and frictions introduced by financial traders.

Chapter 4 starts with risk-neutral probabilities of the Brexit referendum using data from both the options and prediction markets. We then provide a risk-

corrected measure of these probabilities using both non-parametric and parametric methods. While former correction marginally changes the risk-neutral probability, the performance of the latter depends on relative wealth calibration and risk preferences. We estimate subjective Brexit probabilities from past opinion polls and also provide daily estimates of voting intention to leave from BES survey. By comparing the subjective probabilities with our risk-corrected measures, our results show that both FX option and prediction market participants reveal moderate risk seeking preferences before the Brexit referendum.

Chapter 1

Introduction

This thesis consists of three essays on commodity and foreign exchange derivatives. Chapter two proposes a comprehensive option pricing model to capture stylized features in the energy commodity market. Chapter three investigates the impact of speculative trading on the commodity futures risk premium. Chapter four studies information on extreme political events contained in the financial and prediction markets.

In chapter two, we propose a comprehensive option pricing model to capture stylized features in the energy commodity market. Doran and Ronn (2005, 2008) and Back et al. (2013) show that the seasonal pattern in volatility is an important stylized feature for energy commodities. Fernandez-Perez et al. (2018) and Chatrath et al. (2015) document that skewness in commodity return distributions is volatile to some extent. To improve the option pricing model performance in the commodity market, it is crucial to capture the seasonal pattern in volatility (Back et al., 2013), model the volatility as a stochastic process (Schwartz, 1997; Duffie et al., 1999; Anderson, 1985; Larsson and Nossman, 2011) and fit the time-varying behaviour of implied volatility curves (Carr and Wu, 2007).

We use Brent crude oil options as an example to conduct empirical analysis. We find that the Brent crude oil exhibits seasonal pattern in option implied volatility and

time-varying skewness of return distributions. Inspired by the empirical evidence, we propose a comprehensive option pricing model to capture these two stylized features in the energy commodity market. We employ a sine function to capture the seasonal pattern in volatility and use two separate jumps and two independent activity rates to generate time-varying skewness of return distributions for both short and long horizons. Then we test whether and how much the option pricing model performance is improved by each generalization. The empirical results show that the option model pricing performance is significantly improved by capturing the time-varying skewness of return distributions in the crude oil market, but is less affected by capturing seasonality in volatility. This is because the crude oil is closer to financial assets than other commodities, thus, the seasonal pattern in volatility is not as strong as other commodities (such as natural gas). Our option pricing model can be widely applied to price other commodity options, since these two stylized features are not unique to the crude oil market.

In chapter three, we investigate the impact of speculators' trading activities on the time-varying commodity futures risk premium. In particular, we focus on speculators' *spread trade* positions, and study their asset pricing implications for the cross-section of commodity futures returns. Commodity spread trades are intra-commodity investing strategies that involve simultaneously buying and selling the same amount of futures contracts with different maturities within a single commodity. The financialization of the commodity markets from around 2005 has prompted the exponential growth of such strategies (Tang and Xiong, 2012; Singleton, 2014). Speculators take intra-commodity spread positions in order to obtain risk exposures to the change in the shape (slope or curvature, or both) of commodity futures term structures. Hence, the extent to which speculators enter spread trade positions (*spreading pressure*) may reflect the information on the commodity futures term structure and futures returns.

First, we find spreading pressure predicts futures excess returns negatively and significantly even after controlling for important determinants, including basis-momentum,

hedging pressure, and changes in speculators' trading positions. Our Fama-MacBeth cross-sectional regression results show that weekly excess returns decrease by about 1.78 percentage points when smoothed spreading pressure increases by 1 percentage point.[1] Second, our spreading pressure long-short portfolio generates excess returns of as high as 22.52% (with a Sharpe ratio of 0.94) per annum, and it yields higher cumulative returns than other pricing portfolios including basis, momentum, and basis-momentum (Figure 3.6) since 2005.

Third, we show that spreading pressure is a priced factor (*spreading pressure factor*) in the cross-section of commodity futures returns, especially after 2005. The estimated price of risk on the spreading pressure factor is 20.95% per annum, and our single-factor model provides a better cross-sectional fit than the extant two- or three-factor models, which feature R^2 of as high as 66.81%. Interestingly, the pricing power of spreading pressure comes mainly from money managers, including CTAs and hedge funds. Lastly, spreading pressure reflects the expected slopes and curvatures of the commodity futures term structure. The spreading pressure factor is explained by Asian emerging market returns (Tang and Xiong, 2012; Henderson et al., 2015) and by innovations in real economic uncertainty (Bloom, 2009; Ludvigson et al., 2019). It is not captured by liquidity, volatility, inventory, or financial intermediary risk.

In chapter four, we study information on extreme political events contained in the financial and prediction markets. Odds from prediction markets can be employed as probabilities of an extreme event (Belke et al., 2018). In the financial market, the extreme political event may change the return of any asset due to an expectation of a discrete shift in the return distribution (Rogoff, 1977, 1980; Lewis, 2016), thus, probabilities of an extreme event can be inferred from the option market (Borochin and Golec, 2016; Carvalho and Guimaraes, 2018; Kostakis et al., 2020; Langer and Lemoine, 2020).

[1] We refer to the twelve-month average of spreading pressure as *smoothed* spreading pressure. We use a one-year time window to smooth out the effect of seasonality and the maturity of futures contracts on our measure. Kang et al. (2020) use a similar approach to compute their measure of hedging pressure.

However, the event probabilities implied in both the options and prediction markets are risk-neutral probabilities, and it is affected by agents' perception and participants' risk preference. Better estimates of physical probabilities are essential to understanding how well the financial market anticipate event probabilities. Therefore, we construct subjective physical probability proxy of extreme political events by considering a set of political opinion polls. We also use both parametric and non-parametric method to do the risk-correction for the risk-neutral probabilities implied in both markets.

Empirically, we focus on a particular binary political event: the European Union (EU) withdrawal referendum held by the United Kingdom (UK) on the 23^{rd} of June 2016 (Brexit). If UK leave EU, agents would thus be expecting that the sterling (British pound or GBP) value to the other currencies, especially to the United States dollar (USD), would be negatively impacted. Therefore, we investigate the risk-neutral density (RND) extracted from British Pound options. We find that RNDs from short maturities options are bimodal distributed one week before the referendum and risk-neutral tail risk of GBP/USD deviates from its normal level since the beginning of 2016. Therefore, it is reasonable to suppose that agents attached a probability that a discrete change in the economic fundamentals that govern the dynamics of the GBP exchange rate would occur. This is the typical description of a "Peso Problem".

We extract risk-neutral probabilities from the option market using both model-based and model-free methods. Different from Kostakis et al. (2020) and Borochin and Golec (2016), we find that cheap out-of-the-money options carry more information about the probabilities of the 'Brexit' outcome. On average, the options market reveals a higher "Leave" risk-neutral probability by comparison to the betting market, but both market participants seem to closely track opinion poll results when assessing event probabilities. While subjective probabilities extracted from polls rationalize the Brexit surprise, voting intentions estimated from surveys which are determined by persistent characteristics (age, education, income), political views and the risk preferences of the voters, are likely

to be a better guide for physical probabilities. We construct risk-neutral Arrow-Debrew prices from both markets and filter out risk-corrected probabilities from market prices using both a non-parametric (Ross Recovery Theorem) and a parametric (calibrating the stochastic discount factor) approach. Only parametric recovery is likely to have an impact on the level of Brexit probability estimates, albeit under strict parametric assumption. However, we argue that markets could have signalled higher Brexit outcome once we allow for speculative trading triggered by such binary political events in both prediction and option markets. Arguably, reliance on risk-neutral probabilities from both markets were misleading as an indicator for "Leave" outcome.

Chapter 2

Empirical Performance of Alternative Pricing Models of Energy Options

2.1 Introduction

Following the financialazation of the commodity market in 2004 and the poor performance of stocks and Treasuries during the financial crisis, commodities have become an asset class favoured by investors. According to the Futures Industry Association (FIA) Annual Volume Survey in 2015, the total number of commodity futures and options contracts rose from less than 1 billion in 2005 to 4.6 billion in 2015, becoming the asset class with the second highest number of contracts in the futures and options market. This is much more higher than the FX futures and options contracts with the third largest trading volume (2.78 billion), and more than half of the largest trading volume of stock index contracts (8.34 billion). Thus, it is critical to find an appropriate model to price commodity options.

To find an appropriate model to price commodity options, understanding the dy-

namic of volatility and time-varying behaviour of implied volatility curves are important. Brooks and Prokopczuk (2013) illustrate that it is inappropriate to treat different types of commodities as a single asset class, since the volatility behaviours are different across market segments, but are similar to commodities in the same market segment. Thus, we limit our attention to a single sector, the energy sector, since it is the most liquid and the largest sector in the commodity market. Specifically, due to the increase in index investors after the financialazation of the commodity market, the liquidity of the components in the commodity indices (e.g. the S&P Goldman Sachs Commodity Index (S&P GSCI) and the Dow Jones-UBS Commodity Index (DJ-UBSCI)) has increased significantly. As the component with the highest proportion of commodity indices, the energy sector became the most liquid segment. Besides, according to the 2015 FIA Annual Volume Survey, the energy sector has the highest number of traded futures and options contracts in the commodity market, 1.6 billion. Lastly, crude oil and the other commodities in the energy sector are widely used in many economic areas, and are the most important fuels in the modern economy. The valuation studies on crude oil and the other energy commodities derivatives provide insights into risk management for relevant energy companies and have a crucial impact on the economy. Based on the above reasons, this paper focuses on the energy sector and uses crude oil options as an example to conduct empirical analysis.

Energy commodity returns are not normally distributed. Brooks and Prokopczuk (2013) analyse the first four moments of crude oil, gasoline and S&P 500 index returns. It shows that the average returns of these two energy commodities are lower than the S&P 500 index, but the corresponding volatilities are higher, which is consistent with the findings of Regnier (2007). Energy commodity returns distributions are more negatively skewed and less leptokurtic than the S&P 500 index. Alexander (2004) also shows that the natural gas returns distribution has same stylized features. Therefore, the energy commodity returns are not normally distributed and are slightly different from financial

assets.

Different from traditional financial assets, the seasonal pattern in price and volatility has been observed in commodity market. Seasonality in the price level affects the drift term in the spot return process, while it does not affect the futures price, since futures price is a martingale without the drift term under the risk-neutral measure. Commodity options are typically written on futures, thus, seasonality in price level is not important for commodity option pricing (Back et al., 2013). Doran and Ronn (2005, 2008) and Back et al. (2013) show that the seasonal pattern in volatility is an important stylized feature for energy commodities. Looking into realized volatility in the oil market, Doran and Ronn (2008) and Geman and Ohana (2009) document that the oil volatilities are consistent across months and a seasonal pattern is not found, since the oil market is a world market. Doran and Ronn (2005) focus on the options implied volatility and find seasonal pattern in the crude oil volatility, but this seasonal pattern is relatively weaker than the one in the natural gas market. To study the seasonal pattern in the Brent crude oil volatility in the recent years, we examine both realized volatility and options implied volatility. We find that the implied volatility in the crude oil market has a seasonal pattern, while the seasonal pattern in realized volatility is relatively weak.

The variation in the skewness of return distributions can be observed in the financial markets, for example, the currency market (Carr and Wu, 2007; Bakshi et al., 2008) and the stock market (Harvey and Siddique, 1999). In commodity market, the evidence for the time-varying skewness in return distributions is not that straightforward. Chatrath et al. (2015) show that, in the crude oil market, the forecasting of realized volatility can be improved by incorporating the risk-neutral skewness. Fernandez-Perez et al. (2018) construct a skewness factor by using historical returns skewness and find that it is a pricing factor in the commodity market. In some extent, these literature confirms that the skewness of commodity return distributions is volatile. To investigate the variation in crude oil return distributions directly, we follow the method proposed

by Carr and Wu (2007) and use the risk reversal to measure the skewness. We find that the crude oil return skewness is very volatile and the sign also changes over time.

To improve the option pricing model performance in the commodity market, it is crucial to capture the seasonal pattern in volatility and time-varying skewness in return distributions. Back et al. (2013) find that the pricing performance of the commodity option pricing model can be greatly improved with seasonal components in the volatility, under an assumption that volatility is not stochastic. However, Schwartz (1997), Duffie et al. (1999), Anderson (1985) and Larsson and Nossman (2011) show that stochastic volatility is an important feature in oil and energy price process, which follows a mean-reversion process (Wickham, 1996; Abosedra and Laopodis, 1996; Pindyck, 2004; Trolle and Schwartz, 2009). Different from the literature, we propose an option pricing model with seasonal components in the volatility under an assumption of stochastic volatility. Apart from this, previous studies focus on improving the performance of commodity option pricing models by fitting the average behaviour of implied volatility, but keep salient to the time-varying skewness of implied volatility curve. Inspired by the currency option pricing model proposed by Carr and Wu (2007) and Bakshi et al. (2008), we use two independent up and down jumps through two Lèvy processes in the commodity spot return process to generate time-varying skewness.

The contributions and findings of this paper are in two aspects. Theoretically, we contribute to the literature on commodity option pricing models by proposing a new comprehensive option pricing model to adapt to the empirical characteristics of energy commodity, the time-varying skewness in return distributions and seasonal pattern in volatility. This model could be widely applied to the other options and can be easily restricted to capture one of the empirical characteristics only. Empirically, we first show that the skewness in commodity return distributions is very volatile while the kurtosis is persistent. We also examine whether and how much each generalization improves the option pricing model performance and find that capturing time-varying skewness can

improve the option pricing model performance significantly in the crude oil market.

2.2 The Behaviour of Commodity Returns

2.2.1 Data Description

Crude oil is one of the most important products in the commodity market. It accounts for the largest proportion of popular commodity indices (e.g. the S&P Goldman Sachs Commodity Index (S&P GSCI) and the Dow Jones-UBS Commodity Index (DJ-UBSCI)). As the most liquid and highly traded market, crude oil options have a wide range of strike prices and a rich set of maturities. Similar as most of exchange-listed commodity options, ICE-listed crude oil options are American-style and written on futures. Thus, we collect settlement prices of ICE Brent Crude American-style Option Contracts and ICE Brent Crude Futures Contracts from Blomberg. The sample period we used in this paper is between 15 May, 2013 and 17 May, 2017. We use weekly data in the empirical test and we take weekly data on each Wednesday. Thus, our data contains 210 weekly observations. In order to test whether stylized facts of crude oil return are unique in the commodity market, we also examine stylized facts of natural gas return. Therefore, we collect the weekly settlement prices of NYMEX Henry Hub Natural Gas Option Contracts and NYMEX Henry Hub Natural Gas Futures Contracts between 15 May, 2013 and 17 May, 2017.

We use the following procedures to sort the data. First of all, for the liquidity concern, we discard deep out-of-the-money (OTM) options, that is, options with moneyness less than 0.9 or with moneyness greater than 1.1. The moneyness of an option is defined as the strike price divided by the corresponding underlying futures price. Second, we discard options either with long maturities or very short maturities because they are less liquid than the rest of the options. Specifically, we retain options with maturity up to six months and keep two more options expiring in the nearest March,

June, September, or December. We set options with very short maturities as options that expires within 14 days. Third, we discard in-the-money (ITM) options, that is, call options with moneyness less than one and put options with moneyness greater than one. Due to the options observed in our sample are American-style, and our pricing model is for European-style options, we convert the observed American options prices into European options prices. Using at-the-money (ATM) and OTM options in this step can minimize the impact of the early exercise premiums.

Figure 2.1 shows the one-month implied volatilities of ATM Brent crude oil options. By the third quarter of 2014, the implied volatility is around 20%. In the fourth quarter of 2014, the implied volatility soars to around 50%. Since then, the implied volatility remains at a relatively high level. According to the U.S. Energy Information Administration (EIA), Brent crude oil prices experienced a 50% sharp drop in the fourth quarter of 2014 due to global crude oil production exceeding demand. Since then, crude oil price has fluctuated around this level until the end of our sample period. The regime switch in crude oil prices has caused changes in implied volatility to a certain extent.

2.2.2 Seasonality in Volatility

Demand or/and supply uncertainty for most commodities (e.g. energy commodities, agriculture commodities) is highly affected by climate change (Anderson, 1985), which leads to the uncertainty of commodity returns often showing seasonal patterns. To test the seasonal pattern in volatility, we use both realized volatility and implied volatility (Back et al., 2013).

The realized volatility is calculated from the price of the front-month futures contract. We use the return of the front-month futures contract as the daily spot return. The monthly realized volatility is measured by the annualized standard deviation of the daily spot returns during the month. To test the seasonal pattern, we calculate the average realized volatilities grouped by month and fit the data by using a sine function.

Figure 2.2a shows the average realized volatility in the Brent crude oil market. As we can see, the range of averaged realized volatility is from 16% to 38% and we can observe a very weak seasonal pattern.

The implied volatility from the option market reflects the investors' belief as to the futures volatility of the underlying return. The implied volatility from the Brent crude oil options is obtained with the Barone-Adesi and Whaley (BAW) American commodity futures options pricing model (Barone-Adesi and Whaley, 1987). We focus on the ATM options and group implied volatilities by the corresponding maturity months. Figure 2.2b displays the maturity month average implied volatilities from Brent crude oil options and a fitted curve based on a sine function. Compared with the realized volatility, we can observe a stronger seasonal pattern in the implied volatility.

2.2.3 Time-varying Skewness of the Return Distribution

Implied volatility curve reflects the market's expectations of underlying return distribution. It usually exabits smile or smirk shape, which indicates that the underlying returns are not normally distributed under the risk-neutral measure. To examine the implied volatility curve from the Brent crude oil options, we interpolate implied volatility curve for six fixed horizons, one-, two-, three-, six- and twelve- months. We focus on the implied volatilities with seven fixed moneyness levels, 90%, 95%, 97.5%, 100%, 102.5%, 105% and 110%. Following Doran and Ronn (2005), Wayne et al. (2010) and Ederington and Guan (2002), to avoid noise from individual options, we calculate implied volatility for a target moneyness level by taking the average of implied volatilities from three options with same maturity and the moneyness levels closest to the target.

Figure 2.2c shows the average implied volatility curve from Brent crude oil options over three horizons, one-month, three-month and one-year. To display the average implied curves clearly in this figure, we lift up one year implied volatility curve by 2%. The average implied volatility curve for one-month horizon shows a 'smile' shape, and the

average implied volatility curve for three-month and one-year horizons exhibit 'smirk' shapes. Thus, crude oil return distributions are negative skewed, which indicate the average return distributions for different horizons have fat left tails during our sample period.

To investigate the time-series variation of Brent crude oil return distributions, we use time-series risk reversals (RR) and butterfly spreads (BF) to measure the skewness and excess kurtosis of the return distributions, respectively. The 5% risk reversal (RR5) is the implied volatilises difference between a call option with 105% moneyness and a put option with 95% moneyness,

$$RR5 = IV\left(105\%\right) - IV\left(95\%\right), \tag{2.1}$$

where $IV\left(105\%\right)$ and $IV\left(95\%\right)$ represent implied volatility at 105% moneyness level and at 95% moneyness level, respectively. The 5% butterfly spread measures the curvature of implied volatility curve between 95% and 105% moneyness. We calculate it as the difference between the average of implied volatilities at 95% and 105% moneyness levels and implied volatility of at-the-money options,

$$BF5 = \frac{IV\left(95\%\right) + IV\left(105\%\right)}{2} - IV\left(100\%\right), \tag{2.2}$$

where $IV\left(100\%\right)$ is the implied volatility of at-the-money options.

Figure 2.2d shows the three-month 5% risk reversal (RR5) and 5% butterfly spread (5BF) calculated from Brent crude oil options. According to this figure, the 5% risk reversal is very volatile (fluctuates between -5% to 1%) and 5% butterfly spread is relatively persistent from May 2013 to May 2017. Specifically, the 5% risk reversal is negative most of the time, except in July 2014. This indicates the skewness of crude oil returns is time-varying and is mainly negative in our sample period.

Table 2.1 shows the average, standard deviation and weekly autocorrelation of

5% risk reversals and 5% butterfly spreads for five horizons, one-, two-, three-, six- and twelve- months. First of all, in average, the risk reversal is negative from one month to one year horizons. Thus, the out-of-money put options is more expensive than the out-of-money call options in average in our sample period. Moreover, the standard deviation of butterfly spreads is significantly lower than risk reversals. So, in the option pricing model, capturing the time-varying skewness of the crude oil return distribution is more crucial than the time-varying kurtosis. Lastly, both risk reversals and butterfly spreads are strongly serial correlated, and the correlations increase with maturities. This indicates short term contracts and long term contracts are dominated by volatility factors with low persistent and high persistent, respectively. Therefore, we model the long-run mean level of the volatility as a stochastic process.

Figure 2.A-1 shows that the seasonal pattern in volatility and time-varying skewness of return distributions can be observed in the natural gas market as well. Hence, these stylized features are not limited in the crude oil market. Option pricing models that can capture these two features can potentially be applied to the other commodity options.

2.3 Theoretical Model

Standard pricing models of commodity derivatives (e.g. Gibson and Schwartz, 1990; Schwartz, 1997) usually specify a process for commodity spot return and spot cost of carry, respectively. In this paper, we follow Trolle and Schwartz (2009) to specify a process for the forward cost of carry instead of the spot cost of carry. Thus, this section is organized as follows. Firstly, we describe the specification of the commodity spot return process. Then, we specify the forward cost of carry process. After that, we derive the commodity futures price process. Lastly, we show the pricing formula for the commodity futures options.

2.3.1 Commodity Spot Price

We start the model with the specification for the commodity spot return process (Trolle and Schwartz, 2009). Define $S(t)$ as the commodity spot price at time t, where the instantaneous spot cost of carry is $\delta(t)$. Assuming that the spot log-return of the commodity follows a time-changed Lèvy process under the risk-neutral measure $\mathbb{Q}$,

$$s_t = \ln \frac{S(t)}{S(0)} = \int_0^t \delta(u)du + (L^R_{\mathcal{T}_t} - \xi^R \mathcal{T}^R_t) + (L^L_{\mathcal{T}_t} - \xi^L \mathcal{T}^L_t), \tag{2.3}$$

where L^R_t and L^L_t are two Lèvy processes, which can capture the right and left skewness of the commodity return distributions, respectively. ξ^R and ξ^L are known functions used to ensure exponentials of two Lèvy components, $L^R_{\mathcal{T}_t} - \xi^R \mathcal{T}^R_t$ and $L^L_{\mathcal{T}_t} - \xi^L \mathcal{T}^L_t$, to be martingales under the risk-neutral measure $\mathbb{Q}$, respectively. Two independent stochastic time changes $\mathcal{T}^R_t$ and $\mathcal{T}^L_t$ used in Lèvy components can generate independent stochastic volatility (Carr and Wu, 2007).

According to the specification of the commodity spot return process in equation 2.3, this model can generate average implied volatility smiles/smirks at different maturities, and time-varying skewness of the commodity return distributions. First, two Lèvy components can generate non-normally distributed commodity spot returns in the short-term, and stochastic time changes slow down the long-term convergence speed of the return distribution to the normal distribution. So the average shape of the implied volatility curve from both short-term and long-term options can be captured. Besides, two independent stochastic time changes can generate different weights for two Lèvy components over time. When the weight on the right skewed Lèvy component (L^R_t) is lower than the left skewed one (L^L_t), the return distribution is left skewed and a negative risk reversal is generated, and vice versa. Due to the variation of the two Lèvy components' relative weight over time, the sign and the magnitude of the skewness of the return distributions are also time-varying.

Two Lèvy components in equation 2.3 can be decomposed as the following equations:

$$L_t^R = J_t^R + \sigma_S e^{\xi(t)} W_{R1}^Q(\mathcal{T}_t^R), \quad L_t^L = J_t^L + \sigma_S e^{\xi(t)} W_{L1}^Q(\mathcal{T}_t^L), \tag{2.4}$$

where W_{R1}^Q and W_{L1}^Q are two independent Brownian Motions and J_t^R and J_t^L are two pure jump components. For simplicity, we assume that the unconditional returns are relative symmetric distributed. Thus, we set the volatility parameter σ_S and the deterministic function $\xi(t)$ capturing the seasonal pattern in volatility as the same for two Lèvy components. Following Back et al. (2013), we specify $\xi(t)$ as

$$\xi(t) = \theta \sin(2\pi(t + \zeta). \tag{2.5}$$

Following Carr and Wu (2007), the density functions $\pi^R(x)$ and $\pi^L(x)$ for two jumps components J_t^R and J_t^L are defined as the following:

$$\pi^R(x) = \begin{cases} \lambda e^{-\frac{\upsilon_J}{|x|}} \mid x \mid^{-\alpha-1}, & x > 0 \\ 0, & x < 0 \end{cases} \text{ and } \pi^L(x) = \begin{cases} 0, & x > 0 \\ \lambda e^{-\frac{\upsilon_J}{|x|}} \mid x \mid^{-\alpha-1}, & x < 0 \end{cases}. \tag{2.6}$$

This means that the right skewed and left skewed jump components only allow up and down jumps, respectively. For parsimony, we set same parameters ($(\lambda, \upsilon_J) \in \mathbb{R}^+ \, and \, \alpha \in (-\infty, 2]$) in the density function of up and down jumps. Similar to the CGMY model (Carr et al., 2002), λ measures the overall level of activity, υ_J captures the arrival frequency of large jumps relative to small ones, and α controls the jump variation, or activity. The jump process could exhibits finite activity ($\alpha < 0$), infinite activity with finite variation ($0 \leq \alpha < 1$), or infinite variation ($1 \leq \alpha \leq 2$). The magnitude of α is not restricted in this paper.

The activity rates of two Lèvy components (υ_1^R and υ_1^L) are defined as the first-

order differential of stochastic time changes,

$$\upsilon_1^R(t) = \frac{\partial \mathcal{T}_t^R}{\partial t}, \quad \upsilon_1^L(t) = \frac{\partial \mathcal{T}_t^L}{\partial t}. \tag{2.7}$$

We model two activity rates as mean-reversion processes with two stochastic mean levels,

$$d\upsilon_1^j(t) = \kappa_1(\upsilon_2^j(t) - \upsilon_1^j(t))dt + \sigma_{\upsilon 1}\sqrt{\upsilon_1^j(t)}dW_{j3}^Q(t), \tag{2.8}$$

and the long-run mean of $\upsilon_1^j(t)$ is

$$d\upsilon_2^j(t) = (\eta - \kappa_2\upsilon_2^j(t))dt + \sigma_{\upsilon 2}\sqrt{\upsilon_2^j(t)}dW_{j4}^Q(t), \tag{2.9}$$

where $j = R$, L, and $W_{j3}^Q(t)$ and $W_{j4}^Q(t)$ are independent Brownian Motions.

We define ρ_{R1} (ρ_{L1}) as the correlation between the Brownian motions $W_{R1}^Q(t)$ and $W_{L1}^Q(t)$ ($W_{R3}^Q(t)$ and $W_{L3}^Q(t)$), which is

$$\rho_{j1}dt = \mathbb{E}(dW_{j1}^Q(t)dW_{j3}^Q(t)), \tag{2.10}$$

where $j = R$, L. We restrict ρ_{R1} and ρ_{L1} to be positive and negative, respectively (Carr and Wu, 2007). This restriction ensures that the two Lèvy processes (L_t^R and L_t^L) capture the time-varying skewness of commodity spot return distributions at both short and long horizons. Specifically, two pure jump Lèvy components (J_t^R, J_t^L) generate positive and negative skewness at short horizons, respectively. At long horizons, we generate the positive and negative skewness via two correlations ρ_{R1} and ρ_{L1}, respectively.

Let $\bar{J^R}(dt, dx)$ and $\bar{J^L}(dt, dx)$ denote two jump measures of positive and negative jumps size $x(\cdot)$ on $\mathbb{R}^+ \times \mathbb{R}$. Define $\nu^R(dx)$ and $\nu^L(dx)$ as Lèvy measures of positive and

negative jumps and dt as the Lebesgue measure on $[0,t]$. Then we define

$$J^R(dt,dx) = \begin{cases} \bar{J^R}(dt,dx) - \nu^R(dx)dt & if\ 0 < x < R \\ \bar{J^R}(dt,dx) & if\ x \geq R \end{cases} \tag{2.11}$$

and

$$J^L(dt,dx) = \begin{cases} \bar{J^L}(dt,dx) - \nu^L(dx)dt & if\ -R < x < 0 \\ \bar{J^L}(dt,dx) & if\ x \leq -R \end{cases} \tag{2.12}$$

for some $R \in [0,\infty)$.

According to the Ito's Lemma for Ito-Lèvy process, the stochastic differential equation (SDE) of the commodity spot return process is

$$\begin{aligned} \frac{dS(t)}{S(t)} = \delta(t)dt + \int_0^{+\infty}(e^x-1)J^R(dt,dx) + \sigma_S e^{\xi(t)}\sqrt{\upsilon^R(t)}dW^Q_{R1}(t) \\ + \int_{-\infty}^{0}(e^x-1)J^L(dt,dx) + \sigma_S e^{\xi(t)}\sqrt{\upsilon^L(t)}dW^Q_{L1}(t). \end{aligned} \tag{2.13}$$

2.3.2 Forward Cost of Carry

We define $y(t,T)$ as the instantaneous forward cost of carry from time t to T and $t \leq T$, thus, $y(t,t) = \delta(t)$. Assume that the forward cost of carry of the commodity depends on the same volatility factors as the spot return, $\upsilon^R(t)$ and $\upsilon^L(t)$. Therefore, the dynamic process of the forward cost of carry can be written as

$$dy(t,T) = \mu_y(t,T)dt + \sigma_y(t,T)e^{\xi(t)}\sqrt{\upsilon^R(t)}dW^Q_{R2}(t) + \sigma_y(t,T)e^{\xi(t)}\sqrt{\upsilon^L(t)}dW^Q_{L2}(t). \tag{2.14}$$

For parsimony, we set the volatility parameter $\sigma_y(t,T)$ of the forward cost of carry as the same for two independent Brownian motions $W^Q_{R2}(t)$ and $W^Q_{L2}(t)$. We allow the independent Brownian motions $(W^Q_{R2}(t), W^Q_{L2}(t))$ in the forward cost of carry process and $(W^Q_{R1}(t), W^Q_{L1}(t))$ in the spot return process to be correlated, and donate correlations as

(ρ_R, ρ_L). Thus,

$$\rho_j dt = \mathbb{E}(dW_{j1}^Q(t) dW_{j2}^Q(t)), \quad j = R, L. \tag{2.15}$$

Similarly, we denote (ρ_{R2}, ρ_{L2}) as the correlations between the Brownian motions $(W_{R2}^Q(t), W_{L2}^Q(t))$ in the forward cost of carry process and $(W_{R3}^Q(t), W_{L3}^Q(t))$ in the activity rate process,

$$\rho_{j2} dt = \mathbb{E}(dW_{j2}^Q(t) dW_{j3}^Q(t)), \quad j = R, L. \tag{2.16}$$

2.3.3 Commodity Future Price

Define $F(t,T)$ as the commodity futures price at time t expiring at time T. Then, the futures price is

$$F(t,T) = S(t) \exp(\int_t^T y(t,u) du). \tag{2.17}$$

Under the condition of no arbitrage, the futures price is a martingale under the risk-neutral measure $\mathbb{Q}$. So the drift term of the futures return process should be equal to zero. Thus, the process of the futures price is

$$\begin{aligned}
\frac{dF(t,T)}{F(t,T)} =& \sqrt{\upsilon^R(t)} e^{\xi(t)} \left[\sigma_S dW_{R1}^Q(t) + \left(\int_t^T \sigma_y(t,u) du \right) dW_{R2}^Q(t) \right] \\
&+ \sqrt{\upsilon^L(t)} e^{\xi(t)} \left[\sigma_S dW_{L1}^Q(t) + \left(\int_t^T \sigma_y(t,u) du \right) dW_{L2}^Q(t) \right] \\
&+ \int_0^{+\infty} (e^x - 1) J^R(dt, dx) + \int_{-\infty}^0 (e^x - 1) J^L(dt, dx),
\end{aligned}$$

see Appendix 2.B. According to this equation, the futures price depends on two volatility factors, $\upsilon^R(t)$ and $\upsilon^L(t)$. These two volatility factors are driven by $W_{R3}^Q(t)$, $W_{R4}^Q(t)$, $W_{L3}^Q(t)$ and $W_{L4}^Q(t)$, which are not shown in the above equation. Hence, trading on the futures contracts cannot completely hedge instantaneous volatility risk. Since we assume that $(W_{R4}^Q(t), W_{L4}^Q(t))$ are completely uncorrelated with $(W_{R1}^Q(t), W_{L1}^Q(t))$ and $(W_{R2}^Q(t), W_{L2}^Q(t))$, the long-term mean volatility risk is completely unhedgable by trading on futures contracts.

Since the volatility of the long-term forward cost of carry should be less than the short-term forward cost of carry, following Trolle and Schwartz (2009), we specify $\sigma_y(t,T)$ as

$$\sigma_y(t,T) = \alpha e^{-\gamma(T-t)}, \tag{2.18}$$

We denote σ_Y^{Δ} as the integral of $\sigma_y(t,T)$, which is

$$\sigma_Y^{\Delta} = \int_t^T \sigma_y(t,u)du = \int_t^T \alpha e^{-\gamma(u-t)}du = \frac{\alpha}{\gamma} - \frac{\alpha}{\gamma}e^{-\gamma(T-t)}, \tag{2.19}$$

where Δ is a set of parameters (t,T).

According to equation 2.18 and the Ito's lemma, the dynamics of the log futures price $\ln F(t,T)$ is

$$\begin{aligned} d\ln F(t,T) = &\int_0^{+\infty} xJ^R(dt,dx) + \int_{-\infty}^0 xJ^L(dt,dx) \\ &+ \sqrt{\upsilon^R(t)}e^{\xi(t)}\left[\sigma_S dW_{R1}^Q(t) + \sigma_Y^{\Delta}dW_{R2}^Q(t)\right] - \xi^{FR}(t)dt \\ &+ \sqrt{\upsilon^L(t)}e^{\xi(t)}\left[\sigma_S dW_{L1}^Q(t) + \sigma_Y^{\Delta}dW_{L2}^Q(t)\right] - \xi^{FL}(t)dt, \end{aligned} \tag{2.20}$$

where

$$\begin{aligned} \xi^{FR}(t) &= \int_{0<x<R}(e^x - 1 - x)\,\nu^R(dx) + \frac{1}{2}e^{2\xi(t)}\upsilon^R(t)\left[(\sigma_S)^2 + (\sigma_Y^{\Delta})^2 + 2\rho_R\sigma_S\sigma_Y^{\Delta}\right], \\ \xi^{FL}(t) &= \int_{-R<x<0}(e^x - 1 - x)\,\nu^L(dx) + \frac{1}{2}e^{2\xi(t)}\upsilon^L(t)\left[(\sigma_S)^2 + (\sigma_Y^{\Delta})^2 + 2\rho_L\sigma_S\sigma_Y^{\Delta}\right], \end{aligned} \tag{2.21}$$

Then we define two Lèvy processes L_t^{FR} and L_t^{FL} in the futures price process as

$$\begin{aligned} L_t^{FR} &= J_t^R + \sigma_S e^{\xi(t)}W_{R1}^Q(\mathcal{T}_t^R) + \sigma_Y^{\Delta}e^{\xi(t)}W_{R2}^Q(\mathcal{T}_t^R), \\ L_t^{FL} &= J_t^L + \sigma_S e^{\xi(t)}W_{L1}^Q(\mathcal{T}_t^L) + \sigma_Y^{\Delta}e^{\xi(t)}W_{L2}^Q(\mathcal{T}_t^L), \end{aligned} \tag{2.22}$$

then, we can rewrite the futures return process within the Lèvy framework

$$f(t,T) = \ln \frac{F(t,T)}{F(0,T)} = (L^{FR}_{\mathcal{T}^R_t} - \xi^{FR}\mathcal{T}^R_t) + (L^{FL}_{\mathcal{T}^L_t} - \xi^{FL}\mathcal{T}^L_t). \tag{2.23}$$

2.3.4 Commodity Future Option Price

Define the generalized Fourier transform of the commodity futures return $f(t,T)$ as the following

$$\begin{aligned} \phi_f(u) &\equiv E^{\mathbb{Q}}\left(e^{iuf(t,T)}\right) \\ &= E^{\mathbb{Q}}\left[e^{iu(L^{FR}_{\mathcal{T}^R_t} - \xi^{FR}\mathcal{T}^R_t) + iu(L^{FL}_{\mathcal{T}^L_t} - \xi^{FL}\mathcal{T}^L_t)}\right], \end{aligned} \tag{2.24}$$

where $u \in \mathscr{D} \subset \mathbb{C}$, $\mathscr{D}$ is a subset of the complex domain $\mathbb{C}$ where the exponent is well-defined.

Carr and Wu (2004) shows that the generalized Fourier transform of time-changed Lèvy processes is equivalent to the Laplace transform of the random time change under a complex valued measure $\mathbb{M}$. The complex valued measure $\mathbb{M}$ is

$$\frac{d\mathbb{M}}{d\mathbb{Q}} \equiv \exp\left[iu(L^{FR}_t - \xi^{FR}\mathcal{T}^R_t) + iu(L^{FL}_t - \xi^{FL}\mathcal{T}^L_t) + \psi^{FR}\mathcal{T}^R_t + \psi^{FL}\mathcal{T}^L_t\right], \tag{2.25}$$

where $\psi \equiv \left[\psi^{FR}, \psi^{FL}\right]^T$ is the vector of the characteristic exponents of the concavity adjusted right and left skewed Lèvy components in the futures price process, respectively. Then, the generalized Fourier transform under the risk-neutral measure $\mathbb{Q}$ in equation 2.24 can be written as a Laplace transform of $\mathcal{T}_t$ under $\mathbb{M}$:

$$\phi_f(u) = E^{\mathbb{M}}\left(e^{-\psi^T\mathcal{T}_t}\right) \equiv \mathscr{L}^{\mathbb{M}}_{\mathcal{T}}(\psi), \tag{2.26}$$

where the stochastic time change vector $\mathcal{T}_t \equiv \left[\mathcal{T}^R_t, \mathcal{T}^L_t\right]$ is the vector of two separate stochastic time changes applied to the right and left Lèvy components, respectively.

The solution of $\mathscr{L}_{\mathcal{T}}^{\mathbb{M}}(\psi)$ depends on the characteristic exponents ψ and the stochastic time vector $\mathcal{T}_t$.

According to the Lèvy-Khintchine Theorem, the characteristic exponents of a Lèvy component L_t is given by:

$$\begin{aligned}\psi(u) &\equiv \frac{1}{t}\ln E\left[e^{iuL_t}\right] \\ &= -iu\mu + \frac{1}{2}u^2\sigma^2 + \int_{\mathbb{R}^0}\left(1 - e^{iux} + iux1_{|x|<1}\right)\pi(x)\,dx,\end{aligned} \tag{2.27}$$

where μ is the drift of L_t, σ^2 is the variance of the diffusion process of L_t, and the Lèvy density $\pi(x)$ is the arrival rate of jumps with size x.

The Lèvy components in futures return process have two parts, diffusion components and Lèvy jump components. According to the equation 2.27, the characteristic exponent for the concavity adjusted diffusion components is $\frac{1}{2}\left(u^2+iu\right)e^{2\xi(t)}[(\sigma_S)^2+(\sigma_Y^{\Delta})^2+2\rho_j\sigma_S\sigma_Y^{\Delta}]$. According to Carr and Wu (2007), the characteristic exponent of the concavity adjusted right skewed jump component with a free α is

$$\lambda\Gamma(-\alpha)\left[\left(\frac{1}{\upsilon_J}\right)^{\alpha} - \left(\frac{1}{\upsilon_J} - iu\right)^{\alpha}\right] - iu\lambda\Gamma(-\alpha)\left[\left(\frac{1}{\upsilon_J}\right)^{\alpha} - \left(\frac{1}{\upsilon_J} - 1\right)^{\alpha}\right], \tag{2.28}$$

and the characteristic exponent of the concavity adjusted left skewed jump component with a free α is

$$\lambda\Gamma(-\alpha)\left[\left(\frac{1}{\upsilon_J}\right)^{\alpha} - \left(\frac{1}{\upsilon_J} + iu\right)^{\alpha}\right] - iu\lambda\Gamma(-\alpha)\left[\left(\frac{1}{\upsilon_J}\right)^{\alpha} - \left(\frac{1}{\upsilon_J} + 1\right)^{\alpha}\right]. \tag{2.29}$$

To derive the Laplace transform of the stochastic time vector $\mathcal{T}_t$ under the complex measurement $\mathbb{M}$, we change the activity rate process $(\upsilon_1^R, \upsilon_1^L)$ from risk-neutral measure $\mathbb{Q}$ to $\mathbb{M}$ by using Girsanov's Theorem. The diffusion coefficients of υ_1^R and υ_1^L remain the same as $\sigma_{\upsilon 1}^i\sqrt{\upsilon_1^i(t)}$, and the drift terms should be adjusted. The stochastic long-run mean υ_2^R and υ_2^L of two activity rates remain the same. Then the dynamics

under measurement $\mathbb{M}$,

$$\begin{aligned} d\upsilon_1^j(t) &= \left(\kappa\upsilon_2^j(t) - \kappa_j^{\mathbb{M}}\upsilon_1^j(t)\right)dt + \sigma_{\upsilon 1}\sqrt{\upsilon_1^j(t)}dW_{j3}^Q(t) \\ d\upsilon_2^j(t) &= \left(\eta - \kappa_2\upsilon_2^j(t)\right)dt + \sigma_{\upsilon 2}\sqrt{\upsilon_2^j(t)}dW_{j4}^Q(t), \end{aligned} \tag{2.30}$$

where $\kappa_j^{\mathbb{M}} = \kappa + iu\sigma_S\sigma_{\upsilon 1}^j\rho_{j1}e^{\xi(t)} + iu\sigma_Y^{\Delta}\sigma_{\upsilon 1}^j\rho_{j2}e^{\xi(t)}$. Writing the above process as a matrix form $V(t) \equiv \left[\upsilon_1^R(t), \upsilon_1^L(t), \upsilon_2^R(t), \upsilon_2^L(t)\right]^{\mathrm{T}}$, then

$$dV(t) = \left(a - \kappa_V^{\mathbb{M}}V(t)\right)dt + \sqrt{\sum V(t)}dW_V^Q(t), \tag{2.31}$$

where

$$a = \begin{bmatrix} 0 \\ 0 \\ \eta \\ \eta \end{bmatrix}, \quad \kappa_V^{\mathbb{M}} = \begin{bmatrix} \kappa_R^{\mathbb{M}} & 0 & -\kappa & 0 \\ 0 & \kappa_L^{\mathbb{M}} & 0 & -\kappa \\ 0 & 0 & \kappa_2 & 0 \\ 0 & 0 & 0 & \kappa_2 \end{bmatrix}, \quad \sum = \begin{bmatrix} \left(\sigma_{\upsilon 1}^R\right)^2 \\ \left(\sigma_{\upsilon 1}^L\right)^2 \\ \left(\sigma_{\upsilon 2}^R\right)^2 \\ \left(\sigma_{\upsilon 2}^L\right)^2 \end{bmatrix}.$$

The drift term and variance of diffusion term are affine in the activity rates and the long-run mean activity rates under complex measure $\mathbb{M}$. The generalized Fourier transform of the futures return is exponential affine in the current level of the activity rates,$V(t)$,

$$\mathscr{L}_{\mathcal{T}}^{\mathbb{M}}(\psi) = \exp\left(-b(t)^{\mathrm{T}}V_0 - c(t)\right), \tag{2.32}$$

where

$$\begin{aligned} b'(t) &= b_V - \left(\kappa_V^{\mathbb{M}}\right)^{\mathrm{T}}b(t) - \frac{1}{2}\sum \bigodot b(t) \bigodot b(t), \\ c'(t) &= b(t)^{\mathrm{T}}a, \end{aligned} \tag{2.33}$$

with $b_V \equiv \left[\psi^{FR}, \psi^{FL}, 0, 0\right]^{\mathrm{T}}$, $b(0) = 0$ and $c(0) = 0$. The Hadamard product $\bigodot$ is an element-by-element product operation. The coefficients $b(t)$ and $c(t)$ can be solved numerically starting at $b(0)$ and $c(0)$.

Then, we define the payoff of a commodity futures option at option expiry date

T_o as

$$\prod_{T_o,T_f}(k;a,b,c)=\left(a+b\mathrm{e}^{f\left(T_o,T_f\right)}\right)1_{f\left(T_o,T_f\right)\leq c^{\mathrm{T}}k}, \tag{2.34}$$

where $f\left(T_o,T_f\right)=\ln\frac{F\left(T_o,T_f\right)}{F\left(0,T_f\right)}$ and $F\left(T_o,T_f\right)$ is the time-T_o price for a futrue contract expiring on date T_f. Specifically, the terminal payoff of a European call option is $\prod_{T_o,T_f}^{call}\left(-\ln\frac{K}{F(0,T)};-K,F\left(0,T\right),-1\right)$ and the terminal payoff of a European put option is $\prod_{T_o,T_f}^{put}\left(\ln\frac{K}{F(0,T)};K,-F\left(0,T\right),1\right)$

Define $G\left(t,T_o,T_f,K\right)$ as the time-t price of a futures option contract with payoff of equation 2.34 and the strike price K. T_o and T_f are expiry dates of the option contract and its underlying futures contract, respectively. Then,

$$G\left(k;t,T_o,T_f\right)=E_t^{\mathbb{Q}}\left[e^{-\int_t^{T_o}r(s)ds}\prod_{T_o,T_f}(k;a,b,c)\right], \tag{2.35}$$

Assume that the interest rate $r(t)$ and the futures price $F\left(T_o,T_f\right)$ are uncorrelated, then

$$G\left(k;t,T_o,T_f\right)=e^{-\int_t^{T_o}r(s)ds}E^{\mathbb{Q}}\left[\prod_{T_o,T_f}(k;a,b,c)\right]. \tag{2.36}$$

Define $\mathscr{G}\left(z;t,T_o,T_f\right)$ as the generalized Fourier transform of $G\left(t,T_o,T_f,K\right)$, where $z\in\mathscr{C}\subseteq\mathbb{C}$. To apply fast Fourier inversion on the transform (FFT) to compute the Fourier coefficient $G\left(k;t,T_o,T_f\right)$, we treat $G\left(k;t,T_o,T_f\right)$ as the probability density in $\mathscr{G}\left(z;t,T_o,T_f\right)$,

$$\begin{aligned}\mathscr{G}\left(z;t,T_o,T_f\right)&\equiv\int_{-\infty}^{\infty}\mathrm{e}^{izk}G\left(k;t,T_o,T_f\right)dk\\&=e^{-\int_t^{T_o}r(s)ds}\int_{-\infty}^{\infty}\mathrm{e}^{izk}\mathbb{E}^{Q}\left[\prod_{T_o,T_f}(k;a,b,c)\right]dk.\end{aligned} \tag{2.37}$$

According to Carr and Wu (2004), the generalized Fourier transform of the futures option

price $G(k;t,T_o,T_f)$ is

$$\mathscr{G}(z;t,T_o,T_f) = \frac{i}{z}\left(a\phi_{f(T_o,T_f)}(zc) + b\phi_{f(T_o,T_f)}(zc-i)\right), \tag{2.38}$$

where its admissible domain $\operatorname{Im} z$ is $(0,\infty)$, and

$$\mathscr{G}(z;t,T_o,T_f) = \frac{i}{z}\left(a\phi_{f(T_o,T_f)}(-zc) + b\phi_{f(T_o,T_f)}(-zc-i)\right), \tag{2.39}$$

where its admissible domain $\operatorname{Im} z$ is $(-\infty,0)$.

Given $z = z_r + iz_i$, z_r and z_i are the real and imaginary part of z, respectively. The price of the futures option $G(k;t,T_o,T_f)$ with well-defined payoff function can be obtained via the Fourier inversion formula,

$$\begin{aligned} G(k;t,T_o,T_f) &\equiv \frac{1}{2\pi}\int_{iz_i-\infty}^{iz_i+\infty} \mathrm{e}^{-izk}\mathscr{G}(z;t,T_o,T_f)\,dz \\ &= \frac{\mathrm{e}^{z_i k}}{\pi}\int_0^{\infty} \mathrm{e}^{-iz_r k}\mathscr{G}(z_r+iz_i;t,T_o,T_f)\,dz_r. \end{aligned}$$

The discretization of the integral in equation 2.40 is approximately equal to

$$G(k;t,T_o,T_f) \approx G^*(k) = \frac{\mathrm{e}^{z_i k}}{\pi}\sum_{n=0}^{N-1} \mathrm{e}^{-iz_r(n)k}\mathscr{G}(z_r(n)+iz_i;t,T_o,T_f)\triangle z_r, \tag{2.40}$$

where $z_r(n)$ are the nodes of z_r and $\triangle z_r$ are the distance between nodes.

Following the setting in Carr and Madan (1999), we set $z_r(n) = d_z n$, $k_j = -k_L + d_k j$ and $d_z d_j = \frac{2\pi}{N}$ for $j = 0,\ldots,N-1$. According to the FFT, the futures option price is

$$G^*(k_j) = \sum_{n=0}^{N-1} \mathrm{e}^{-jn\frac{2\pi}{N}i} f_n, \tag{2.41}$$

with

$$f_n = \frac{1}{\pi}\mathrm{e}^{z_i k_j + ik_L d_z n}\mathscr{G}(d_z n + iz_i;t,T_o,T_f)\,d_z, \tag{2.42}$$

where d_z and d_k are the spacing for integration and the log of moneyness k, respectively. The range of the log of moneyness is between -k_L and $d_k N - k_L$. To ensure the middle point of k_j is the at-the-money option ($k = 0$), we set $k_L = \frac{d_k N}{2}$.

2.4 Estimation Procedure

2.4.1 Specification of the market price of risk

The cross-sectional dynamic of commodity futures options implied volatilities can be captured well under the risk-neutral measure $\mathbb{Q}$. To capture the time-series variation of implied volatilities, we specify the process of activity rates under the real probability measure$\mathbb{P}$. Assume that the market price of risk on activity rates is $\gamma\left(\upsilon_n^j(t)\right)$ for $j = R, L$ and $n = 1, 2$:

$$\gamma\left(\upsilon_n^j(t)\right) = \gamma_n \sqrt{\upsilon_n^j(t)}, \tag{2.43}$$

The dynamics of activity rates under $\mathbb{P}$ are

$$\begin{aligned} d\upsilon_1^j(t) &= (\kappa_1 \upsilon_2^j(t) - \kappa_1^{\mathbb{P}} \upsilon_1^j(t))dt + \sigma_{\upsilon 1} \sqrt{\upsilon_1^j(t)} dW_{j3}^Q(t), \\ d\upsilon_2^j(t) &= (\eta - \kappa_2^{\mathbb{P}} \upsilon_2^j(t))dt + \sigma_{\upsilon 2} \sqrt{\upsilon_2^j(t)} dW_{j4}^Q(t), \end{aligned} \tag{2.44}$$

where $\kappa_1^{\mathbb{P}} = \kappa_1 - \sigma_{\upsilon 1}\gamma_1$ and $\kappa_2^{\mathbb{P}} = \kappa_2 - \sigma_{\upsilon 2}\gamma_2$.

2.4.2 Kalman Filter and Maximum Likelihood Estimation

To estimate parameters in the analytic solution of option price, we cast the model into a state-space model and do the estimation by using the Kalman filter and Maximum Likelihood. In the state-space model, both activity rates and long-run mean of activity rates are unobservable variables. The discretization of activity rates under statistical

measure $\mathbb{P}$ can be written as

$$\begin{aligned} V_1^j(t) &= (1-\varphi_{1j})\kappa_1^{\mathbb{P}} V_2^j(t) + \varphi_{1j} V_1^j(t-1) + \sigma_{v1}\sqrt{V_1^j(t-1)\Delta t}\varepsilon_1^j(t), \\ V_2^j(t) &= (1-\varphi_{2j})\kappa_2^{\mathbb{P}}\eta + \varphi_{2j} V_2^j(t-1) + \sigma_{v2}\sqrt{V_2^j(t-1)\Delta t}\varepsilon_2^j(t), \end{aligned} \tag{2.45}$$

where $j = R, L$, $\varphi_{1j} = \exp\left(-\kappa\left(v_1^j\right)\Delta t\right)$ and $\varphi_{2j} = \exp\left(-\kappa\left(v_2^j\right)\Delta t\right)$. φ_{1j} and φ_{2j} are the auto-correlation coefficients of each activity rates between the time interval Δt. The vector of error terms $\left[\varepsilon_1^R(t), \varepsilon_1^L(t), \varepsilon_2^R(t), \varepsilon_2^L(t)\right]$ is an i.i.d. four-variate standard normal innovation.

Assume that the option pricing error is additive and normally distributed, the measurement equation under the risk-neutral measure is

$$\frac{O\left(V_t\right)}{\mathcal{V}_t} = \frac{\hat{O}\left(V_t\right)}{\mathcal{V}_t} + u_t, \quad u_t \sim iid\, N\left(0, \Omega\right), \tag{2.46}$$

where $O\left(V_t\right)$ is the actual options prices, $\hat{O}\left(V_t\right)$ is the estimated options prices, $\mathcal{V}_t$ is the corresponding Black (1976) Vegas ($\mathcal{V}_t = \frac{\partial O(V_t)}{\partial \sigma}\,|_{\sigma=\hat{\sigma}_t}$), u_t is the measurement errors with zero mean and Ω covariance matrix following the normal distribution.

We do not fit the options prices or implied volatilities directly in the measurement equation due to the following reasons. The options prices are unstable in moneyness, time to maturity and time-series dimensions. Fitting the options prices may cause the pricing error (u_t) mainly affected by expensive options (i.e. in-the-money and long-term options). Implied volatility is more stable in the above three dimensions because it intuitively weights options prices based on moneyness and expiration time. However, it is difficult to fit the implied volatility directly, because the use of numerical inversion to convert the estimated options prices into the implied volatilities increases the error and complexity of the estimation. Instead of fitting implied volatility directly, we follow Carr and Wu (2007), Bakshi et al. (2008) and Trolle (2014) to fit options prices scaled by the corresponding Black (1976) Vegas, since $\frac{O(V_t)}{\mathcal{V}_t} - \frac{\hat{O}(V_t)}{\mathcal{V}_t} \approx \sigma_t - \hat{\sigma}_t$.

We use Kalman filter to update state variables. When the state vector is linearly correlated to the transition equation and the measurement equation, the general Kalman filter is appreciate. However, our measurement equation is nonlinear. One possible way to address the non-linearity is to use the Extended Kalman Filter, but it can only accurately capture the posterior mean and covariance of the first-order options prices. To handle the high-order nonlinearity in our model, we use the unscented Kalman filter (Wan and Van Der Merwe, 2000), which can accurately capture the third-order posterior distribution.

Define y_{t+1} as the actual options prices scaled by Vega at time-$t+1$, $\bar{y}_{t+1}$ as the time-(t+1) estimated options prices scaled by Vega and $\bar{Py}y_{t+1}$ as the covariance matrix from measurement equation. And we can obtain these values from unscented Kalman filter. Assume that pricing errors are normally distributed, then the log-likelihood value (Carr and Wu, 2007) at at time-$t+1$ is

$$l_{t+1} = -\frac{1}{2}\log \mid \bar{Py}y_{t+1} \mid -\frac{1}{2}\left(y_{t+1} - \bar{y}_{t+1}\right)^T \left(\bar{Py}y_{t+1}\right)^{-1}\left(y_{t+1} - \bar{y}_{t+1}\right). \tag{2.47}$$

Then, we can get a set of model parameters Θ from

$$\Theta = \arg\max_{\Theta} \sum_{t=1}^{T} l_t\left(\Theta\right). \tag{2.48}$$

2.4.3 Model Specifications

The benchmark model in this paper is the option pricing model proposed by Trolle and Schwartz (2009). This model sets that both volatility and its long-run mean level are stochastic, but excluding seasonal components and jumps used to capture time-varying skewness. According to this specification, we restrict $\theta = \zeta = 0$ and $\lambda = \upsilon_J = \alpha_J = 0$. We also restrict that one activity rate only in the system and set $\rho_L = \rho_{1L} = \rho_{2L} = 0$, $\rho = \rho_R$, $\rho_1 = \rho_{1R}$ and $\rho_2 = \rho_{2R}$. So the set of parameters in this model is $\Theta =$

$\{\rho, \rho_1, \rho_2, \sigma_S, \sigma_1, \sigma_2, \kappa_1, \kappa_2, \alpha, \gamma, \eta, \kappa_1^{\mathbb{P}}, \kappa_2^{\mathbb{P}}\}$. To test whether and what extent the pricing performance can be improved by capturing the time-varying skewness of the return distribution and/or seasonality in volatility, we specify three other models.

In the second model specification (SSV), we capture the time-varying skewness of the return distribution. This model includes two lèvy components with two jumps and two activity rates, but excludes seasonal components by setting $\theta = \zeta = 0$. The parameters in this model are $\Theta = \{\rho_R, \rho_{1R}, \rho_{2R}, \rho_L, \rho_{1L}, \rho_{2L}, \sigma_S, \sigma_1, \sigma_2, \kappa_1, \kappa_2, \alpha, \gamma, \eta, \kappa_1^{\mathbb{P}}, \kappa_2^{\mathbb{P}}, \lambda, \upsilon_J, \alpha_J\}$.

The third model specification (SV-S) is to capture seasonality in volatility. Different from the benchmark model, we relax the restrictions on θ and ζ. The parameters we have in this model are $\Theta = \{\rho, \rho_1, \rho_2, \sigma_S, \sigma_1, \sigma_2, \kappa_1, \kappa_2, \alpha, \gamma, \eta, \kappa_1^{\mathbb{P}}, \kappa_2^{\mathbb{P}}, \theta, \zeta\}$.

The last model specification (SSV-S) is the comprehensive model can capture the time-varying skewness of the return distribution and seasonality in volatility. The parameters are $\Theta = \{\rho_R, \rho_{1R}, \rho_{2R}, \rho_L, \rho_{1L}, \rho_{2L}, \sigma_S, \sigma_1, \sigma_2, \kappa_1, \kappa_2, \alpha, \gamma, \eta, \kappa_1^{\mathbb{P}}, \kappa_2^{\mathbb{P}}, \lambda, \upsilon_J, \alpha_J, \theta, \zeta\}$.

2.5 Empirical Results

2.5.1 Data

To evaluate the pricing performance of the four model specifications , we use the Brent crude oil data described in Section 2.2.1 to estimate parameters. As we discussed before, the Brent crude oil options in our sample are American-style, but the option pricing model in this paper are for European-style options. Thus, we convert the observed American options prices to European options prices by following Broadie et al. (2007) and Trolle and Schwartz (2009). First, we use the Barone-Adesi and Whaley (BAW) American commodity futures options pricing model (Barone-Adesi and Whaley, 1987) to obtain the BAW implied volatilities from American options prices. Then, we take the BAW implied volatility into Black formula (Black, 1976) to calculate the corresponding

European option price.

We estimate model parameters by using in-sample data from 15 May, 2013 to 04 May, 2016 (156 weekly observations) and use data between 11 May, 2016 and 17 May, 2017 for out-of-sample tests (54 weekly observations). The average daily number of option contracts is approximately 116.

2.5.2 Parameter Estimation and Pricing Performance

Table 2.2 displays estimated parameters by using in-sample data under four model specifications, the benchmark model, SSV specification to capture the time-varying skewness, SV-S specification to capture the seasonality in volatility and SSV-S specification to capture both time-varying skewness and seasonality in volatility.

The correlations among Brownian motions under the benchmark model and SV-S specification denote as ρ, ρ_1 and ρ_2. Under SSV and SSV-S specifications, the correlation parameters are ρ_R, ρ_{1R}, ρ_{2R}, ρ_L, ρ_{1L} and ρ_{2L}. Under the benchmark model and SV-S specification, correlations between the innovations in spot return and the innovations in the forward cost of carry (ρ) is negative. It implies that the volatility is positively related to the backwardation magnitude (Routledge et al., 2000; Trolle and Schwartz, 2009). Since the ρ_L is more negative than ρ_R under SSV and SSV-S specifications, the backwardation magnitude is largely affected by the downside risk, for example, downside risk is high when the crude oil is in surplus and lack of demand. Under SSV and SSV-S specifications, the right skewed Lèvy components in the spot return is positively related to its volatility factor (ρ_{1R}), while the left skewed Lèvy components is negatively related to its volatility factor (ρ_{1L}). This two correlations with different signs ensure that the model generates the time-varying skewness of long-term expiring contracts. According to the magnitude of ρ_1 and ρ_2 (or (ρ_{1R}, ρ_{1L}) and (ρ_{2R}, ρ_{2L})), the activity rates are more correlated with spot price, rather than the forward cost of carry.

Based on the model set up, both volatility factor v_1 and v_2 are mean-reverting

processes. According to the estimated reversion coefficient of two volatility factors in Table 2.2, volatility factor v_1 has a higher mean reverting speed than v_2 under risk-neutral and real probability measures across four model specifications, since κ_1 is higher than κ_2 under the risk-neutral measure and $\kappa_1^{\mathbb{P}}$ is higher than $\kappa_2^{\mathbb{P}}$ under the real probability measure. So, v_1 is much more less persistent than v_2. Volatility factor v_1 mainly captures the transitory shocks, while its long run mean v_2 captures the persistent shocks. However, the risk premiums of two volatility factors are different. Under all model specifications, κ_1 is greater than $\kappa_1^{\mathbb{P}}$, while κ_2 is less than $\kappa_2^{\mathbb{P}}$. Thus, the market price of risk on volatility factor v_1 is positive, but the market price of the volatility factor v_2 is negative. This shows that investors in the crude oil market are averse to both high persistent risk and high variation in the persistent risk.

The level and variance of jumps are captured by λ and v_J. According to the estimated value of these two parameters, the level and variance of jumps do not change much even after capturing seasonality in volatility. α_J is between zero and one under the SSV and SSV-S specifications. This means that the jumps in the crude oil market have infinite activity and finite variance. Thus, the number of jumps in our sample period is infinite, but the tails of the jump distribution are relatively "thin enough", both the upper and the lower part can converge to a finite value. Parameters to control seasonality in volatility (θ and ζ) are significant before and after controlling the time-varying skewness.

Table 2.3 shows the pricing performance of our four model specification. We measure the pricing performance by using the mean absolute errors (MAE) and the log likelihood values. Compared with the benchmark model, in term of MAE, the SV-S specification has a poor in-sample and out-of-sample performance. After capturing the time-varying skewness of crude oil return distributions, both in-sample and out-of-sample mean absolute errors and log likelihood values indicate SSV and SSV-S models have better performance than the benchmark model. In term of MAE, the difference in

pricing performance between SSV and SSV-S specifications is insignificant.

Figure 2.3 shows the the pricing errors (MAE) in moneyness dimension by using full sample data. According to Carr and Wu (2007), if the shape of implied volatility curve is well captured by the option pricing model, the pricing errors (MAE) in the moneyness dimensions should not display significant structural pattern. Compared with SSV (Figure 2.3b) and SSV-S (Figure 2.3d) model specifications, the pricing errors of the benchmark (Figure 2.3a) and SV-S (Figure 2.3c) models have significant structural patterns along the moneyness across one-month, three-month and one-year maturities and especially in the short horizon. Thus, the option pricing model that captures time-varying skewness can account for the shape of implied volatility curve.

Therefore, we conclude that capturing time-varying skewness of crude oil return distributions can improve the pricing performance significantly, but capturing seasonal pattern in volatility cannot. This may be because the crude oil market is a world market, and the seasonal pattern in volatility is not as strong as some other commodities, for example, soybeans, natural gas, heating oil and etc.

2.5.3 The Activity Rate Dynamics and Stochastic Skewness

According to the analysis in the previous section, the pricing performance of the option pricing model in the Brent crude oil market is related to whether the model can capture the time-vary skewness of return distributions, but not the seasonal pattern in volatility. Therefore, in this section, we focus our investigation on the benchmark model and SSV specification.

The activity rates are updated by using the unscented Kalman filter. Figure 2.4 shows time-series activity rates v_1 under the benchmark model and SSV specification. Under the benchmark model, the overall fluctuation of the time-series activity rate in Figure 2.4a has a similar pattern to the ATM implied volatility in the figure 2.1. This means that the stochastic volatility is well captured by the benchmark model. According

to Figure 2.4b, the activity rate of the left skewed Lèvy component is mostly higher than that of the right skewed Lèvy component, especially after the fourth quarter of 2014. This indicates the market demand of out-of-the-money put options is much more higher than the demand of out-of-the-money call options. It is not surprising since Brent crude oil price drops more than a half during the fourth quarter of 2014 and fluctuate around this level since then. It is also consistent with the story from the implied volatility 'smirk' in Figure 2.2c, that is, during our sample period, OTM put options are more expensive than OTM call options in average. However, according to the central tendency of activity rates in Figure 2.5b, the long-term demands of OTM call and OTM put options are more balanced than the short-term.

Figure 2.6 shows the actual and model implied three-month 5% risk reversals. The model implied risk reversals are generated by using the benchmark model and the SSV specification. Compared with the actual risk reversal, the estimated risk reversal under the benchmark model in Figure 2.6a is more persistent. In contrast, we observe estimated risk reversals under the SSV specification in Figure 2.6b is more volatile. The estimated risk reversals are very close to actual risk reversals before the fourth quarter of 2014, which is the period with relatively low implied volatility. During the period of high implied volatility, estimated risk reversals deviate from actual risk reversals. Thus, following Carr and Wu (2007), we also plot the 5% risk reversals scaled by the ATM implied volatility with same maturity. Figure 2.6d shows that the scaled 5% risk reversals generated by SSV-model is close to the scaled actual level.

2.6 Conclusion

In this paper, we propose a comprehensive option pricing model to capture stylized features in the energy commodity market, one is the seasonal pattern in volatility, and the other is time-varying skewness of return distributions. Empirically, we use the Brent

crude oil futures and options data to test the pricing performance of the comprehensive model and investigate how much the pricing performance changes by capturing each stylized feature.

Our results show that the Brent crude oil market exhibits seasonal pattern in volatility and time-varying skewness of return distributions. The comprehensive option pricing model we proposed in this paper is enable to capture these two stylized features in the commodity market. We employ a sine function to capture the seasonal pattern in volatility and use two separate jumps and two independent activity rates to generate time-varying skewness of return distributions for both short and long horizons. We use Brent crude oil options to test whether and how much the option pricing model performance is improved by each generalization. The empirical results show that the option model pricing performance is significantly improved by capturing the time-varying skewness of return distributions in the crude oil market, but is less affected by capturing seasonality in volatility. This is because the crude oil market is a world market, and crude oil is closer to financial assets than other commodities, thus, the seasonal pattern in volatility is not as strong as other commodities (such as natural gas). Our option pricing model can be used to price other commodity options, since these two stylized features are not unique to the crude oil market.

Table 2.1: **Summary Statistics of Risk Reversals and Butterfly Spreads**

This table presents the average, standard deviation and weekly autocorrelation of 5% risk reversals and 5% butterfly spreads for five horizons, one-, two-, three-, six- and twelve- month. The 5% risk reversal (RR5) is the implied volatilises difference between a call option with 105% moneyness and a put option with 95% moneyness. The 5% butterfly spread is the difference between the average of implied volatilities at 95% and 105% moneyness levels and implied volatility of at-the-money option. The sample period is between 15 May, 2013 and 17 May, 2017.

	RR5			BF5		
Maturity	Mean	Std	Auto	Mean	Std	Auto
1 Month	-2.41	1.28	0.84	0.60	0.43	0.94
2 Months	-2.14	0.89	0.89	0.30	0.22	0.95
3 Months	-1.99	0.73	0.92	0.20	0.14	0.96
6 Months	-1.76	0.57	0.93	0.11	0.07	0.96
12 Months	-1.47	0.48	0.94	0.05	0.04	0.91

Table 2.2: **Parameter Estimation**

This table presents the in-sample estimated parameters by using the benchmark model, SSV specification, SV-S specification and SSVS specification, respectively. The sample period is from 15 May, 2013 to 04 May, 2016 (156 weekly observations).

Parameters		Benchmark	SSV	SV-S	SSV-S
ρ	ρ_R	-0.3669	-0.2639	-0.2999	-0.1732
		(-0.0097)	(-0.0106)	(-0.0100)	(-0.0023)
ρ_1	ρ_{1R}	-0.7864	0.3355	-0.9300	0.3608
		(-0.0098)	(0.0092)	(-0.0093)	(0.0091)
ρ_2	ρ_{2R}	-0.6204	-0.0622	-0.5694	-0.0606
		(-0.0101)	(-0.0100)	(-0.0020)	(-0.0101)
ρ_L	ρ_L	-	-0.6949	-	-0.7240
			(-0.0099)		(-0.0021)
ρ_{1L}	ρ_{1L}	-	-0.5197	-	-0.5273
			(-0.0099)		(-0.0089)
ρ_{2L}	ρ_{2L}	-	-0.0707	-	-0.1567
			(-0.0101)		(-0.0084)
σ_S	σ_S	0.2567	0.1073	0.2157	0.1079
		(0.0087)	(0.0098)	(0.0071)	(0.0038)
σ_1	σ_1	1.265	1.3137	1.5847	1.3800
		(0.0129)	(0.0100)	(0.0978)	(0.0054)
σ_2	σ_2	1.2848	1.2154	1.6583	1.2668
		(0.0095)	(0.0100)	(0.0112)	(0.0193)
κ_1	κ_1	19.2988	9.8020	19.7706	9.7419
		(0.0100)	(0.0102)	(0.0089)	(0.0095)
κ_2	κ_2	1.3091	0.4544	0.6087	0.4615
		(0.0108)	(0.0097)	(0.0087)	(0.0043)
α	α	0.3815	0.2435	0.1601	0.2645
		(0.0095)	(0.0095)	(0.0093)	(0.0067)
γ	γ	1.8794	1.3411	1.1141	1.3409
		(0.0099)	(0.0101)	(0.0089)	(0.0091)
η	η	0.9098	0.3504	0.8116	0.3518
		(0.0110)	(0.0100)	(0.0079)	(0.0103)
$\kappa_1^{\mathbb{P}}$	$\kappa_1^{\mathbb{P}}$	8.5987	4.4797	2.0438	4.4722
		(0.0100)	0.0112	(0.0088)	(0.0034)
$\kappa_2^{\mathbb{P}}$	$\kappa_2^{\mathbb{P}}$	1.9021	1.0906	1.3819	1.1716
		(0.0126)	(0.0099)	(0.0032)	(0.0056)
λ	λ	-	0.3933	-	0.4025
			(0.0099)		(0.0078)
υ_J	υ_J	-	0.1051	-	0.1077
			(0.0100)		(0.0063)
α_J	α_J	-	0.8072	-	0.7627
			(0.0123)		(0.0098)
θ	θ	-	-	0.2169	0.1178
				(0.0270)	(0.0376)
ζ	ζ	-	-	0.4033	0.5342
				(0.0108)	(0.0068)

Table 2.3: **Pricing Performance**

This table presents the log likelihood values ($\mathscr{L}(\Theta)$) and the mean absolute errors (MAE) of the benchmark model, SSV specification, SV-S specification and SSVS specification, respectively. The last rows in each panel (MAE Difference with Benchmark) report the MAE difference between benchmark model and the other model specifications, SSV specification, SV-S specification and SSVS specification, and present the t-statistics in parentheses. In-sample data is from 15 May, 2013 to 04 May, 2016 (156 weekly observations) and out-of-sample data is between 11 May, 2016 and 17 May, 2017 (54 weekly observations).

	Benchmark	SSV	SV-S	SSV-S
In-sample performance				
$\mathscr{L}(\Theta)$	-275896.83	-255634.20	-265240.95	-242715.03
MAE(%)	2.40	2.27	2.46	2.27
MAE Difference with Benchmark		-0.13	0.06	-0.13
		(-4.68)	(2.46)	(-4.61)
Out-of-sample performance				
$\mathscr{L}(\Theta)$	-101435.52	-97132.01	-98799.54	-855147.10
MAE(%)	2.90	2.83	3.15	2.82
MAE Difference with Benchmark		-0.07	0.25	-0.08
		(-2.62)	(5.59)	(-2.73)

Figure 2.1: **Implied volatility of One-month ATM Option**

This figure shows the one-month implied volatilities of at-the-money Brent crude oil options between 15 May, 2013 and 17 May, 2017. The sample is weekly frequency.

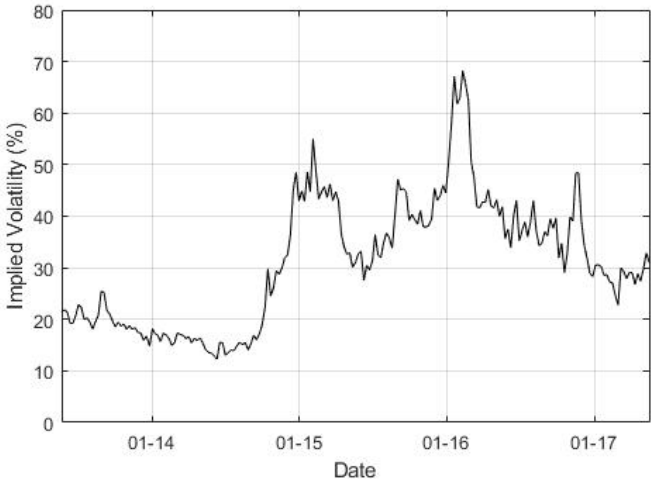

Figure 2.2: **Dynamic Behaviour of the Crude Oil Return**

This figure shows the seasonal pattern in volatility, average implied volatility curves, risk reversals and butterfly spreads in the Brent crude oil market. Figure 2.2a and 2.2b display the seasonal pattern in the realized volatility and the option-implied volatility, respectively. Figure 2.2c shows the average implied volatility curve from Brent crude oil options over three horizons, one-month (1M), three-month (3M) and one-year (1Y, curve raised up by 2%). Figure 2.2d shows three-month 5% risk reversals (RR5) and three-month 5% butterfly spreads (5BF) calculated from Brent crude oil options. The sample period is between15 May, 2013 and 17 May, 2017.

(a) **Seasonality Pattern of Realized Volatility**

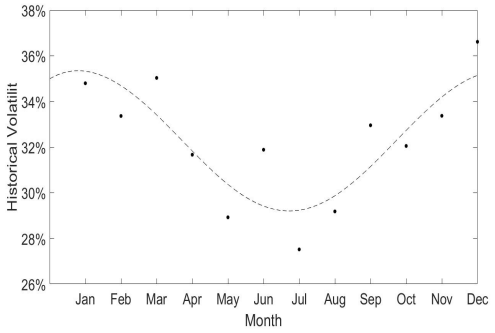

(b) **Seasonality Pattern of Implied Volatility**

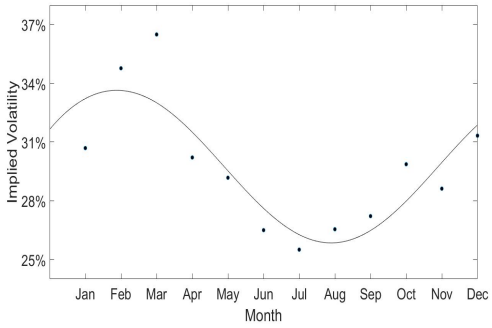

(c) **Average Implied Volatility Curve**

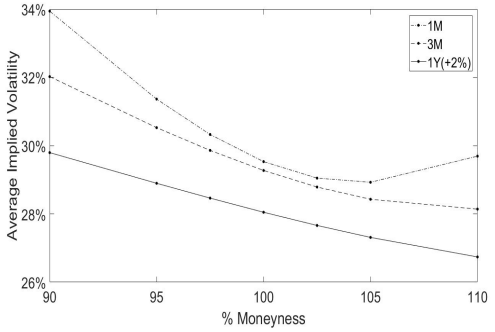

(d) **Time-varying Risk Reversals and Butterfly Spreads**

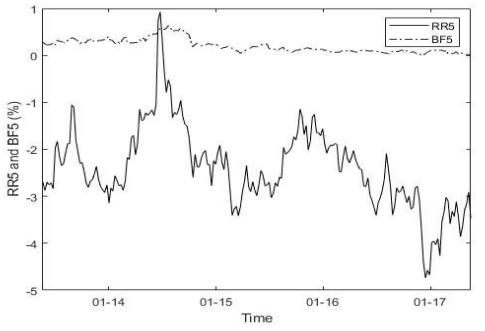

Figure 2.3: **MAE in the Moneyness and Maturity Demotion**

This figure presents the the mean absolute pricing errors (MAE) in moneyness dimension for one-month (1M), three-month (3M) and twelve-month (1Y) horizons in full sample. Figure 2.3a, 2.3b, 2.3c and 2.3d are MAEs of the benchmark model, SSV specification, SV-S specification and SSVS specification, respectively. The sample period is between15 May, 2013 and 17 May, 2017.

(a) **Benchmark Model**

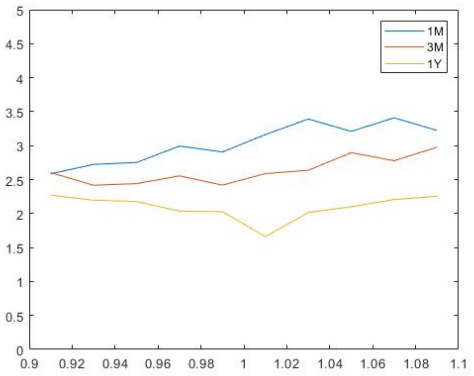

(b) **SSV Specification**

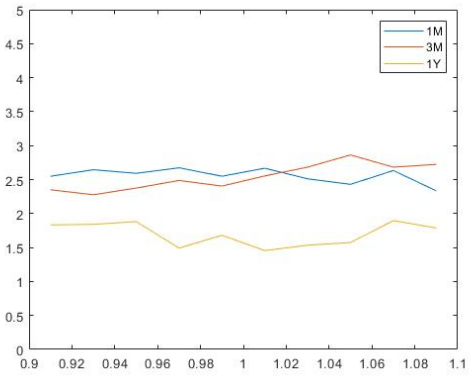

(c) **SV-S Specification**

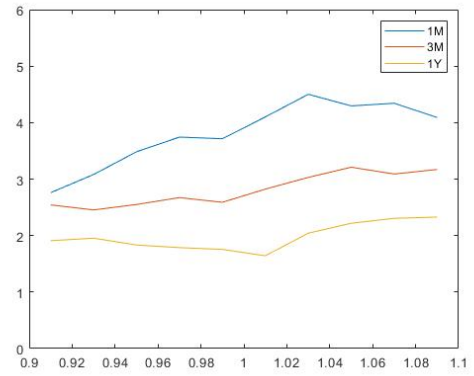

(d) **SSV-S Specification**

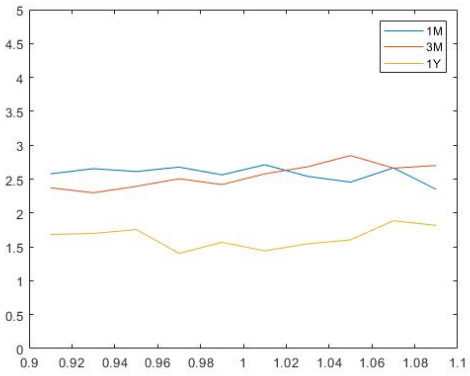

Figure 2.4: **Dynamics of Estimated Activity Rate**

This figure presents time-series activity rates v_1 under the benchmark model and SSV specification in full sample. The activity rates are updated by the unscented Kalman filter. Figure 2.4a displays the activity rate in the benchmark model. Figure 2.4b displays the activity rate of the right skewed Lèvy component (black line) and the activity rate of the left skewed Lèvy component (red line) under SSV specification. The sample period is between15 May, 2013 and 17 May, 2017.

(a) **Benchmark Model**

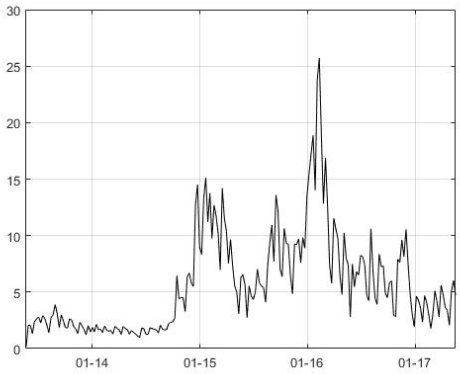

(b) **SSV Specification**

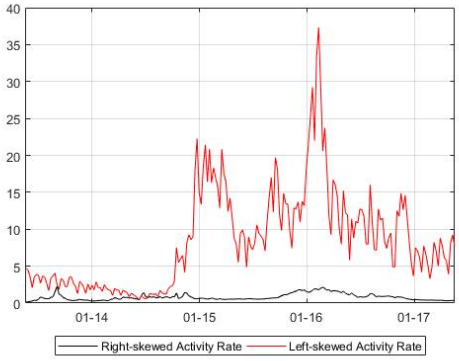

Figure 2.5: **Dynamics of Long-Run Mean of Activity Rate**

This figure presents the activity rates' long-run average, v_2, under the benchmark model and SSV specification in full sample. The long-run mean of activity rates are updated by the unscented Kalman filter. Figure 2.5a displays the long-run mean of activity rate in the benchmark model. Figure 2.5b displays the long-run mean of the activity rate of the right skewed Lèvy component (black line) and the long-run mean of the activity rate of the left skewed Lèvy component (red line) under SSV specification. The sample period is between15 May, 2013 and 17 May, 2017.

(a) **Benchmark Model**

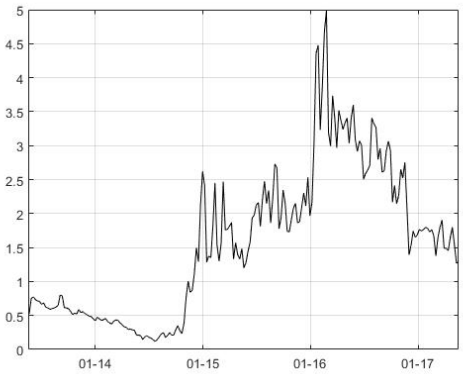

(b) **SSV Specification**

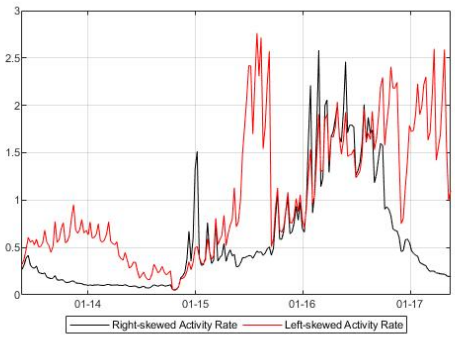

Figure 2.6: **Actual and Estimated Risk Reversal**

This figure presents the actual and model implied three-month 5% risk reversals under the benchmark model and SSV specification. Figure 2.6a and Figure 2.6b display model implied three-month 5% risk reversals (red line) under the benchmark model and the SSV specification, respectively. The black line is the actual three-month 5% risk reversals, Figure 2.6c and Figure 2.6d display model implied three-month 5% risk reversals scaled by 3-month ATM model implied volatility (red line) under the benchmark model and the SSV specification, respectively. The black line is the actual three-month 5% risk reversals scaled by 3-month ATM actual implied volatility. The sample period is between15 May, 2013 and 17 May, 2017.

(a) **Benchmark Model**

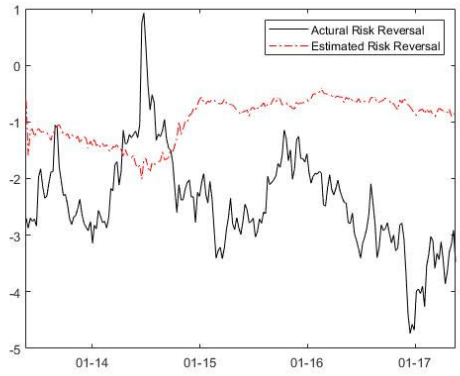

(b) **SSV Specification**

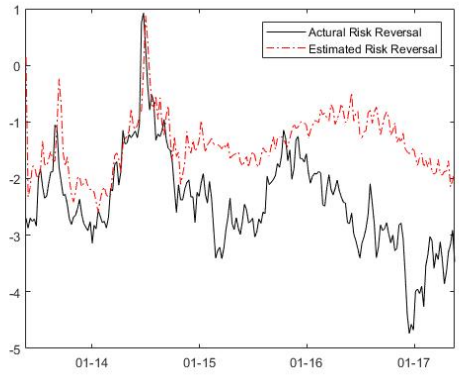

(c) **Benchmark Model (Scaled RR)**

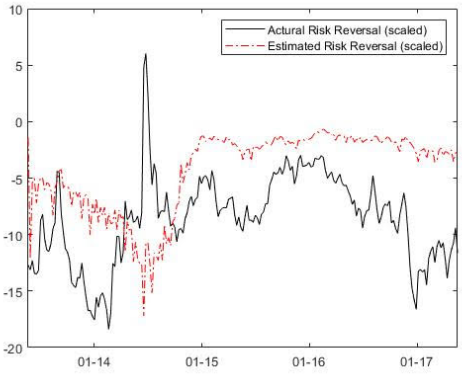

(d) **SSV Specification (Scaled RR)**

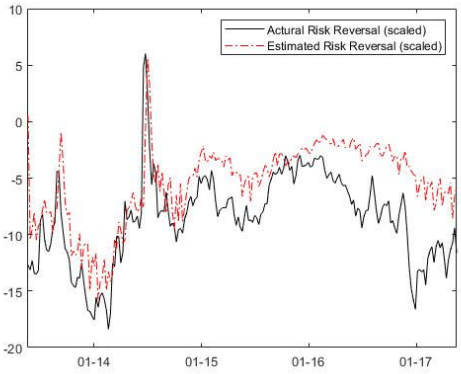

Appendix 2.A Dynamic Behaviour of the Natural Gas Return

Figure 2.A-1: **Dynamic Behaviour of the Natural Gas Return**

This figure shows the seasonal pattern in volatility, average implied volatility curves, risk reversals and butterfly spreads in the Henry Hub natural gas market. Figure 2.A-1a and 2.A-1b display the seasonal pattern in the realized volatility and the option-implied volatility, respectively. Figure 2.A-1c shows the average implied volatility curve from Henry Hub natural gas options over three horizons, one-month (1M), three-month (3M) and one-year (1Y, curve raised up by 2%). Figure 2.A-1d shows three-month 5% risk reversals (RR5) and three-month 5% butterfly spreads (5BF) calculated from Henry Hub natural gas options. The sample period is between15 May, 2013 and 17 May, 2017.

(a) **Seasonality Pattern of Realized Volatility**

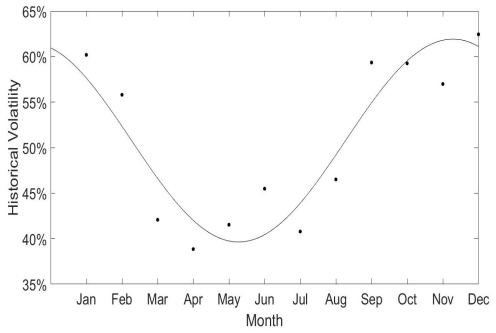

(b) **Seasonality Pattern of Implied Volatility**

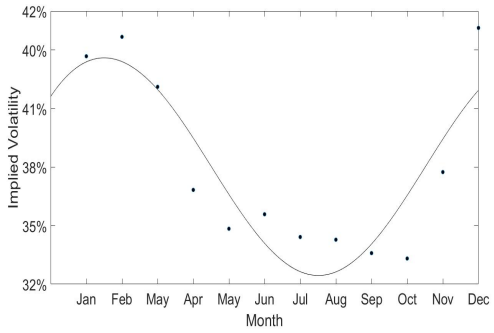

(c) **Average Implied Volatility Curve**

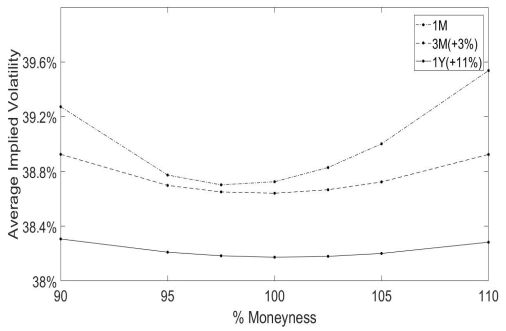

(d) **Time-varying Risk Reversals and Butterfly Spreads**

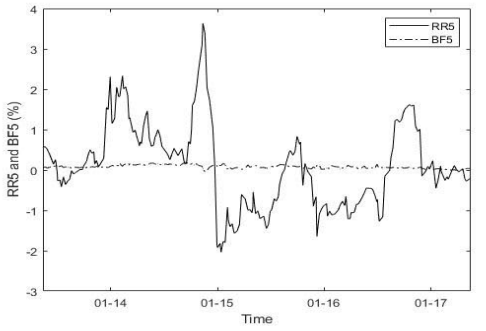

Appendix 2.B Commodity Future Price

We define $Y(t,T) = \int_t^T y(t,u)du$. Then,

$$dF(t,T) = Y(t,T)dS(t) + F(t,T)dY(t,T) + \frac{1}{2}F(t,T)(dY(t,T))^2 + Y(t,T)dS(t)dY(t,T), \tag{2.49}$$

which could be written as

$$\frac{dF(t,T)}{F(t,T)} = \frac{dS(t)}{S(t)} + dY(t,T) + \frac{1}{2}(dY(t,T))^2 + \frac{dS(t)}{S(t)}dY(t,T). \tag{2.50}$$

Specifically,

$$\begin{aligned} dY(t,T) = &\left[-\delta(t) + \int_t^T (\mu_y(t,u))\, du\right] dt \\ &+ \left(\int_t^T \sigma_y(t,u)du\right) e^{\xi(t)} \left[\sqrt{\upsilon^R(t)}dW_{R2}^Q(t) + \sqrt{\upsilon^L(t)}dW_{L2}^Q(t)\right], \end{aligned}$$

$$(dY(t,T))^2 = \left(\int_t^T \sigma_y(t,u)du\right)^2 e^{2\xi(t)} \left[\upsilon^R(t) + \upsilon^L(t)\right] dt, \tag{2.51}$$

$$\frac{dS(t)}{S(t)}dY(t,T) = \sigma_S e^{2\xi(t)} \left(\int_t^T \sigma_y(t,u)du\right) \left[\upsilon^R(t)\rho_R + \upsilon^L(t)\rho_L\right] dt. \tag{2.52}$$

Therefore,

$$
\begin{aligned}
\frac{dF(t,T)}{F(t,T)} = &\left[\int_t^T \mu_y(t,u)du\right]dt + \frac{1}{2}\left(\int_t^T \sigma_y(t,u)du\right)^2 e^{2\xi(t)}\left[\upsilon^R(t)+\upsilon^L(t)\right]dt \\
&+ \sigma_S e^{2\xi(t)}\left(\int_t^T \sigma_y(t,u)du\right)\left[\upsilon^R(t)\rho_R+\upsilon^L(t)\rho_L\right]dt \\
&+ \sqrt{\upsilon^R(t)}e^{\xi(t)}\left[\sigma_S dW^Q_{R1}(t) + \left(\int_t^T \sigma_y(t,u)du\right)dW^Q_{R2}(t)\right] \\
&+ \sqrt{\upsilon^L(t)}e^{\xi(t)}\left[\sigma_S e^{\xi(t)} dW^Q_{L1}(t) + \left(\int_t^T \sigma_y(t,u)du\right)dW^Q_{L2}(t)\right] \\
&+ \int_0^{+\infty}(e^x-1)J^R(dt,dx) + \int_{-\infty}^0 (e^x-1)J^L(dt,dx).
\end{aligned}
$$

The process of drift of the forward cost of carry is

$$
\begin{aligned}
\mu_y(t,T) = &\upsilon^R(t)\sigma_y(t,T)e^{2\xi(t)}\left[\sigma_S\rho_R + \int_t^T \sigma_y(t,u)du\right] \\
&\upsilon^L(t)\sigma_y(t,T)e^{2\xi(t)}\left[\sigma_S\rho_L + \int_t^T \sigma_y(t,u)du\right]
\end{aligned}
\tag{2.53}
$$

Chapter 3

Speculator Spreading Pressure and the Commodity Futures Risk Premium

3.1 Introduction

According to the Futures Industry Association (FIA) annual survey, the trading volume of global commodity futures increased markedly in recent years, from 2.19 billion contracts in 2009 to 5.74 billion in 2018. This dramatic increase, and the subsequent sharp decrease in commodity prices over the 2008/2009 crisis, has triggered heated debates about whether and how speculators' trading activity impacts commodity price swings. Some studies have found no impact. Rather, they posit that speculators' activities moderate prices, bringing them closer to fundamentals (e.g., Brunetti et al., 2016). Others argue that the financialization of commodity markets has enabled *uninformed* speculators, particularly with the influx of index traders, to affect commodity prices and volatilities by bringing about increased financial investment in the market (Basak and Pavlova, 2016; Brogaard et al., 2019).

In a recent theoretical paper, Goldstein and Yang (2019) reconcile both sides of this argument. They show that financial traders can bring both noise and information to the market, while the overall effect of financialization can be time-varying. Building upon the latter standpoint, we aim here to investigate the impact of speculators' trading activities on the time-varying commodity futures risk premium. In particular, we focus on speculators' *spread trade* positions, and study their asset pricing implications for the cross-section of commodity futures returns.

Commodity spread trades are intra-commodity investing strategies that involve simultaneously buying and selling the same amount of futures contracts with different maturities within a single commodity. Intra-commodity spread trading strategies include *calendar spread* (e.g., rolling activity (Mou, 2011) or speculative trades such as curve momentum (Paschke et al., 2020) and *butterfly spread* positions. They have gained in popularity among speculators in commodity futures markets due to their lower barriers/costs to entry (i.e., no short-selling constraint, lower margin requirement to obtain high leverage).[1] The financialization of the commodity markets from around 2005 has prompted the exponential growth of such strategies (Tang and Xiong, 2012; Singleton, 2014). Speculators take intra-commodity spread positions in order to obtain risk exposures to the change in the shape (slope or curvature, or both) of commodity futures term structures.[2] Hence, the extent to which speculators enter spread trade positions (*spreading pressure*) may reflect the information on the commodity futures term structure and futures returns.

We use data from the Commodity Futures Trading Commission (CFTC) on traders' weekly positions, and daily prices of futures contracts from Bloomberg for twenty-six commodities from 1992 to 2018. We find four main results for the relationship between spreading pressure and excess returns in commodity futures markets.

[1] In a recent paper, Robe and Roberts (2019) document substantial spread activity in the agricultural commodity futures market.

[2] For instance, the calendar spread entails the risk of both slope and curvature changes of futures curves; the butterfly spread is only related to risk of changes in curvature.

Because there was a structural break in the commodity market due to financialization and a surge in index investment, significant changes in futures risk premia have occurred since 2005 (Buyuksahin et al., 2008; Hamilton and Wu, 2014; Tang and Xiong, 2012; van Huellen, 2020). Therefore, we report our results separately: for our full sample, and for two subsamples (pre- and post-2005).

First, spreading pressure predicts futures excess returns negatively and significantly even after controlling for important determinants, including basis-momentum, hedging pressure, and changes in speculators' trading positions. Our Fama-MacBeth cross-sectional regression results show that weekly excess returns decrease by about 1.78 percentage points when smoothed spreading pressure increases by 1 percentage point.[3] Second, our spreading pressure long-short portfolio generates excess returns of as high as 22.52% (with a Sharpe ratio of 0.94) per annum, and it yields higher cumulative returns than other pricing portfolios including basis, momentum, and basis-momentum (Figure 3.6) since 2005.

Third, we show that spreading pressure is a priced factor (*spreading pressure factor*) in the cross-section of commodity futures returns, especially after 2005. The estimated price of risk on the spreading pressure factor is 20.95% per annum, and our single-factor model provides a better cross-sectional fit than the extant two- or three-factor models, which feature R^2 of as high as 66.81%. Interestingly, the pricing power of spreading pressure comes mainly from money managers, including CTAs and hedge funds. Lastly, spreading pressure reflects the expected slopes and curvatures of the commodity futures term structure. The spreading pressure factor is explained by Asian emerging market returns (Tang and Xiong, 2012; Henderson et al., 2015) and by innovations in real economic uncertainty (Bloom, 2009; Ludvigson et al., 2019). It is not captured by liquidity, volatility, inventory, or financial intermediary risk.

[3]We refer to the twelve-month average of spreading pressure as *smoothed* spreading pressure. We use a one-year time window to smooth out the effect of seasonality and the maturity of futures contracts on our measure. Kang et al. (2020) use a similar approach to compute their measure of hedging pressure.

We note several hints that our results may be linked to frictions that are introduced via commodity index investment. For example, our results are stronger in the post-2005 period, after commodity financialization, especially the short leg (high spreading pressure) of our trading strategy.[4] The spreading pressure predicts the shape of the futures curve, especially in certain states, i.e., positive slope and negative curvature (concave futures curve), when index pressure is likely to prevail (Van Huellen, 2020). Moreover, data from the disaggregated Commitment of Traders (DCOT) report suggest that pricing results come mainly from positions of managed money investors, although we cannot isolate the index positions in those reports. On the other hand, quarterly index investment reports from the CFTC (over a shorter sample, 2007Q4-2015Q3) indicate a positive relation between changes in spread and index investment positions. Finally, we find that the short (long) leg of our trading strategy predominantly includes index (non-index) commodities. However, a strategy that shorts only index commodities does not exhibit a similar performance.

Our results can be interpreted within the framework of models of commodity financialization (Basak and Pavlova, 2016; Brunetti and Reiffen, 2014; Sockin and Xiong, 2015; Goldstein and Yang, 2019). Models based on symmetric information and uninformed trading (e.g., Basak and Pavlova, 2016; Brunetti and Reiffen, 2014) imply that the entry of uninformed speculators (e.g., index traders) who do not trade based on economic fundamentals results in higher valuations (and lower expected returns) for index commodities. Models based on asymmetric information (Sockin and Xiong, 2015; Goldstein and Yang, 2019), on the other hand, highlight the dual role of financial traders who bring both information (via speculative trades) and noise (via hedge-based trades) to the market. They can potentially distort price signals for commodity users and producers (Brogaard et al., 2019). Goldstein and Yang (2019) also show that informational

[4] After mid-2004, (Buyuksahin et al., 2008) document structural changes in the trading of commodity futures across maturities and cointegration relation of commodity futures prices across maturities due to increased calendar spread positions.

friction is time-varying. Thus, in a market with few financial traders (e.g., during the early days of commodity financialization), a positive information effect dominates until the mass reaches a certain threshold.

Our cross-sectional strategy that invests in low spreading pressure commodities and shorts commodities with high spreading pressure delivers a high trading performance. The profitability of such a strategy stems from the fact that the long leg of the portfolio is immune to these informational frictions. It is driven primarily by fundamentals such as global economic growth expectations, and it is highly exposed to shocks in real economic uncertainty. The short leg is exposed to such informational frictions through financial investors, especially after the influx of index traders. The performance of this strategy is superior to alternative strategies suggested in the literature (e.g., momentum, basis-momentum), and only declines during the early days of commodity financialization when shorting index commodities was not profitable.

The extant literature on commodity futures factor pricing has proposed a number of risk factors. Szymanowska et al. (2014), Yang (2013) and Bakshi et al. (2019) introduce a carry factor based on a term structure signal called Basis. They find that low-basis commodity futures carry higher carry factor risk premiums than their high-basis counterparts. Gorton et al. (2013) and Bakshi et al. (2019) show that the risk premium on a momentum factor is significant, while Fernandez-Perez et al. (2018) find that commodity futures with a negative skewness have significantly higher returns than positive skewness ones. Boons and Prado (2019) introduce a so-called basis-momentum factor based on the slope and curvature of the futures term structure. Research has also explored other pricing factors, such as value (Asness et al., 2013), volatility (Bakshi et al., 2019), liquidity (Marshall et al., 2012), and inflation (Hong and Yogo, 2012).

The spreading pressure factor we propose here differs from the aforementioned studies in that it is based on the positions of market participants rather than on futures prices. Regarding traders' position-based risk factors in commodity markets, hedging

pressure has been extensively studied in the literature (Bessembinder, 1992; Basu and Miffre, 2013; Dewally et al., 2013). Commodity futures with high shorting demand from hedgers tend to have larger risk premiums on a hedging pressure factor than futures with lower shorting demand. Our paper is closely related to Boons and Prado (2019), in that both studies examine the pricing of a large cross-section of commodity futures with a parsimonious factor model, where the risk factor reflects the information on commodity futures curves.

This paper contributes to the aforementioned literature of commodity futures pricing in several key aspects. First, we document the predictability of spreading pressure on commodity futures excess returns. Second, we propose a novel pricing factor, and we describe the superiority of a parsimonious single-factor model over multifactor models. Third, we establish a link between speculators' spread positions and the commodity futures risk premium. We also contribute to the literature on the role of speculators and index investors in particular, and financial intermediation in general in the commodity futures markets. Finally, this paper is one of the first studies to explore the economic determinants and information contents of spreading pressure.

3.2 Data and Summary Statistics

3.2.1 Commodity Futures Returns

We obtain daily prices for individual commodity futures contracts from Bloomberg. Our sample period is October 6, 1992 through December 30, 2018. Our analysis focuses on twenty-six commodity futures contracts with different maturities covering five major sectors: 1) energy (heating oil, natural gas, RBOB/unleaded gasoline, and WTI crude oil), 2) grains (corn, oats, rough rice, soybean oil, soybean meal, soybeans, and wheat), 3) meats (feeder cattle, lean hogs, live cattle, and frozen pork belly),[5] 4) metals (high-

[5]Frozen pork belly futures were delisted on July 15, 2011.

grade copper, palladium, platinum, silver, and gold), and 5) soft (cocoa, coffee, cotton, lumber, orange juice, and sugar).

To match the weekly frequency of the CFTC's trader positions data, we calculate weekly (Tuesday to Tuesday) excess returns on fully collateralized futures positions (e.g., Gorton et al., 2013; Koijen et al., 2018; Bakshi et al., 2019; Boons and Prado, 2019)

$$R_{t+1}^{(n)} = \frac{F_{t+1}^{(n)}}{F_t^{(n)}} - 1, \quad n \geqslant 1 \tag{3.1}$$

where $F_t^{(n)}$ is the n-th nearby futures contract, i.e., the contract with the n-th shortest maturity, at the end of week t among all available contracts. Our return calculations mainly use the prices of front month contracts (i.e., first or second nearby contracts depending on calendar dates) in order to ensure sufficient liquidity.[6]

Table 3.1 shows the summary statistics for annualized excess returns of front month contracts of the twenty-six commodities for the full sample of 1,369 weeks (October 6, 1992-December 30, 2018), and the two subperiods of pre- and post-January 4, 2005 (639 and 730 weeks, respectively). Twenty-one (twenty) of the twenty-six commodities' front month contracts have Sharpe ratios lower than 0.25 in the full sample period (post-2005 period). This implies that investing in a single commodity futures contract may not have an attractive risk-return profile. Futures returns seem to be serially uncorrelated, as the magnitude of first-order autocorrelations is shown to be very low for most commodities. It is also notable that corn has the highest open interest before 2005, and WTI crude oil is the most liquid futures contract since 2005.

[6] A first nearby contract is defined as the shortest-maturity contract whose first notice day comes after the end of the week in order to avoid a case where the contract is required to take a physical delivery of underlying commodities (Bakshi et al., 2019). In such a case, the definition of front months would also depend on the calendar date on which the week ends. More specifically, for weeks that end prior to the seventh calendar day of the month, we would use a first nearby contract; for weeks that end on or after the seventh calendar day, we would use a second nearby contract (Kang et al., 2020).

3.2.2 Trader Positions

Commodity futures position data by different types of traders come from the Commodity Futures Trading Commission (CFTC). CFTC releases weekly COT reports that contain the aggregate long and short positions of three types of traders: commercial, non-commercial, and non-reportable. It also reports the spread trades positions for non-commercial investors. Following the standard in the literature, we view commercials as hedgers, non-commercials as speculators, and non-reportables as small speculators. The data capture traders' weekly positions from Tuesday to Tuesday, and they are published on Friday of the same week. The CFTC has published DCOT data since 2006, from which we can break down trader positions even further, splitting non-commercials into money managers and other reportables.[7]

Following the COT report, we capture the size of traders' positions and their trading behavior based on five measurements: 1) percentage of the total market held by the different trader types, 2) hedging pressure (HP), 3) spreading pressure (SP), 4) net trading (Q) by hedgers and speculators, and 5) the propensity to trade (PT) by speculators with long or short positions only, and speculators with spread positions only. We calculate each measure separately for each type (i.e., hedgers, speculators, and small speculators). For speculators, we distinguish their spreads positions further as either long- or short-only positions.

Next, we define the sector-level measure of market shares by trader type as the open interest-weighted average of percentage market shares at the commodity level. These are calculated as total positions (both long and short), divided by open interest,

[7]Money managers are traders who engage in managing and conducting organized futures trading on behalf of clients. The category includes commodity trading advisers (CTAs), commodity pool operators (CPOs), and unregistered funds identified by the CFTC. Other reportables are non-commercials other than money managers.

as follows:

$$percentage\, market\, held\, by\, trader\, i\, at\, t = \frac{Long_{i,t} + Short_{i,t}}{2 \times Open\, Interest_t} \tag{3.2}$$

Figure 3.1 reports the evolution of relative positions by futures trader type over time for each commodity sector (energy, metals, soft, grains, and meats). Several interesting patterns emerge. First, it is commonly observed across sectors that speculators' total positions (i.e., those with and without spread trades) began gradually increasing in early 2000. The increase in speculator positions coincides with the decrease in hedger positions in a certain sector (or, energy). Second, speculators' positions on spread trades are largest in the energy sector, exceeding even those of directional speculators. Third, speculator positions in the energy sector experienced exponential growth since 2005, the period coinciding with the era of financialization of the commodity markets.

Fourth, speculators' spread positions in the metals sector show an interesting pattern around the 2008/2009 crisis, increasing markedly before the crisis, and dropping significantly afterward. Fifth, contrary to the notion that traders opt for a spread position when a commodity market is highly uncertain (Boons and Prado, 2019), we do not find a significant increase in spread positions during the crisis for any sector. Lastly, we find no significant correlation in trade positions between spread and directional speculators.

We construct a series of trader position variables for each trader type (e.g., hedgers, spread speculators, directional speculators, etc.). We define our main variable, spreading pressure (SP) of commodity i, as speculators' spread positions divided by open interest:

$$SP_{i,t} = \frac{Spread_{speculators,i,t}}{Open\, Interest_{i,t}} \tag{3.3}$$

Next, we construct control variables that include hedging pressure, net trading, and trade propensity as follows. We use hedging pressure of commodity i to capture hedging

demand, defined as hedgers' net short positions divided by open interest:

$$HP_{i,t} = \frac{Short_{hedger,i,t} - Long_{hedger,i,t}}{Open\,Interest_{i,t}} \tag{3.4}$$

where net trading (Q) is defined as the change in traders' net long positions divided by open interest:

$$Q_{i,t} = \frac{NetLong_{i,t} - NetLong_{i,t-1}}{Open\,Interest_{t-1}} \tag{3.5}$$

A limitation of this measure is that speculators' net trading only reflects changes in trade positions for directional speculators (i.e., long-only or short-only), not for spread speculators, since their $NetLong$ is always zero. As in Kang et al. (2020), we also construct the measure of propensity to trade (PT), defined as the sum of absolute changes in long and short positions between $t-1$ and t, divided by total long and short positions at $t-1$:

$$PT_{i,t} = \frac{abs(Long_{i,t} - Long_{i,t-1}) + abs(Short_{i,t} - Short_{i,t-1})}{Long_{i,t-1} + Short_{i,t-1}} \tag{3.6}$$

Figure 3.2 shows the evolution of spreading pressure over time for six selected commodities: three high-SP commodities (natural gas, WTI crude oil, and lean hogs) and three low-SP ones (platinum, palladium, and oats). It also provides a further breakdown of speculator spread positions since 2006 into money managers and others. It appears to show a structural break around 2005 in level of spreading pressure, but only for high-SP commodities. Specifically, the mean of spreading pressure for natural gas, WTI crude oil, and lean hogs experienced a dramatic jump in value after 2005, but we do not observe the same trend for platinum, palladium, and oats. It is important to note, however, that all three commodities in the high-SP group are also constituents of popular commodity indexes (S&P GSCI Index and Dow Jones-UBS Commodity Index), while

their lower-SP counterparts are all non-index commodities.[8] These observations imply that speculators' spread positions may be related to the financialization of commodity markets, or, more accurately, to the presence of rapidly growing index investments in the markets since 2005 (Tang and Xiong, 2012; Singleton, 2014).

To look more closely at the behavior of spreading pressure within the calendar year, we plot the weekly average of spreading pressure for two commodities (palladium and WTI crude oil) in Figure 3.3 for the pre-and post-2005 periods. The figure clearly shows there is a maturity effect on the level of spreading pressure, especially post-2005. Pre-2005, we note that the spreading pressure for palladium only tended to reach the peak when the date got closer to maturity (the first notice day or last trading day, whichever comes first), before subsequently plummeting to its lowest level after maturity. Post-2005, however, this pattern is seen for WTI crude oil as well, and it becomes even stronger for palladium. This implies that spread trades mainly involve front month rather than longer-maturity contracts.

Table 3.2 reports the summary statistics of traders' position variables (spreading pressure, hedging pressure, net trading, and propensity to trade) across the twenty-six commodities. There are a number of important observations. For spreading pressure, the energy sector has the largest value at the commodity level, and the mean of spreading pressures has increased significantly since 2005 for both market levels (9.41% for the full sample, 6.06% for pre-2005, and 12.39% for post-2005) and commodity levels (e.g., 7.05% vs. 33.84% for natural gas, and 6.82% vs. 27.22% for WTI crude oil). Regarding hedging pressure, the average is positive for all commodities except natural gas, feeder cattle, and frozen pork belly, and metals (meats) has the highest (lowest) hedging pressure at the sector level. The means of absolute net trading changes for hedgers and speculators are 3.45% and 3.08%, respectively. As for propensity to trade, spread speculators exhibit

[8] According to CFTC index investment reports, there is a significant increase in managed money flows to platinum, along with an increase in index investment. Not surprisingly, this coincides with the diminishing role of platinum in the low-SP group (see Online Appendix, Figure 3.A-4).

a higher propensity to trade than directional speculators.

3.3 Spreading Pressure and Futures Excess Return

3.3.1 Trader Positions and Futures Excess Return

In this section, we investigate whether spreading pressure exhibits predictive power for futures excess returns by employing a cross-sectional regression across the twenty-six commodities. To gain a sense of the relationship, we first simply examine a cross-sectional fit between average returns and average spreading pressure for the full sample period (Figure 3.4) and the post-2005 period (Figure 3.5). To compare as precisely as possible, we also provide a cross-sectional fit for the other trader categories (hedgers, directional speculators, and small directional speculators).

The results show that excess returns are negatively related only with spreading pressure. The relation is positive for all other categories regardless of which sample we use. Compared with hedging pressure and speculating pressure, spreading pressure has the largest magnitude of slopes and exhibits relatively high explanatory power (R^2= 34.97%), especially since 2005. The positive relation between excess returns and hedging pressure is consistent with the normal backwardation theory, where hedgers hold a net short position, and an increase in short demand will discount futures prices in order to find counterparties. For the same reason, the theory suggests that speculators' net long positions is positively related to returns, because speculators are the counterparties of hedgers, which is confirmed in our results.

To test the return predictability of trade positions more formally, we next conduct a Fama-MacBeth cross-sectional regression by trader type, as follows:

$$R_{i,t+1} = b_0 + b_j Pressure_{j,t} + \epsilon_{i,t+1} \tag{3.7}$$

where $R_{i,t+1}$ is weekly excess returns on the front month contract of commodity i at week $t+1$, and $Pressure_{j,t}$ is trader position variables at week t by different trader categories j, as defined earlier (i.e., hedging pressure, spreading pressure, speculating pressure, and pressure from small speculators). Table 3.3 confirms that spreading pressure has significant predictive power over next week's futures returns; trade positions by the other three categories lack this predictive ability for the full sample period and for the two subsamples (pre-and post-2005).

3.3.2 Does Spreading Pressure Predict Excess Returns?

We construct spreading pressure portfolios weekly by sorting commodities based on spreading pressure, and calculating their post-ranking returns. To remove any seasonality and maturity effects, we use smoothed spreading pressure (i.e., past the fifty-two-week average) as a trading signal. Portfolios Low3 (High3) represent the portfolio of the three lowest (highest) spreading pressure commodities; portfolios Mid include the remaining twenty commodities. For comparison, we also construct portfolios based on basis-momentum as a benchmark, which has been shown to perform better than other trading signals, such as carry (basis) and momentum (Boons and Prado, 2019).[9]

Table 3.4 reports the summary statistics of spreading pressure portfolios and a long-short portfolio strategy. We observe that long-short spreading pressure portfolios yield large returns and high Sharpe ratios for the full sample and both subsamples, but they are largest for the post-2005 period (22.52% and 0.94 for excess returns and

[9]Basis-momentum denotes the difference between momentum signals from front-month and second-month futures strategies:

$$BM_t = \prod_{s=t-52}^{t} \left(1 + R^{(1)}_{long,s}\right) - \prod_{s=t-52}^{t} \left(1 + R^{(2)}_{long,s}\right)$$

The literature shows that Carry (C_t) and Momentum (M_t) are:

$$C_t = \frac{\ln F^2_t - \ln F^1_t}{T_2 - T_1}, \qquad M_t = \prod_{s=t-52}^{t} \left(1 + R^{(1)}_{long,s}\right)$$

Sharpe ratios, respectively). Compared with basis-momentum portfolios, the performance of spreading pressure long-short portfolios is superior in terms of both excess returns (22.52% vs. 18.66%) and Sharpe ratios (0.94 vs. 0.76) since 2005.[10]

Figure 3.6 shows cumulative excess returns of carry (basis), momentum, and basis-momentum portfolios, along with spreading pressure portfolios. We observe that the spreading pressure portfolio performs the second-best behind the basis-momentum portfolio in the full sample, but is the best alternative since 2005. We also notice that the performance of the spreading pressure portfolio is particularly weak in the early days (2001-2005) of commodity financialization. We will further explore the time-varying performance of this strategy in a later section.

To examine the predictability of spreading pressure more fully after controlling for other factors, we follow Kang et al. (2020) to conduct Fama-MacBeth cross-sectional predictive regressions as follows:

$$R_{i,t+k} = b_0 + b_{\overline{SP}}\overline{SP}_{i,t} + b_{BM}BM_{i,t} + b_Q^h Q_{i,t}^h + b_Q^s Q_{i,t}^s + \epsilon_{i,t+1} \tag{3.8}$$

where $\overline{SP}_{i,t}$ is the smoothed (fifty-two-week average) spreading pressure of commodity i at week t, $BM_{i,t}$ is basis-momentum, $Q_{i,t}^h$ is the change in hedgers' net positions, and $Q_{i,t}^s$ is the change in speculators' net positions. Basis-momentum is documented to predict commodity futures excess returns with stronger predictive power than more well-known trading signals such as carry or momentum (Boons and Prado, 2019). Also, the change in hedgers' (speculators') net positions is shown to predict excess returns positively (negatively) (Kang et al., 2020) .

[10]The results of long-short strategies are robust to the number of commodities used to construct the portfolios, and remain largely unchanged after accounting for sector-fixed effects. For example, the patterns in portfolio returns remain similar when we take into account for transaction costs (Online Appendix, Table 3.A-1), when we change the number of commodities in each leg of the long-short strategies from three to four (Online Appendix, Table 3.A-2), when we scale the spreading pressure by its fifty-two week standard deviation (Online Appendix, Table 3.A-3), or when we construct within-sector long-short portfolios (Online Appendix, Table 3.A-4). Spreading pressure portfolios can generate positive excess returns for all sectors except Metals, and especially high returns for Energy (30.4%).

Panel A in Table 3.5 shows that commodities with higher spreading pressure in week t tend to have significantly lower excess returns in week $t+1$ (coefficient = -1.78 and t-statistics = -3.00) for the full sample period (Model 1). The significance of the predictability of spreading pressure remains unchanged even after controlling for other well-known factors, i.e., $BM_{i,t}$, $Q^h_{i,t}$, and/or $Q^s_{i,t}$ (Models 5 to 8). Comparing the results for the two subsamples (pre-2005 in Panel B, and post-2005 in Panel C), we note that predictive power is stronger in later periods. In addition, spreading pressure exhibits the highest explanatory power on futures returns (R^2 = 6.8%) among the four predictors since 2005.[11]

3.3.3 Is Spreading Pressure a Priced Factor?

In this section, we investigate whether spreading pressure is a priced commodity factor by employing time series and cross-sectional tests. We construct a spreading pressure portfolio by going long Low3 and shorting High3 spreading pressure portfolios. In a similar vein, we construct other pricing factors, such as basis-momentum (Boons and Prado, 2019), and three factors from Bakshi et al. (2019), a carry, a momentum, and the equal-weighted average excess return on all commodities as a commodity market factor.

Before conducting the formal test, we first glance at the correlations among commodity pricing factors. Table 3.6, Panel A, shows that the magnitude of correlations between the spreading pressure factor and other well-known factors is not large (with correlation coefficients lower than 0.30). Table 3.6, Panel B, presents correlations between the spreading pressure factor and average market returns for five commodity sectors (energy, grain, meats, metals, and soft). The correlations are fairly low, suggesting that the spreading pressure factor has its own variation, and does not depend on a particular commodity sector.

[11] As a robustness test, we vary the number of weeks ahead to longer than one week in order to gauge whether spreading pressure can have long-term predictive power. Table 3.A-5 in the Online Appendix shows that spreading pressure can also predict excess returns significantly and negatively for two, three, and four weeks ahead.

Next, we employ a time series test by regressing our spreading pressure factor on other pricing factors to determine whether it generates a significant alpha (i.e., intercept). The idea is that, if the spreading pressure factor is not captured by existing factors, we should observe a significant time series alpha (Barillas and Shanken, 2017, 2018):

$$R_{SP} = \alpha + \sum_{i=1}^{K} \beta_i F_{i,t} + \epsilon_t \tag{3.9}$$

where K is the number of factors, and $F_{i,t}$ is factor i at time t.

Table 3.7 shows multivariate regressions of the spreading pressure factor on a set of commodity factors proposed by Boons and Prado (2019) and Bakshi et al. (2019). The intercepts of the time series regressions are highly significant, and their economic magnitudes are large for all pricing models, especially for the post-2005 period. Specifically, abnormal returns on the spreading pressure factor-mimicking portfolio are 19.83% (20.01%) using Boons and Prado (2019) (Bakshi et al. (2019)) as a benchmark model. The Newey-West t-statistics of abnormal returns are as high as 2.96 (3.21). The GRS test shows we can reject the null hypothesis that the abnormal returns of our spreading portfolios (Low3, Mid, and High3) are jointly equal to zero.[12] Note that the time series test results suggest that the spreading pressure factor is not captured by the extant commodity factor models, and can improve mean-variance efficiency when added to the benchmark models.

Next, we turn to a cross-sectional test to gauge whether the spreading pressure factor is priced into the cross-section of commodity futures returns. We also compare it with the extant commodity factor pricing models. As a portfolio-level test, we use test assets that are comprised of seventeen portfolios constructed by univariate-sorting commodity futures, with three each on carry, momentum, basis-momentum, and spreading

[12]Table 3.A-6 in the Online Appendix confirms that our spreading pressure portfolios cannot be explained by the alternative three-factor (Szymanowska et al., 2014) model, nearby returns of the basis long-short portfolio, the spreading returns of the high-basis portfolio, or the spreading returns of the low-basis portfolio.

pressure, and five on sector. We also conduct a model comparison for the six candidate models nested in:

$$R_{t,i} = \gamma_{t,0} + \lambda_{t,\overline{SP}}\beta_{t,\overline{SP}} + \lambda_{t,BM}\beta_{t,BM} + \lambda_{t,C}\beta_{t,C} + \lambda_{t,M}\beta_{t,M} + \lambda_{t,Avg}\beta_{t,Avg} + \epsilon_{t,i} \quad (3.10)$$

where λ is factor risk premia, and we estimate β_t as a fixed parameter using the entire sample.

The first model specification is $\lambda_{t,BM} = \lambda_{t,C} = \lambda_{t,M} = \lambda_{t,Avg} = 0$, which means spreading pressure is the only factor in this model. The second specification is $\lambda_{t,C} = \lambda_{t,M} = \lambda_{t,Avg} = 0$, i.e., a two-factor model with spreading pressure and basis-momentum. The third specification is $\lambda_{t,\overline{SP}} = \lambda_{t,C} = \lambda_{t,M} = 0$, which is a two-factor model with basis-momentum and average commodity market factor (Boons and Prado, 2019). The fourth specification is $\lambda_{t,\overline{SP}} = \lambda_{t,BM} = 0$, i.e., a three-factor model in Bakshi et al. (2019), with carry, momentum, and average commodity market factor. The fifth and sixth specifications are used to test whether spreading pressure remains priced in after accounting for both the Boons and Prado (2019) and Bakshi et al. (2019) models, which are with $\lambda_{t,C} = \lambda_{t,M} = \lambda_{t,Avg} = 0$ and $\lambda_{t,BM} = 0$, respectively.

Table 3.8 reports our cross-sectional asset pricing test with portfolio-level results, where we present the estimates of annualized risk premia on each pricing factor under different model specifications. The t-statistics are based on standard errors calculated as per Shanken (1992) and Kan et al. (2013).[13]

The estimation results in Model (1) show that risk premia on the spreading pressure factor are significant in the full sample and the post-2005 sample, but insignificant in the pre-2005 sample. Model (2) shows that spreading pressure is still a priced factor even after controlling for basis-momentum, while Model (3) has slightly better regression

[13]Shanken (1992) standard error corrects for the presence of errors in in the first-stage betas, and the Kan et al. (2013) standard error additionally corrects for conditional heteroskedasticity and model misspecification.

results (high R^2) for the pre-2005 period. Model (4) shows that the risk premia on the carry factor are significant in the post-2005 subsample, but the momentum factor's risk premia are significant pre-2005. In the post-2005 sample, Models (5) and (6) show that the spreading pressure factor remains significantly priced after adding it to each of the two benchmark models. Lastly, we find that a single-factor model, Model (1), provides a good cross-sectional fit, with R^2 of 66.81%.[14]

To summarize, both time series and cross-sectional tests suggest that the spreading pressure factor reflects a unique dimension of the risk in the commodity futures market. We find it is in fact priced into the cross-section of commodity futures returns, at both the portfolio and individual commodity levels (Lewellen et al., 2010). Our subsample tests confirm that the pricing effect of spreading pressure has strengthened since 2005, which is in line with the evidence of a structural break in commodity risk premia during the era of financialization of commodity markets (Hamilton and Wu, 2014; Tang and Xiong, 2012).

3.4 Unraveling Spreading Pressure

3.4.1 Commodity Futures Term Structure

A number of researchers have explored the slope and curvature of the futures term structure based on observable economic fundamentals. They show that its shape can depend on the behavior of different types of market participants. Karstanje et al. (2015) link the slope of futures curves to hedging pressure, housing (construction growth), and

[14]The cross-sectional test results are robust to our choice of test assets. In contrast to Table 3.8, whose results are based on nearby returns of seventeen different portfolios, Table 3.A-7 in the Online Appendix gives results with the number of test assets doubling up to thirty-four by using spreading returns and nearby returns. The thirty-four commodity-sorted portfolios include these returns for seventeen constructed portfolios, i.e., twelve sorted on spreading pressure, basis momentum, and basis-momentum (High3, Mid, and Low3 portfolios sorted on each signal), and five sector portfolios (Energy, Grains, Meats, Metals, and Softs). The spreading return is defined as the difference between the equal-weighted average return of the first- and second-nearby contracts. Online Appendix Table 3.A-8 reports results of the cross-sectional asset pricing test using the twenty-six individual (as opposed to portfolio-level) commodities as test assets.

inventories, and find that curvature is positively related to interest rates and business inventories (new order growth), and negatively related to industrial production. Focusing on the oil futures market, Heidorn et al. (2015) find that only fundamental investors (producers, merchants, processors, and users) influence the level of the futures term structure, and financial traders (swap dealers and money managers) affect the slope and curvature.

More recently, Van Huellen (2020) relates the shape of term structures to index investment, and shows that index pressure can drive futures curves to become upward-sloping and concave, while hedging pressure induces downward-sloping and convex curves. However, when index traders' long positions exceed hedgers' short positions, the term structure of commodity futures can exhibit wave-like shapes. In a similar vein, we explore in this section the relationship between spreading pressure and commodity futures curves.

Following the literature, we define the slope and curvature of commodity futures curves as basis and the difference between basis, as follows:

$$slope_t = \frac{\ln F_t^3 - \ln F_t^1}{T_3 - T_1} \tag{3.11}$$

$$curvature_t = \frac{\ln F_t^3 - \ln F_t^2}{T_3 - T_2} - \frac{\ln F_t^2 - \ln F_t^1}{T_2 - T_1} \tag{3.12}$$

where F_t^n is the price of the n-th nearby contract with time-to-maturity T_n at week t. Positive (negative) slopes denote the futures curve is upward (downward), and positive (negative) curvatures indicate a convex (concave) futures curve.

Speculators tend to enter spread positions to bet on the change in futures term structure. For example, calendar spread is a bet on the slope, while butterfly spread is more of a bet on the curvature. As such, it is conceivable that spreading pressure contains information such as speculators' expectations about relative changes in futures prices for contracts of differing maturities. Likewise, hedging pressure reflects hedgers'

demands for price insurance. Their high demands on short positions may limit speculators' construction of spread positions.

We investigate whether spreading pressure contains information about traders' expectations about the shape of the commodity futures curve. To this end, we conduct a predictive pooled regression of the one-week-ahead slope and curvature of the futures term structure on current spreading pressure with time and commodity fixed effects:

$$\{Slope_{t+1}, Curvature_{t+1}\} = \alpha_{t+1} + \beta_{SP} SP_t + \beta_{HP} HP_t + \varepsilon_{i,t+1}. \tag{3.13}$$

As control variables, we use hedging pressure and time to the earliest maturity date, which are also related to the shape of the commodity futures term structure. In addition, our analysis is based on data from four states with different futures curve shapes.

Table 3.9, reports the regression results after controlling for time fixed effects and commodity fixed effects for the post-2005 sample.[15] We first note that the most likely state in the data is an upward-sloping concave curve (48.15% of the time). The last row of the table shows that the spreading pressure predicts a steeper curve, regardless of the state. The only state for which it cannot significantly predict the curve's slope is when the futures curve is downward and convex (or when hedging pressure dominates). On the other hand, the spreading pressure can only significantly predict the curvature of the term structure when the futures curve is concave (when index pressure prevails, in line with evidence in Van Huellen (2020)).

3.4.2 Spreading Pressure by Trader Category

Our previous empirical tests are all based on weekly COT data from the CFTC that begin from the earliest available date, October 6, 1992. The CFTC also publishes the DCOT report (disaggregated COT), with more detailed trader categories beginning from

[15] In Online Appendix Table 3.A-9, we repeat the analysis in the pre-2005 sample.

June 13, 2006. Although the DCOT sample period is relatively short, we can still obtain further insights into spreading pressure by analyzing the spread positions held by more detailed trader types.

DCOT data break down trader positions into two subcategories: 1) producers/merchants/ processors/users, and 2) swap dealers for commercials, as well as two additional subcategories of 1) money managers and 2) other reportables for non-commercials. The non-reportables from the DCOT report remain the same as those in the COT report, which contains data on spread positions held by swap dealers, money managers, and other reportables. The spread positions held by commercials in the COT report are equal to the sum of those held by money managers and other reportables. So we construct an alternative proxy for the spreading pressure factor by using DCOT data, and investigating the determinants of commodity futures risk premia on spreading pressure from total speculators. As an intermediary in the commodity futures market defined by the CFTC, swap dealers' spreading pressure is of interest to us. We aim to analyze whether information carried by swap dealers' spreading pressure differs from that of non-commercials.

Similarly to the construction of our original spreading pressure factor, we construct a spreading pressure factor from the managed money category (other reportables or swap dealers) by buying three commodities with the lowest spreading pressure and shorting three commodities with the highest spreading pressure.[16] We then conduct cross-sectional tests for six asset pricing factor models, nested in:

$$\begin{aligned} R_{t,i} =& \gamma_{t,0} + \lambda_{t,\overline{SP}}\beta_{t,\overline{SP}} + \lambda_{\overline{SP}}^{ManagedMoney}\beta_{t,\overline{SP}\_ManagedMoney} \\ &+ \lambda_{\overline{SP}}^{OtherReportable}\beta_{t,\overline{SP}\_OtherReportable} + \lambda_{\overline{SP}}^{SwapDealer}\beta_{t,\overline{SP}\_SwapDealers} + \epsilon_{t,i} \end{aligned} \tag{3.14}$$

The specifications of Models (1) to (4) are single-factor models that use spreading pres-

[16]Detailed results of long-short strategies on spreading pressure by trader category are reported in Online Appendix Table 3.A-10.

sure from the overall commercial, managed money, other reportables, or swap dealer categories as pricing factors, respectively. Model (5) is the two-factor model with spreading pressure from the managed money and other reportables categories. We include Model (5) to investigate which non-commercial traders' activities contribute most heavily to the risk premia of the spreading pressure from overall non-commercials. The Model (6) two-factor model, with spreading pressure from overall speculators and swap dealers, tests whether spreading pressure from intermediaries carries different types of information with respect to speculators' spreading pressure.

Table 3.10 shows that spreading pressure from overall non-commercials, managed money, other reportables, and swap dealers is all priced by using a single-factor model (Models (1)-(4)). The single-factor model by using spreading pressure from managed money exhibits the highest R^2, 62.36%, which is not significantly different than that using overall spreading pressure (Model (1)). Model (2) with spreading pressure from other reportables has the lowest R^2. Model (5) shows that the risk premia on spreading pressure from other reportables is insignificant after adding spreading pressure from money managers. This suggests that the risk premia of spreading pressure are mainly caused by spreading pressure from managed money.

Kang et al. (2020) also document that money managers' positions tend to be more speculative. So the risk premia on spreading pressure come mainly from spread position movements with a speculative purpose. However, we cannot determine whether this is informed speculation or uninformed (liquidity) trading by commodity index investors. We will explore this point in more detail in the next section. Model (6) shows that the spreading pressure from swap dealers does not carry any additional useful information for commodity futures excess returns beyond that of non-commercials.

3.4.3 Spreading Pressure Factor over Time

Prior literature documents structural changes in the commodity futures market due to commodity financialization and an influx of index traders around 2004-2005 (e.g., Buyuksahin et al., 2008; Hamilton and Wu, 2014), speculative trades leading to the oil price boom and bust between 2003 and 2008 (Kilian and Murphy, 2014), the positive informational effect of financial traders in the early days of commodity financialization (Goldstein and Yang, 2019), and the rise of electronic trading platforms for commodity futures markets in the last quarter of 2006 (Raman et al., 2017). We first test how these events affect the spreading pressure (SP) factor return, and the returns of the long (low spreading pressure) and short (high spreading pressure) legs of the SP portfolio. In particular, we run the regression of spreading pressure (and its long and short legs) on different time dummy variables:

$$R_{i,t} = \alpha + \beta_j I_j + \gamma_i R_{i,t-1} + \varepsilon_t \tag{3.15}$$

where $R_{i,t}$ includes returns of spreading pressure ($R_{i,t}$), returns of the spreading pressure long leg ($R_{Long,t}$), and returns of the spreading pressure short leg ($R_{Short,t}$). The time dummy used in Model (1) is $I_{t\geq 2005}$, which equals 1 when the time is post-2005. Similarly, the time dummy variables used in Models (2) and (3) are $I_{2001\leq t\leq 2005}$ and $I_{2003\leq t\leq 2008}$ respectively. In Model (4), we use two time dummies, $I_{t\geq 2005}$ and $I_{2006Sep\leq t\leq 2006Dec}$. We include the lag of return $R_{i,t-1}$ as a control variable.

Table 3.11 reveals some key observations about the time series properties of spreading pressure portfolio returns. While the SP factor return is not significantly higher during the post-2005 period, the superior performance of such a strategy in the recent sample comes from the short leg of the portfolio. In other words, it is significantly more profitable to short high spreading pressure commodities in the post-2005 period. This observation confirms the importance of financialization plays to the SP portfolio

returns.

Interestingly, the SP factor returns dropped significantly in the earlier days (2001-2005) due to positive (negative) returns for holding (shorting) high spreading pressure commodities. Returns to the long leg (low spreading pressure) of the portfolio are not affected by either time dummy. We can rationalize this evidence with the Goldstein and Yang (2019) model, which predicts a positive informational effect, that is, signalling via speculation-based trades dominates the noise generated via hedge-based trades. However, this effect only prevails in the short leg of the SP portfolio, since the long leg is immune to the frictions caused by commodity financialization.[17] In fact, an investor who put money into the SP portfolio in 1993 would have earned more by exiting the commodity markets (and, say, keeping the money in T-bills) during the early days of financialization (2001-2005), and then returning in 2005. Reinvesting in the SP portfolio at that time would have earned the highest Sharpe ratio (0.90) over the entire sample period.

The third specification in Table 3.11 shows that the so-called "bubble view," or "Masters Hypothesis," is not behind the SP portfolio's profitability (Masters, 2008; Cheng and Xiong, 2014). In other words, the speculative activity in the commodity futures market that led to the oil price boom and bust (2003 and 2008) does not explain the returns to the SP factor, or to either legs of the portfolio. Finally, Raman et al. (2017) argue that an important dimension of commodity financialization is the rise of electronic futures markets in the last quarter of 2006. When we include an electronification dummy along with the 2005 dummy in the final specification, we see that the SP factor return is significantly larger in this period due to the lower returns in the short leg of the portfolio.

[17] In Online Appendix Figure 3.A-1, we show that the information inefficiency of the short leg of the SP portfolio increased substantially post-2005. We observe no such increase in the long leg of the SP portfolio.

3.4.4 Spreading Pressure Factor and Asset Returns

Another important prediction of the commodity financialization models is the increased correlation of commodity returns with other asset classes, especially equity markets (e.g., Cheng and Xiong, 2014; Basak and Pavlova, 2016). We next test for a correlation between SP factors, including both legs of the portfolio with other asset classes. We focus on U.S. market returns (S&P 500), MSCI Emerging Markets Asia index returns, as well as U.S. Dollar Index Futures Contracts returns and JP Morgan Treasury Bond Index returns. Following the literature (Tang and Xiong, 2012; Henderson et al., 2015), we also control for the growth rate of the Baltic Dry Index, the change in the ten-year break-even inflation rate, and the lagged return variables. In particular, we regress the SP factor (as well as its long and short legs separately) on asset returns and control variables:

$$R_{i,t} = \alpha + \beta_k R^a_{k,t} + \gamma_j C_{j,t} + \varepsilon_t \tag{3.16}$$

In Table 3.12, we note that the only variable that explains the spreading pressure factor (and both of its legs) is MSCI Emerging Markets Asia index returns. They exhibit a stronger effect on the long leg of the SP portfolio, suggesting that economic fundamentals, such as global economic growth expectations, particularly in Asia, play an important role in explaining SP portfolio returns. Both S&P 500 and the USD index returns correlate with individual components of the SP portfolio, but the effect cancels itself out in the long-short strategy without an overall effect on the SP factor.

3.4.5 Spreading Pressure Factor and Economic Uncertainty

There is a solid literature on the impact of uncertainty shocks on economic activity and business cycles (Bloom, 2009; Ludvigson et al., 2019), and growing interest in the implications for commodity markets (Watugala, 2019). Cheng et al. (2015) investigate how changes in the CBOE Volatility Index (VIX), an implied volatility measure based on

S&P 500 index options, affected the trading activity of commodity market participants around the global financial crisis. Ludvigson et al. (2019) highlight the importance of distinguishing financial or macroeconomic uncertainty from real economic uncertainty. The latter is related to shocks to production, and constructed with seventy-three real activity variables. Negative shocks to production increase real economic uncertainty, which indicates a bad economic state. Arguably, this is a better measure of uncertainty for commodity markets.

In this section, we aim to examine whether commodities in the long and short legs, as well as the spreading pressure factor, are sensitive to uncertainty shocks.[18] In order to test the exposure to uncertainty shocks, we regress the SP factor (and its long and short legs) on changes in different uncertainty measures ($\Delta Uncertainty_t$). We use the VIX, macroeconomic, financial, and real economic uncertainty (Ludvigson, Ma, and Ng, 2019), and control the past returns:

$$R_{i,t} = \alpha + \beta_{k,Uncertainty} \Delta Uncertainty_{k,t} + \gamma_j C_{j,t} + \varepsilon_t \tag{3.17}$$

Table 3.13 shows that both the VIX and financial uncertainty shocks reduce the returns of both legs of the strategy. Hence, there is no effect on the spreading pressure factor, as it is only significantly and negatively related to changes in real economic uncertainty. Specifically, the return from the long leg with low spreading pressure commodities is significantly exposed to real economic uncertainty shocks (coefficient = -19.34 and t-statistics = -3.28). But the short leg (high spreading pressure commodities) return is immune to such shocks. This could also be considered evidence for market segmentation in the commodity futures market, where the return dynamics of each leg of the strategy are driven by different trading motives (Goldstein et al., 2014). The long leg is more sensitive to fundamental and real economic uncertainty shocks that are relevant for

[18] We collect these data from Sydney C. Ludvigson's website.

hedgers, while the short leg suffers from the informational frictions from commodity financialization.

Next, to conduct a commodity-level analysis, we also regress the excess return of each commodity i on changes in real economic uncertainty. We then sort each commodity according to its turnover in the long and short legs, respectively. Figure 3.7 shows that commodities in the long (short) leg of the SP portfolio have strong (weak) exposure to changes in real economic uncertainty. These appear to be related to their portfolio turnover. However, we note that there are only a few commodities in the investment opportunity set of the long (i.e., low spreading pressure) leg of the strategy. We also observe that most commodities in the long portfolio are not part of a major index such as the S&P GSCI Index or the Bloomberg Commodity Index, DJ-UBSCI (at least for most of the sample), while we only short index commodities. This suggests at least some link between spread positions and commodity index investment. We confirm this conjecture in Table 3.14, where we collect data from CFTC quarterly index investment reports (over a shorter period, 2007Q4-2015Q3). These data indicate a positive relation between changes in spread positions and index investment positions, which is driven mainly by the spread positions of managed money investors.

Our cross-sectional strategy investing in some non-index commodities (low spreading pressure) and shorting some index commodities (high spreading pressure) delivers positive returns and high Sharpe ratios in the recent sample. However, note that our spreading pressure strategy is not a mere manifestation of index effects. Cumulative excess returns generated by the SP portfolio are higher than those obtained by simply going long all non-index commodities and short all their index counterparts (Figure 3.A-2).

3.4.6 Something Else in Disguise?

In the previous section, we show how commodities in the long and short legs of the spreading pressure strategy differ in terms of index participation and exposure to economic fundamentals via frictions introduced through financial investors. But are they also different in terms of exposure to risk factors such as volatility, liquidity, inventory, or financial intermediary risk? For example, we may expect index commodities to be more liquid thanks to liquidity provisions by index traders (Brunetti and Reiffen, 2014; Tang and Xiong, 2012). That relation is actually more complex because of the dual roles of financial investors (Cheng and Xiong, 2014). Or index participation could potentially increase commodity volatility (Tang and Xiong, 2012; Basak and Pavlova, 2016).[19] One could argue that the priced spreading pressure factor compensates for other commodity market risks such as inventory (Gorton et al., 2013) or financial intermediary risk (He et al., 2017).

To test the role of these alternative risk channels, we repeat our cross-sectional asset pricing test in Table 3.15 by constructing volatility, liquidity, inventory, and financial intermediary risk factors. Volatility factors are the innovations in aggregate and average commodity market variances ($\Delta var_{mkt,t}$ and $\Delta var_{avg,t}$), and the liquidity measure is innovations in the aggregate Amihud measure ($\Delta liquidity_{AMI}$). We construct aggregate commodity market variance ($var_{mkt,t}$) as the sum of daily squared returns of equal-weighted commodity portfolio in week t. Average commodity market variance ($var_{avg,t}$) is the equally-weighted average of the sum of the daily squared return of all commodities in week t. We compute commodity i's Amihud measure as the annual average of daily $\frac{|R_{n,d}|}{Vol_{n,d}}$ by using dollar volume $Vol_{n,d}$ for both front- and second-month contracts ($n = 1, 2$) at day d. The aggregate Amihud measure is the mean of the median of front- and second-month Amihud illiquidity over all commodities (Boons and Prado,

[19] Figure 3.A-3 shows no significant difference in volatility. The short leg of the spreading pressure portfolio appears slightly more volatile than the long leg. In contrast, we observe a great deal of difference in liquidity between the two portfolio legs, i.e., the long leg is much more illiquid than the short leg.

2019).

Following Gorton et al. (2013), we collect inventory data from the National Agricultural Statistics Service of the U.S. Department of Agriculture (NASS-USDA), the Energy Information Administration (EIA), etc. We then calculate the normalized inventory level for each commodity at time t as the ratio of the inventory level at time t to its past twelve-month moving average from $t-1$ to $t-12$. We construct the inventory risk factor as the return of the long-short portfolio constructed by going long three commodities with the lowest normalized inventory levels, and short three commodities with the highest normalized inventory levels. Following He et al. (2017), we also construct the intermediary capital risk factor on a weekly basis, computed as the AR(1) innovations to the intermediary capital ratio (i.e., shocks to the equity capital ratio of the primary dealer counterparties of the New York Federal Reserve), scaled by the lagged intermediary capital ratio.[20]

The results of accounting for the alternative risk factors are in Table 3.15. It shows that, while volatility and liquidity factors are priced in a two-factor model with a market average factor, this is not the case for inventory or financial intermediary risk factors. More importantly, none of these factors survive when we augment the model with our SP factor. These results suggest that the signal extracted from spread positions is not driven solely by volatility, liquidity, inventory, or intermediary risk factors.

3.5 Conclusion

In this paper, we find that speculators' intra-commodity spread trades carry important information about commodity futures risk premiums, especially during the era of financialization of the commodity markets. In contrast, speculators' directional betting via either long- or short-only trades do not offer comparable information content. Spec-

[20]These data come from Zhiguo He's website.

ulators' spreading pressure, defined as spread trade positions scaled by open interest, negatively predicts commodity futures returns. Moreover, a long-short portfolio based on spreading pressure is priced in the cross-section of commodity futures returns, while a single-factor model with our spreading pressure factor exhibits a better fit than the extant multifactor models. The estimated price of risk on the spreading pressure factor is 20.95% per annum, and it generates R^2 as high as 66.81%.

Our spreading pressure factor is constructed by purchasing commodities with low spreading pressure, typically non-index commodities, and shorting those with high spreading pressure (index commodities). The profitability of the long leg of this strategy stems from the fact that commodities in the long portfolio do not suffer from frictions introduced by financial traders, e.g., noise generated by hedge-based index traders. Their returns are driven by economic fundamentals such as growth in emerging (Asia) markets, and reflect a compensation for exposure to real economic uncertainty shocks. Shorting commodities with high spreading pressure is profitable precisely because they suffer from the negative effects of commodity financialization, except for during earlier years, when speculative trades brought commodity futures prices closer to fundamentals. To counteract these effects, we would recommend a more detailed reporting of spread positions across a larger cross-section of commodity futures. This key source of risk in the modern commodity futures market is ultimately too big to be dismissed.

Table 3.1: **Summary Statistics of Commodity Futures Returns**

This table presents the summary statistics of commodity futures returns for which we report annualized mean (Mean), standard deviation (SD), Sharpe ratios (Sharpe) and first-order autocorrelation (AR(1)) of futures front-month returns, as well as average open interest (OI) for each of the twenty-six commodities used in our sample. The first part of the columns shows the statistics for the full sample (October 6, 1992 through December 26, 2018); the second part is for the pre-2005 period (October 6, 1992 through January 4, 2005); and the third part is the post-2005 period (January 4, 2005 through December 26, 2018). The front-month excess return of a commodity in month $t+1$ is defined as $R^{(1)}_{long,t+1} = \frac{F^{(1)}_{t+1}}{F^{(1)}_{t}} - 1$, where $F^{(1)}_t$ is the price of the front-month futures contract at time t.

Sector	Commodity	Full Sample					Pre-2005					Post-2005				
		Mean	SD	Sharpe	AR(1)	OI	Mean	SD	Sharpe	AR(1)	OI	Mean	SD	Sharpe	AR(1)	OI
Energy	Heating Oil	5.71	30.84	0.19	0.01	230,497	11.94	30.82	0.39	-0.03	148,299	0.26	30.86	0.01	0.05	302,336
	Natural Gas	-11.47	45.16	-0.25	0.01	654,085	7.11	48.76	0.15	-0.01	266,957	-27.74	41.67	-0.67	0.04	992,425
	WTI Crude Oil	5.46	32.81	0.17	-0.03	1,038,331	18.11	31.62	0.57	-0.05	465,567	-5.62	33.76	-0.17	-0.01	1,538,911
	Unleaded/RBOB Gasoline	11.42	32.66	0.35	0.00	193,703	19.21	31.06	0.62	-0.04	98,089	4.60	33.99	0.14	0.02	277,267
Grains	Corn	-4.56	25.73	-0.18	-0.02	1,110,982	-8.19	21.05	-0.39	0.01	942,732	-1.39	29.23	-0.05	-0.04	1,258,258
	Oats	2.41	31.15	0.08	-0.03	21,709	0.73	27.99	0.03	-0.03	33,917	3.88	33.69	0.12	-0.03	11,008
	Rough Rice	-7.36	24.94	-0.30	0.05	9,183	-7.83	27.09	-0.29	0.02	5,499	-6.95	22.91	-0.3	0.08	12,403
	Soybean Oil	-0.92	22.86	-0.04	0.00	229,604	-0.97	21.57	-0.04	0.02	120,132	-0.87	23.94	-0.04	-0.01	325,430
	Soybean Meal	11.64	25.35	0.46	-0.02	196,443	8.43	23.1	0.36	-0.01	115,598	14.46	27.18	0.53	-0.03	267,210
	Soybeans	5.53	22.36	0.25	0.00	507,836	3.80	20.49	0.19	0.01	440,631	7.05	23.9	0.29	-0.01	566,663
	Wheat	-6.54	28.16	-0.23	-0.01	323,737	-7.19	23.03	-0.31	0.00	226,253	-5.98	31.99	-0.19	-0.02	409,068
Meats	Feeder Cattle	2.80	14.94	0.19	-0.04	27,334	3.63	13.58	0.27	-0.08	16,003	2.08	16.05	0.13	-0.02	37,252
	Lean Hogs	-1.94	25.38	-0.08	0.05	129,574	0.67	26.21	0.03	0.03	40,465	-4.22	24.64	-0.17	0.06	207,574
	Live Cattle	2.19	15.47	0.14	-0.07	197,569	4.50	15.79	0.29	-0.07	97,510	0.16	15.19	0.01	-0.06	285,155
	Frozen Pork Belly	10.76	35.61	0.30	0.09	5,196	16.02	37.04	0.43	0.09	5,727	-8.12	29.88	-0.27	0.08	2,187
Metal	High Grade Copper	6.90	24.03	0.29	0.05	111,946	4.80	21.50	0.22	-0.01	66,945	8.74	26.06	0.34	0.09	151,336
	Palladium	14.60	32.92	0.44	0.02	15,723	12.13	34.75	0.35	0.05	5,186	16.76	31.24	0.54	-0.02	23,879
	Platinum	6.12	21.38	0.29	-0.02	30,129	11.76	19.04	0.62	-0.03	14,120	1.18	23.22	0.05	-0.01	44,141
	Silver	6.41	28.20	0.23	0.00	120,204	3.35	23.24	0.14	0.03	92,569	9.10	31.92	0.28	-0.02	144,393
	Gold	3.58	16.04	0.22	0.01	312,738	-0.77	13.57	-0.06	0.02	177,685	7.39	17.92	0.41	0.01	430,956
Soft	Cocoa	0.81	28.68	0.03	0.01	138,438	-1.32	30.53	-0.04	-0.01	89,839	2.66	26.97	0.10	0.03	180,913
	Coffee	0.53	36.51	0.01	-0.02	106,964	7.83	41.97	0.19	-0.02	50,077	-5.87	30.94	-0.19	-0.02	156,681
	Cotton	-1.61	25.80	-0.06	0.02	131,981	-4.72	23.97	-0.2	0.02	66,645	1.11	27.32	0.04	0.02	189,083
	Lumber	-4.26	31.90	-0.13	0.07	5,311	2.39	33.11	0.07	0.14	3,281	-10.09	30.81	-0.33	0.00	7,071
	Orange Juice	2.55	32.38	0.08	0.00	24,551	-6.51	28.71	-0.23	0.02	26,310	10.48	35.27	0.30	-0.01	23,014
	Sugar	2.86	30.63	0.09	0.00	466,244	8.86	28.96	0.31	0.03	168,008	-2.40	32.03	-0.07	-0.03	726,894
	Average	2.45	27.77	0.10	0.00	243,847	4.14	26.87	0.14	0.00	145,540	0.41	28.18	0.03	0.01	329,673

Table 3.2: **Summary Statistics of Commodity Futures Trader Positions**

This table presents the summary statistics of traders' positions variables for each of the twenty-six commodities, which are calculated using data obtained from the CFTC Commitment of Traders (COT) report. *Hedging Pressure* is defined as $HP_t = \frac{Short_{hedger,t} - Long_{hedger,t}}{Open\ Interest_t}$, and *P(HP¿0)* is the probability of short hedging. *Spreading Pressure* is defined as $SP_t = \frac{Spread_{speculators,t}}{Open\ Interest_t}$, *Net trading* as $Q_{i,t} = \frac{NetLong_{i,t} - NetLong_{i,t-1}}{Open\ Interest_{t-1}}$, where $NetLong_{i,t}$ is the net long position of trader i in month t, and propensity to trade (PT) of traders i in month t as $PT_{i,t} = \frac{abs(Long_{i,t} - Long_{i,t-1}) + abs(Short_{i,t} - Short_{i,t-1})}{Long_{i,t-1} + Short_{i,t-1}}$. The first part of the columns shows the statistics for the full sample (October 6, 1992 through December 26, 2018); the second part for the pre-2005 period (October 6, 1992 through January 4, 2005); and the third part for the post-2005 period (January 4, 2005 through December 26, 2018).

Commodity	Spreading Pressure %									Hedging Pressure (HP) %			|Net Trading| %		Average PT %	
	Full Sample			Pre-2005			Post-2005									
	Mean	SD	AR(1)	Mean	SD	AR(1)	Mean	SD	AR(1)	Mean	SD	P(HP>0)	Hedger	Specs	Specs (no spread)	Specs (spread)
Heating Oil	10.11	5.52	0.98	5.28	2.27	0.91	14.33	3.80	0.94	9.15	8.75	83.93	2.47	1.79	13.96	12.09
Natural Gas	21.35	14.12	1.00	7.05	5.52	0.98	33.84	3.44	0.94	-0.45	11.37	47.92	1.61	1.38	10.88	8.48
WTI Crude Oil	17.71	11.29	1.00	6.82	3.07	0.97	27.22	6.03	0.98	6.91	10.07	75.31	1.74	1.41	9.79	6.79
Unleaded/RBOB Gasoline	8.47	5.34	0.98	4.61	1.85	0.84	11.84	5.11	0.97	15.95	11.26	88.39	2.91	2.22	13.40	16.13
Corn	10.17	4.61	0.98	6.35	2.71	0.97	13.52	3.08	0.95	2.09	13.03	57.05	2.36	2.21	8.19	8.44
Oats	3.47	2.96	0.88	4.11	3.14	0.88	2.90	2.67	0.86	31.28	18.04	93.86	4.07	2.99	13.24	64.44
Rough Rice	6.81	3.84	0.84	6.81	3.42	0.82	6.81	4.17	0.85	8.09	23.44	61.58	3.84	2.92	13.46	31.13
Soybean Oil	14.46	4.89	0.95	12.28	4.89	0.96	16.38	4.01	0.93	12.74	16.98	73.12	3.92	2.98	11.75	9.81
Soybean Meal	10.90	3.86	0.95	9.10	3.84	0.94	12.48	3.12	0.93	19.02	14.59	86.27	3.49	2.71	12.07	11.15
Soybeans	12.23	3.68	0.96	9.94	3.20	0.94	14.23	2.80	0.92	9.65	16.65	70.05	2.78	2.59	9.19	8.70
Wheat	12.57	5.75	0.97	7.80	3.19	0.92	16.74	3.97	0.94	0.77	14.79	45.87	3.06	2.69	7.99	11.23
Feeder Cattle	10.16	5.08	0.94	6.30	3.00	0.86	13.55	4.00	0.90	-7.65	10.70	24.62	2.11	3.03	9.43	18.87
Lean Hogs	14.20	5.77	0.96	9.51	3.79	0.89	18.30	3.70	0.92	1.55	12.94	57.34	2.48	2.69	9.10	12.43
Live Cattle	11.83	4.70	0.97	8.30	3.27	0.94	14.92	3.40	0.94	5.85	10.92	66.91	1.78	2.16	7.40	10.09
Frozen Pork Belly	6.44	4.53	0.78	6.17	4.36	0.81	8.00	5.13	0.66	-1.87	16.22	45.90	3.70	5.89	17.16	71.57
High Grade Copper	7.63	5.54	0.97	2.62	2.05	0.92	12.01	3.56	0.90	7.13	20.50	61.36	3.97	3.21	11.11	32.46
Palladium	2.00	2.24	0.83	1.57	2.52	0.85	2.33	1.93	0.81	40.29	29.92	82.40	4.74	3.87	9.92	77.86
Platinum	1.54	1.70	0.84	1.28	1.59	0.77	1.77	1.76	0.87	48.36	22.78	95.40	5.98	5.21	10.92	107.62
Silver	11.10	6.10	0.97	7.04	4.09	0.96	14.67	5.28	0.95	38.63	17.03	99.56	3.68	3.41	8.54	10.80
Gold	10.13	4.94	0.97	8.21	2.37	0.92	11.82	5.90	0.97	23.89	26.70	79.33	4.96	4.08	10.66	9.26
Cocoa	7.42	5.51	0.98	3.75	3.53	0.97	10.64	4.89	0.96	13.26	16.39	76.41	2.77	2.42	9.49	21.63
Coffee	10.07	5.04	0.97	6.10	2.79	0.92	13.54	3.86	0.94	11.87	16.44	68.74	3.69	3.34	10.72	14.06
Cotton	6.38	2.67	0.92	4.73	1.83	0.86	7.81	2.45	0.90	9.65	22.54	66.18	4.43	3.79	11.11	14.16
Lumber	6.11	4.35	0.87	3.61	2.52	0.69	8.27	4.45	0.84	9.54	19.95	64.79	4.49	4.42	12.85	43.34
Orange Juice	4.94	3.13	0.92	6.04	2.82	0.87	3.98	3.08	0.93	22.92	23.55	82.32	4.83	4.03	11.52	28.08
Sugar	6.44	4.68	0.99	2.17	1.65	0.94	10.17	2.98	0.95	14.94	18.05	75.97	3.72	2.62	10.91	33.54
Average	9.41	5.07	0.94	6.06	3.05	0.90	12.39	3.79	0.91	13.60	17.06	70.41	3.45	3.08	10.95	26.7

Table 3.3: **Trader Positions and Futures Returns by Trader Type**

This table reports the average slope coefficients and R^2s from weekly Fama-MacBeth cross-sectional regressions of commodity-level excess returns on one week-lagged trader positions (pressure) for each of four trader categories: hedgers (commercials), spread speculators (non-commercials with spread positions only), non-spread speculators (non-commercials with long or short, but not both, positions only), and small speculators (non-reportables). Pressure from hedgers refers to hedging pressure, measured by hedgers' net short positions scaled by total open interest; pressure from speculators with spread positions only is spreading pressure, defined as speculators' spread positions scaled by total open interest; and pressure from the other two categories, large speculators with long or short positions only and small speculators, is calculated as traders' net long positions scaled by total open interest, respectively. Newey-West t-statistics with four lags are in parentheses. Panel A presents results for the full sample from October 6, 1992 through December 26, 2018. Panels B and C show subsample results for October 6, 1992 through January 4, 2005, and January 4, 2005 through December 26, 2018, respectively.

Model	Hedgers	Speculators (spread)	Speculators (non-spread)	Small Speculators
Panel A: Full Sample				
$Pressure_{i,t}$	-0.07	-0.94	-0.09	0.03
	(-0.59)	(-1.95)	(-0.60)	(0.14)
R^2	5.44%	5.75%	5.29%	4.43%
Panel B: Pre-2005				
$Pressure_{i,t}$	-0.21	-0.38	-0.23	-0.12
	(-1.19)	(-0.42)	(-1.07)	(-0.41)
R^2	4.78%	4.85%	4.48%	4.35%
Panel C: Post-2005				
$Pressure_{i,t}$	0.04	-1.39	0.03	0.16
	(0.24)	(-3.00)	(0.17)	(0.41)
R^2	5.97%	6.48%	5.94%	4.49%

Table 3.4: **Spreading Pressure Portfolio**

This table presents the summary statistics of commodity futures weekly portfolio returns, where portfolios are constructed by sorting commodity futures on the fifty-two week average of spreading pressure or basis-momentum. Basis-momentum is calculated following Boons and Prado (2019) as $\prod_{s=t-11}^{t}\left(1+R_{long,s}^{(0)}\right)-\prod_{s=t-11}^{t}\left(1+R_{long,s}^{(1)}\right)$. *Low3* (*High3*) consists of commodity futures ranked in the bottom (top) three for spreading pressure or basis-momentum, and the rest of twenty commodities constitute the portfolio called *Mid*. *Low3-High3* represents a long-short portfolio strategy of buying Low3 and shorting High3. Portfolios' excess returns are calculated as equal-weighted average excess returns of portfolio constituents. Panel A presents results for the full sample from October 6, 1992 through December 26, 2018. Panels B and C show subsample results for October 6, 1992 through January 4, 2005, and for January 4, 2005 through December 26, 2018, respectively.

Panel A: Full Sample

	Spreading Pressure				Basis-Momentum			
	Low3	Mid	High3	Low3-High3	Low3	Mid	High3	High3-Low3
Mean	10.57	2.08	-6.37	16.94	-7.56	1.70	14.10	21.66
Std. Dev.	20.90	12.34	20.22	23.87	20.90	13.06	19.98	25.78
Sharpe ratio	0.51	0.17	-0.31	0.71	-0.36	0.13	0.71	0.84
Skewness	-0.13	-0.10	-0.03	0.00	0.10	-0.06	-0.09	-0.05
Kurtosis	5.15	5.00	4.02	3.90	3.82	5.36	4.33	3.47

Panel B: Pre-2005

	Spreading Pressure				Basis-Momentum			
	Low3	Mid	High3	Low3-High3	Low3	Mid	High3	High3-Low3
Mean	13.05	2.82	3.05	10.00	-6.65	3.42	18.74	25.39
Std. Dev.	18.90	10.47	16.39	23.87	20.14	10.17	21.21	27.10
Sharpe ratio	0.69	0.27	0.19	0.42	-0.33	0.34	0.88	0.94
Skewness	-0.09	0.05	0.10	0.14	0.14	0.06	-0.06	-0.13
Kurtosis	4.09	3.25	3.66	4.13	3.24	3.06	4.06	3.44

Panel C: Post-2005

	Spreading Pressure				Basis-Momentum			
	Low3	Mid	High3	Low3-High3	Low3	Mid	High3	High3-Low3
Mean	8.58	1.49	-13.93	22.52	-8.30	0.32	10.36	18.66
Std. Dev.	22.39	13.66	22.79	23.85	21.50	14.99	18.94	24.68
Sharpe ratio	0.38	0.11	-0.61	0.94	-0.39	0.02	0.55	0.76
Skewness	-0.14	-0.14	0.00	-0.11	0.08	-0.07	-0.15	0.03
Kurtosis	5.39	5.10	3.68	3.75	4.15	5.05	4.56	3.46

Table 3.5: **Fama-MacBeth Cross-Sectional Regressions**

This table presents the average coefficients from running Fama-MacBeth cross-sectional regressions of futures excess returns on the lagged (fifty-two week average) spreading pressure ($\overline{SP}$). Included as control variables are basis-momentum (BM), hedgers' net position changes (Q_h), and/or speculators' net position changes (Q_s):

$$R_{i,t+k} = b_0 + b_{\overline{SP}}\overline{SP}_{i,t} + b_{BM}BM_{i,t} + b_Q^h Q_{i,t}^h + b_Q^s Q_{i,t}^s + \epsilon_{i,t+1}$$

Newey-West t-statistics with four lags and average R^2 are reported for each model specification. Panel A presents results for the full sample from October 6, 1992 through December 26, 2018. Panels B and C show subsample results for October 6, 1992 through January 4, 2005, and January 4, 2005 through December 26, 2018, respectively.

Model	(1)	(2)	(3)	(4)	(5)	(6)	(7)	(8)
Panel A: Full Sample								
$b_{\overline{SP}}$	-1.78				-1.69	-1.97	-1.96	-1.91
	(-3.00)				(-2.89)	(-3.17)	(-3.13)	(-3.00)
b_{BM}		1.56			1.47			1.65
		(3.17)			(3.02)			(3.09)
b_Q^h			3.02			3.32		2.59
			(5.21)			(5.55)		(1.58)
b_Q^s				-3.50			-3.66	-0.87
				(-5.77)			(-5.80)	(-0.51)
R^2	5.94%	6.95%	4.89%	4.66%	12.63%	10.83%	10.61%	21.66%
Panel B: Pre-2005								
$b_{\overline{SP}}$	-2.20				-2.09	-2.49	-2.43	-2.45
	(-1.89)				(-1.83)	(-2.04)	(-1.97)	(-1.96)
b_{BM}		2.04			1.87			2.05
		(2.76)			(2.48)			(2.57)
b_Q^h			2.76			3.05		4.81
			(4.60)			(4.91)		(3.20)
b_Q^s				-2.44			-2.70	1.86
				(-3.59)			(-3.79)	(1.06)
R^2	4.88%	7.59%	4.75%	4.35%	12.19%	9.52%	9.16%	21.02%
Panel C: Post-2005								
$b_{\overline{SP}}$	-1.45				-1.37	-1.56	-1.59	-1.47
	(-2.80)				(-2.65)	(-2.84)	(-2.92)	(-2.68)
b_{BM}		1.17			1.15			1.33
		(1.79)			(1.81)			(1.85)
b_Q^h			3.22			3.53		0.80
			(3.49)			(3.70)		(0.30)
b_Q^s				-4.35			-4.43	-3.07
				(-4.63)			(-4.53)	(-1.11)
R^2	6.80%	6.43%	5.00%	4.91%	12.99%	11.89%	11.78%	22.17 %

Table 3.6: **Spreading Pressure Factor**

This table presents the summary statistics of spreading pressure factor, i.e., the excess return of long-short spreading pressure portfolios ($R_{\overline{SP}}$). Panel A reports the correlation between the spreading pressure factor and other well-known commodity futures risk factors such basis-momentum (R_{BM}), carry (R_C) , momentum (R_M) and the market factor (R_{Avg}). Panel B shows the correlation between spreading pressure portfolios and each of four commodity futures sector portfolios (energy, grain, meats, metals, and soft). Low3 (High3) consists of commodity futures ranked in the bottom (top) three for spreading pressure, and the remaining twenty commodities constitute the portfolio called Mid. Low3-High3 represents a long-short portfolio strategy of buying Low3 and shorting High3. Portfolios' excess returns are calculated as equal-weighted average excess returns of portfolio constituents. The full sample spans October 6, 1992 through December 26, 2018; pre-2005 (post-2005) is from October 6, 1992 through January 4, 2005 (January 4, 2005 through December 26, 2018).

Panel A. Commodity Futures Risk Factor Correlations				
	R_{Avg}	$R_{\overline{SP}}$	R_{BM}	R_C
(1) Full Sample				
$R_{\overline{SP}}$	-0.01			
R_{BM}	-0.03	0.13		
R_C	0.05	0.18	0.19	
R_M	0.04	0.16	0.19	0.43
(2) Pre-2005				
$R_{\overline{SP}}$	-0.01			
R_{BM}	0.03	0.12		
R_C	0.09	0.08	0.24	
R_M	0.10	0.05	0.32	0.45
(3) Post-2005				
$R_{\overline{SP}}$	-0.00			
R_{BM}	-0.07	0.15		
R_C	0.03	0.26	0.14	
R_M	0.00	0.25	0.05	0.41

Panel B: Spreading Pressure Factor and Commodity Sector Return Correlations					
	Energy	Grain	Meats	Metal	Soft
(1) Full Sample					
Low3	0.28	0.44	0.06	0.71	0.48
Mid	0.64	0.73	0.31	0.60	0.67
High3	0.62	0.51	0.20	0.37	0.29
Low3-High3	-0.28	-0.04	-0.12	0.30	0.17
(2) Pre-2005					
Low3	0.11	0.19	0.01	0.65	0.36
Mid	0.63	0.60	0.39	0.37	0.53
High3	0.26	0.57	0.24	0.15	0.14
Low3-High3	-0.10	-0.24	-0.16	0.41	0.19
(3) Post-2005					
Low3	0.40	0.57	0.10	0.73	0.55
Mid	0.66	0.80	0.26	0.70	0.74
High3	0.85	0.48	0.19	0.47	0.37
Low3-High3	-0.43	0.08	-0.09	0.24	0.16

Table 3.7: **Pricing Model Comparison: Spanning Regressions and GRS Tests**

This table presents the results of spanning regressions and GRS tests by regressing spreading pressure factors on commodity futures risk factors proposed by the extant pricing models. Panel A reports the regression coefficients on two factors (basis-momentum and the average commodity market factor) from Boons and Prado (2019), and Panel B reports three factors (carry, momentum, and the average commodity market factor) from Bakshi et al. (2019). Newey-West t-statistics with one lag are calculated, and F-statistics and the p-value of the joint GRS test are also provided in the last two rows. We report the results for the full sample from October 6, 1992 through December 26, 2018, and the two subsamples (pre- and post-2005).

	Full Sample	Pre-2005	Post-2005
Panel A. Boons and Prado (2019)			
α	14.30	7.55	19.83
	(2.87)	(1.02)	(2.96)
β_{BM}	0.12	0.10	0.14
	(4.00)	(2.43)	(3.32)
β_{Avg}	0.00	-0.04	0.01
	(-0.06)	(-0.38)	(0.19)
R^2	1.75%	1.37%	2.2%
GRS-F	3.43	0.68	3.63
p-val	0.02	0.57	0.01
Panel B. Bakshi et al. (2019)			
α	15.56	10.05	20.01
	(3.26)	(1.38)	(3.21)
β_{Avg}	-0.03	-0.05	-0.01
	(-0.53)	(-0.50)	(-0.18)
β_C	0.12	0.06	0.17
	(3.62)	(1.27)	(3.72)
β_M	0.08	0.02	0.15
	(2.65)	(0.42)	(3.57)
R^2	3.99%	0.71%	9.36%
GRS-F	3.96	1.08	3.98
p-val	0.01	0.36	0.01

Table 3.8: **Asset Pricing Tests with Spreading Pressure Factor**

This table presents the estimated risk premium on commodity futures risk factors by running Fama-MacBeth cross-sectional asset pricing tests. Six different model specifications are considered, and are nested in $R_{t,i} = \gamma_{t,0} + \lambda_{t,\overline{SP}}\beta_{t,\overline{SP}} + \lambda_{t,BM}\beta_{t,BM} + \lambda_{t,C}\beta_{t,C} + \lambda_{t,M}\beta_{t,M} + \lambda_{t,Avg}\beta_{t,Avg} + \epsilon_{t,i}$. We use seventeen commodity futures portfolios as test assets, broken down as carry (3), momentum (3), basis-momentum (3), spreading pressure (3), and commodity sector (5). Model (1) is a single-factor model that contains the spreading pressure factor only, Model (2) adds the basis-momentum factor, Model (3) is the Boons and Prado (2019) model, and Model (4) is the Bakshi et al. (2019) model. Models (5) and (6) add the spreading pressure factor to Models (3) and (4), respectively. We report two versions of the t-statistics, following Shanken (1992) (in parentheses) and Kan et al. (2013) (in square brackets). OLS R^2 and GLS R^2 (in parentheses) are in the last column. Panel A presents results for the full sample from October 6, 1992 through December 26, 2018. Panels B and C show subsample results for October 6, 1992 through January 4, 2005, and January 4, 2005 through December 26, 2018, respectively.

Panel A: Full Sample							
Model	γ_0	$\lambda_{\overline{SP}}$	λ_{BM}	λ_C	λ_M	λ_{Avg}	R^2
(1)	2.55	16.32					38.57%
	(1.00)	(2.99)					(27.87%)
	[0.86]	[2.91]					
(2)	2.71	12.90	21.34				75.83%
	(1.06)	(2.41)	(4.01)				(59.23%)
	[0.92]	[2.38]	[3.87]				
(3)	-0.61		24.25			2.81	63.33%
	(-0.14)		(4.37)			(0.56)	(39.69%)
	[-0.15]		[4.28]			[0.55]	
(4)	2.52			6.58	17.65	-0.43	36.15%
	(0.58)			(1.23)	(2.96)	(-0.09)	(13.02 %)
	[0.56]			[1.17]	[3.09]	[-0.08]	
(5)	-2.13	13.73	21.49			4.49	79.28%
	(-0.49)	(2.59)	(4.03)			(0.91)	(59.90%)
	[-0.56]	[2.51]	[3.97]			[0.88]	
(6)	-0.33	14.71		4.86	16.15	2.65	57.19%
	(-0.08)	(2.78)		(0.92)	(2.72)	(0.54)	(37.44%)
	[-0.07]	[2.77]		[0.85]	[2.99]	[0.48]	

Table 3.8 - **Continued**

Panel B: Pre-2005							
Model	γ_0	$\lambda_{\overline{SP}}$	λ_{BM}	λ_C	λ_M	λ_{Avg}	R^2
(1)	4.77	11.55					10.28%
	(1.51)	(1.49)					(6.71%)
	[1.64]	[1.32]					
(2)	4.26	8.00	24.37				47.74%
	(1.35)	(1.05)	(2.74)				(37.31%)
	[1.38]	[0.99]	[3.04]				
(3)	-2.64		24.50			6.85	51.36%
	(-0.37)		(2.75)			(0.89)	(34.35%)
	[-0.48]		[3.08]			[1.09]	
(4)	-0.2			0.49	26.75	4.30	48.94%
	(-0.03)			(0.06)	(2.81)	(0.55)	(28.43%)
	[-0.03]			[0.06]	[3.34]	[0.61]	
(5)	-4.1	10.17	23.22			8.21	55.93%
	(-0.57)	(1.35)	(2.64)			(1.06)	(38.20%)
	[-0.69]	[1.19]	[2.98]			[1.25]	
(6)	-3.2	11.65		-0.77	26.12	7.15	58.28%
	(-0.44)	(1.54)		(-0.09)	(2.74)	(0.92)	(35.20%)
	[-0.43]	[1.48]		[-0.09]	[3.23]	[0.93]	
Panel C: Post-2005							
Model	γ_0	$\lambda_{\overline{SP}}$	λ_{BM}	λ_C	λ_M	λ_{Avg}	R^2
(1)	0.92	20.95					66.81%
	(0.24)	(2.88)					(33.01%)
	[0.22]	[2.80]					
(2)	1.51	18.85	17.61				84.36%
	(0.40)	(2.62)	(2.61)				(47.39%)
	[0.33]	[2.51]	[2.26]				
(3)	0.25		23.33			0.19	47.87%
	(0.05)		(3.30)			(0.03)	(23.33%)
	[0.05]		[2.77]			[0.03]	
(4)	3.31			14.17	12.04	-3.02	33.91%
	(0.66)			(1.98)	(1.54)	(-0.49)	(5.26%)
	[0.65]			[1.93]	[1.49]	[-0.45]	
(5)	-1.16	19.23	18.16			2.11	85.35%
	(-0.23)	(2.68)	(2.72)			(0.34)	(49.36%)
	[-0.25]	[2.53]	[2.35]			[0.29]	
(6)	0.98	20.02		9.74	7.29	-0.13	68.20%
	(0.20)	(2.87)		(1.40)	(0.97)	(-0.02)	(34.12%)
	[0.20]	[2.67]		[1.40]	[1.03]	[-0.02]	

Table 3.9: **Spreading Pressure and the Term Structure of Futures Prices**

This table reports the predictive regression of the one week-ahead slope and curvature of the commodity futures term structure on spreading pressure and hedging pressure:

$$\{Slope_{t+1}, Curvature_{t+1}\} = \alpha_{t+1} + \beta_{SP} SP_t + \beta_{HP} HP_t + \varepsilon_{i,t+1}.$$

We define the slope of futures curves as $slope_t = \frac{\ln F_t^3 - \ln F_t^1}{T_3 - T_1}$, and the curvature as $curvature_t = \frac{\ln F_t^3 - \ln F_t^2}{T_3 - T_2} - \frac{\ln F_t^2 - \ln F_t^1}{T_2 - T_1}$. We report the results for four subgroups as well as for the whole. *Group* indicates the sub-sample depending on the shape of the term structure at time t, i.e., 1) positive slope, positive curvature, 2) positive slope, negative curvature, 3) negative slope, positive curvature, and 4) negative slope, negative curvature. *Percentage* (*Mean of SP*) is the proportion of the sample (average spreading pressure) for each group. The regression controls for both time- and commodity-fixed effects, as well as for time to earliest maturity date for each commodity at each point in time. t-statistics based on standard errors clustered at the time dimension are in parentheses. The sample period is January 4, 2005 through December 26, 2018.

Group	Percentage	Mean of SP	$Slope_{t+1,i} \times 100$			$Curv_{t+1,i} \times 100$		
			$SP_{t,i}$	$HP_{t,i}$	R^2	$SP_{t,i}$	$HP_{t,i}$	R^2
(1) $+Slope$, $+Curv$	24.72%	12.98%	0.99	-0.07	48.43%	0.08	-0.07	15.49%
			(9.31)	(-3.07)		(0.41)	(-1.87)	
(2) $+Slope$,$-Curv$	48.15%	12.72%	0.17	-0.18	32.04%	-0.13	-0.05	22.65%
			(2.62)	(-11.47)		(-1.82)	(-2.54)	
(3) $-Slope$, $+Curv$	10.49%	11.38%	-0.06	-0.25	42.28%	0.06	-0.19	43.82%
			(-0.66)	(-7.4)		(0.39)	(-3.64)	
(4) $-Slope$, $-Curv$	16.64%	11.96%	-0.31	-0.04	42.42%	-0.57	-0.17	36.11%
			(-2.62)	(-0.83)		(-3.05)	(-2.25)	
(5) All states	100%	12.54%	0.17	-0.31	19.71%	0.08	-0.07	6.65%
			(2.27)	(-20.08)		(0.90)	(-3.86)	

Table 3.10: **Asset Pricing Test with Disaggregated Spreading Pressure Factors**

This table reports the results of cross-sectional asset pricing tests with different versions of spreading pressure factors depending on disaggregated spread trader categories from the DCOT report (i.e., money manager, swap dealer, and other reportable):

$$\begin{aligned} R_{t,i} &= \gamma_{t,0} + \lambda_{t,\overline{SP}}\beta_{t,\overline{SP}} + \lambda_{\overline{SP}}^{ManagedMoney}\beta_{t,\overline{SP}\_ManagedMoney} + \lambda_{\overline{SP}}^{OtherReportable}\beta_{t,\overline{SP}\_OtherReportable} \\ &\quad + \lambda_{\overline{SP}}^{SwapDealer}\beta_{t,\overline{SP}\_SwapDealers} + \epsilon_{t,i} \end{aligned}$$

We use seventeen portfolios as test assets, constructed by sorting on carry (3), momentum (3), basis-momentum (3), spreading pressure (3), and sector (5). $\lambda_{t,\overline{SP}}$ is the estimated risk premium on the spreading pressure factor based on spreading pressure from overall speculators (i.e., money managers and others), $\lambda_{\overline{SP}}^{ManagedMoney}$ and $\lambda_{\overline{SP}}^{OtherReportable}$ are based on sub-categories of speculator, i.e., money managers and others, respectively, and $\lambda_{\overline{SP}}^{SwapDealer}$ is based on financial intermediaries, i.e., swap dealers. Two versions of t-statistics are reported following Shanken (1992) (in parentheses) and Kan et al. (2013) (in square brackets). The sample period is June 13, 2006 through December 26, 2018.

Model	γ_0	$\lambda_{\overline{SP}}$	$\lambda_{\overline{SP}}^{ManagedMoney}$	$\lambda_{\overline{SP}}^{OtherReportable}$	$\lambda_{\overline{SP}}^{SwapDealers}$	R^2
(1)	-0.94	18.97				64.84%
	(-0.21)	(2.38)				
	[-0.21]	[2.44]				
(2)	0.34		22.32			62.36%
	(0.08)		(2.29)			
	[0.07]		[2.50]			
(3)	-3.53			20.74		49.08%
	(-0.78)			(2.15)		
	[-0.65]			[2.21]		
(4)	2.60				21.32	50.19%
	(0.62)				(2.05)	
	[0.56]				[2.22]	
(5)	-0.59		20.81	13.96		63.61%
	(-0.15)		(1.98)	(1.35)		
	[-0.15]		[1.97]	[1.25]		
(6)	-0.01	18.15			14.25	66.06%
	(-0.00)	(2.31)			(1.29)	
	[-0.00]	[2.44]			[1.27]	

Table 3.11: **Spreading Pressure Factor over Time**

This table presents the regression of spreading pressure (and its long and short legs) on different time dummy variables,

$$R_{i,t} = \alpha + \beta_j I_j + \gamma_i R_{i,t-1} + \varepsilon_t$$

where $R_{i,t}$ includes the return of spreading pressure ($R_{i,t}$), return of spreading pressure long leg ($R_{Long,t}$), and the return of spreading pressure short leg ($R_{Short,t}$). The time dummy used in Model (1) is $I_{t\geq 2005}$, which equals to one when the time is after 2005. Similarly, the time dummy variables used in Model (2) and (3) are $I_{2001\leq t\leq 2005}$ and $I_{2003\leq t\leq 2008}$ respectively. In Model (4), we use two time dummies, $I_{t\geq 2005}$ and $I_{2006Sep\leq t\leq 2006Dec}$. We include the lag of return $R_{i,t-1}$ as a control variable. t-statistics are in parentheses. The sample period is October 5, 1993 through December 26, 2018.

Model	Variable	$R_{SP,t}$	$R_{Long,t}$	$R_{Short,t}$
(1)	α	0.18	0.25	0.06
		(1.33)	(2.06)	(0.49)
	$\beta_{t\geq 2005}$	0.22	-0.09	-0.32
		(1.18)	-(0.54)	-(2.08)
(2)	α	0.42	0.24	-0.21
		(4.10)	(2.66)	-(2.43)
	$\beta_{2001\leq t\leq 2005}$	-0.59	-0.20	0.44
		-(2.59)	(-0.98)	(2.26)
(3)	α	0.31	0.24	-0.09
		(2.99)	(2.62)	-(1.04)
	$\beta_{2003\leq t\leq 2008}$	-0.05	-0.18	-0.13
		-(0.24)	-(0.93)	-(0.70)
(4)	α	0.18	0.25	0.06
		(1.33)	(2.06)	(0.5)
	$\beta_{t\geq 2005}$	0.18	-0.09	-0.29
		(0.97)	-(0.58)	-(1.86)
	$\beta_{2006Sep\leq t\leq 2006Dec}$	1.65	0.28	-1.52
		(2.04)	(0.40)	-(2.21)

Table 3.12: **Spreading Pressure Factor and Asset Returns**

This table presents the relationship between the spreading pressure factor and the returns of MSCI Emerging Markets Asia Index, S&P 500, U.S. Dollar Index Futures Contracts, and JP Morgan Treasury Bond Index. We regress the spreading pressure factor (as well as its long and short legs separately) on normalized returns of indices ($R^a_{k,t}$), $R_{i,t} = \alpha + \beta_k R^a_{k,t} + \gamma_j C_{j,t} + \varepsilon_t$, where R^a_k is the return of MSCI Emerging Markets Asia Index (Panel A), S&P 500 (Panel B), U.S. Dollar Index Futures Contracts (Panel C) and JP Morgan Treasury Bond Index (Panel D). The control variables ($C_{j,t}$) in this regression are the growth rate of the Baltic Dry Index, the change in the ten-year breakeven inflation rate and the lag of the spreading pressure return, long or short leg return. We report β_i, its t-statistics and the R^2 of the above regression. The sample period is January 4, 2005 through December 26, 2018 (weekly frequency).

	β	t-stat	R^2(%)
Panel A: MSCI Emerging Markets Asia Index Return			
Spreading Pressure Factor	12.04	3.18	2.58
Long, low spreading pressure commodities	32.62	8.95	24.83
Short, high spreading pressure commodities	20.19	4.71	16.51
Panel B: S&P 500 Return			
Spreading Pressure Factor	3.95	1.14	1.19
Long, low spreading pressure commodities	23.06	5.78	18.23
Short, high spreading pressure commodities	18.75	3.78	15.79
Panel C: U.S. Dollar Index Future Contracts Return			
Spreading Pressure Factor	-5.03	-1.51	1.33
Long, low spreading pressure commodities	-29.29	-7.85	23.45
Short, high spreading pressure commodities	-24.23	-8.39	19.39
Panel D: JP Morgan Treasury Bond Index Return			
Spreading Pressure Factor	2.81	0.71	1.11
Long, low spreading pressure commodities	-0.82	-0.20	11.88
Short, high spreading pressure commodities	-4.35	-1.00	11.91

Table 3.13: **Spreading Pressure Factor and Economic Uncertainty**

This table presents the relationship between the spreading pressure factor and shocks to different measures of uncertainty, namely the VIX index, and macroeconomic, financial, and real economic uncertainty. We regress the spreading pressure factor (and its long and short legs separately) on normalized changes in uncertainty measures ($\Delta Uncertainty_t$), $R_{SP,t} = \alpha + \beta_{i,Uncertainty}\Delta Uncertainty_{i,t} + +\gamma_j C_{j,t} + \varepsilon_t$. The control variable ($C_{j,t}$) used in this regression is the lag of the spreading pressure return, long or short leg return. We report $\beta_{Uncertainty}$, its t-statistics and R^2 of the above regression. The sample period is January 4, 2005 through December 26, 2018 (monthly frequency).

	β	t-stat	$R^2(\%)$
Panel A: Real Economic Uncertainty			
Spreading Pressure Factor	-19.34	-3.28	5.08
Long, low spreading pressure commodities	-24.07	-1.88	7.48
Short, high spreading pressure commodities	-1.83	-0.20	0.35
Panel B: VIX			
Spreading Pressure Factor	-7.45	-1.23	0.96
Long, low spreading pressure commodities	-29.42	-3.56	11.53
Short, high spreading pressure commodities	-21.66	-3.67	6.70
Panel C: Financial Uncertainty			
Spreading Pressure Factor	-12.02	-1.85	2.10
Long, low spreading pressure commodities	-24.74	-2.74	7.81
Short, high spreading pressure commodities	-9.05	-1.67	1.40
Panel D: Macro Uncertainty			
Spreading Pressure Factor	-13.02	-1.67	2.44
Long, low spreading pressure commodities	-29.40	-2.54	10.60
Short, high spreading pressure commodities	-10.88	-1.40	1.89

Table 3.14: **Spread Positions and Index Investment**

This table presents pooled regressions for two models with time and commodity fixed effects, nested in

$$\Delta SpreadPosition_{i,t} = \alpha_t + \mu_i + \beta_{IndexPosition} \Delta IndexPosition_{i,t} + \epsilon_{i,t}$$

where $IndexPosition_{i,t}$ includes $\{LongIndexPosition_{i,t}, NetIndexPosition_{i,t}\}$, α_t and μ_i are used to control time and commodity fixed effects. $LongIndexPosition_{i,t}$ is total long position held by index investors, and $NetIndexPosition_{i,t}$ is net long position held by index investors. $\Delta Position_{i,t} = Position_{i,t}/Position_{i,t-1} - 1$. Panel A shows the results for non-commercials' spread positions. Panels B and C show results for spread positions held by money managers and other reportables, respectively. In Panel D, we show swap dealers' spread positions. The sample period is December, 2007 through September, 2015 (quarterly frequency). Non-commercials spread positions are collected from weekly COT reports, while spread position data at a trader category level come from DCOT reports. The panel shows commodity investment data for twenty commodities, excluding frozen pork belly, lumber, rough rice, oats, orange juice, and palladium.

Model	$\beta_{LongIndexPosition}$	$\beta_{NetIndexPosition}$	R^2
Panel A: Spread Positions (non-commercials) and Index Positions			
(1)	0.19		16.79%
	(2.15)		
(2)		0.18	16.81%
		(2.15)	
Panel B: Spread Positions (managed money) and Index Positions			
(3)	0.23		14.21%
	(2.80)		
(4)		0.20	14.11%
		(2.39)	
Panel C: Spread Positions (other reportables) and Index Positions			
(5)	0.21		16.79%
	(1.30)		
(6)		0.23	16.81%
		(1.53)	
Panel D: Spread Positions (swap dealers) and Index Positions			
(7)	0.46		11.33%
	(0.38)		
(8)		-1.55	11.87%
		(-1.34)	

Table 3.15: **Cross-Sectional Asset Pricing Tests for Alternative Risk Channels**

This table presents cross-sectional tests for whether volatility, liquidity, intermediary capital or inventory risks are priced in the commodity market:

$$\begin{aligned} R_{t,i} &= \gamma_{t,0} + \lambda_{t,SP}\beta_{t,SP} + \lambda^{mkt}_{t,var}\beta^{mkt}_{t,var} + \lambda^{avg}_{t,var}\beta^{avg}_{t,var} + \lambda^{AMI}_{t,liquidity}\beta^{AMI}_{t,liquidity} \\ &\quad + \lambda^{HKM}_{t,ICR}\beta^{HKM}_{t,ICR} + \lambda^{GHR}_{t,INV}\beta^{GHR}_{t,INV} + \lambda_{t,Avg}\beta_{t,Avg} + \epsilon_{t,i} \end{aligned}$$

Volatility factors are the innovations in aggregate and average commodity market variance ($\Delta var_{mkt,t}$ and $\Delta var_{avg,t}$). We construct aggregate commodity market variance ($var_{mkt,t}$) as the sum of daily squared returns of equal-weighted commodity portfolio in week t. Average commodity market variance ($var_{avg,t}$) is the equally-weighted average of the sum of the daily squared returns of all commodities in week t (Boons and Prado, 2019). The liquidity measure is the innovations in the aggregate Amihud measure ($\Delta liquidity_{AMI}$). We compute commodity i's Amihud measure as the annual average of daily $\frac{|R_{n,d}|}{Vol_{n,d}}$ by using dollar volume $Vol_{n,d}$ for both front- and second-month contract ($n = 1, 2$) at day d. The aggregate Amihud measure is the mean of the median of front- and second-month Amihud illiquidity over all commodities (Boons and Prado, 2019). The intermediary capital risk factor (ICR) is the AR(1) innovations to the intermediary capital ratio scaled by the lagged intermediary capital ratio from He et al. (2017). Inventory risk factor (INV) is the return of the long-short portfolio constructed by going long the three commodities with the lowest normalized inventory levels, and shorting the three commodities with the highest normalized inventory levels. Normalized inventory level at time t is the ratio of the level at time t to its past twelve-month moving average from $t-1$ to $t-12$, which is defined by Gorton et al. (2013). We use seventeen portfolios sorted on carry (3), momentum (3), basis-momentum (3), spreading pressure (3), and sector portfolios (5). Models (1) to (5) are two-factor models contain the market factor and one of either the volatility or the liquidity factors. Models (6) to (10) add the spreading pressure factor. t-statistics of the estimated prices of risk (λ) are in parentheses below each estimate, which are calculated following Shanken (1992) (in parentheses) and Kan et al. (2013) (in square brackets). The sample period is January 4, 2005 through December 26, 2018.

Table 3.15 - **Continued**

Model	γ_0	λ_{SP}	λ_{var}^{mkt}	λ_{var}^{avg}	$\lambda_{liquidity}^{AMI}$	λ_{ICR}^{HKM}	λ_{INV}^{GHR}	λ_{Avg}	R^2
(1)	-3.06		-1.22					3.52	36.46%
	(-0.49)		(-1.86)					(0.49)	
	[-0.47]		[-1.87]					[0.42]	
(2)	-4.57			-2.15				5.21	40.97%
	(-0.68)			(-1.95)				(0.68)	
	[-0.63]			[-1.78]				[0.56]	
(3)	-5.80				-0.02			6.61	44.44%
	(-0.67)				(-1.86)			(0.71)	
	[-0.70]				[-2.24]			[0.64]	
(4)	2.87					18.42		-2.54	2.32%
	(0.52)					(0.41)		(-0.38)	
	[0.25]					[0.13]		[-0.19]	
(5)	3.96						21.81	-3.89	5.25%
	(0.79)						(0.78)	(-0.62)	
	[0.75]						[0.49]	[-0.58]	
(6)	2.29	22.24	0.32					-1.36	67.78%
	(0.40)	(3.18)	(0.46)					(-0.20)	
	[0.41]	[2.81]	[0.43]					[-0.18]	
(7)	0.91	21.05		0.00				-0.01	66.82%
	(0.15)	(3.07)		(-0.00)				(-0.00)	
	[0.14]	[2.78]		[-0.00]				[-0.00]	
(8)	-3.23	18.71			-0.01			4.29	73.70%
	(-0.50)	(2.59)			(-1.30)			(0.58)	
	[-0.44]	[2.47]			[-0.96]			[0.50]	
(9)	-3.80	23.86				76.11		4.69	75.18%
	(-0.69)	(3.30)				(1.76)		(0.71)	
	[-0.65]	[3.14]				[1.40]		[0.67]	
(10)	0.73	21.26					-16.52	0.30	68.52%
	(0.15)	(2.96)					(-0.60)	(0.05)	
	[0.14]	[2.81]					[-0.51]	[0.04]	

Figure 3.1: **Commodity Futures Positions by Traders Type**

This figure presents the market share for each of four categories (commercials, non-commercials with- or without spread positions, and non-reportables for each of five commodity sectors; energy, metals, soft, grains, and meats. The market share of trader type i is calculated as $\frac{Long_{i,t}+Short_{i,t}}{2\times Open\,Interest_t}$. The sample period is October 6, 1992 through December 26, 2018.

(a) **Energy**

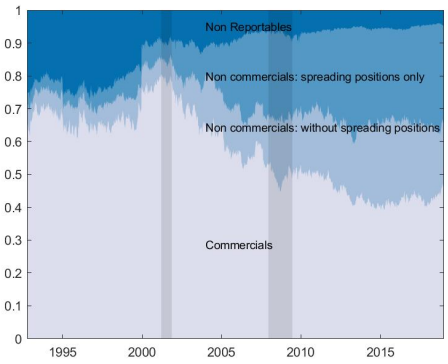

(b) **Metals**

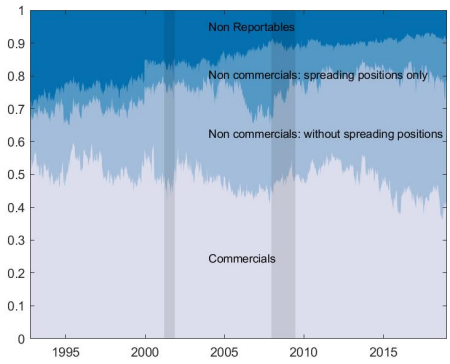

(c) **Softs**

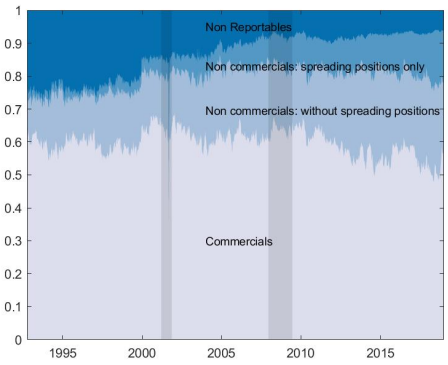

(d) **Grains**

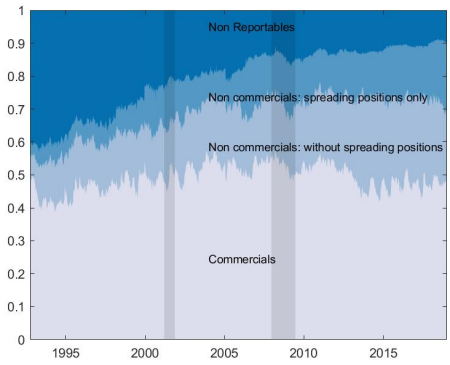

(e) **Meats**

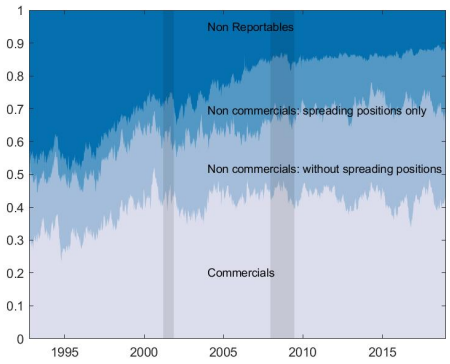

Figure 3.2: **Spreading Pressure Over Time**

This figure presents the time-series of spreading pressure by aggregated non-commercials (black line) and disaggregated commercials, i.e., money managers (dark blue area) and other reportables (light blue area). It reports six selected commodities, with three of high spreading pressure (natural gas, WTI crude oil, and lean hogs), and three of low spreading pressure (palladium, platinum, and oats). The sample period is October 6, 1992 through December 26, 2018, for aggregated pressure, and June 13, 2006 through December 26, 2018, for disaggregated pressure.

(a) **Natural Gas**

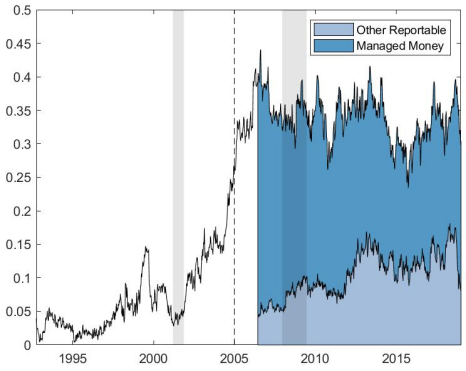

(b) **WTI Crude Oil**

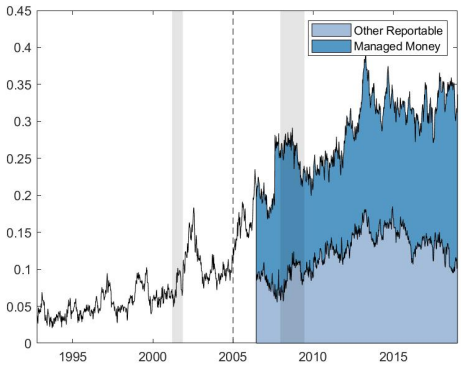

(c) **Lean Hogs**

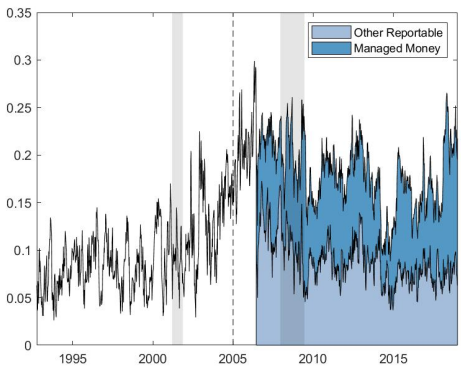

(d) **Platinum**

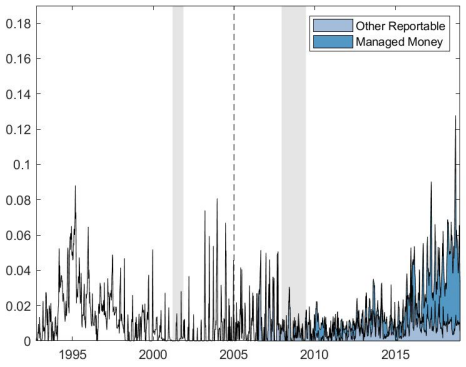

(e) **Palladium**

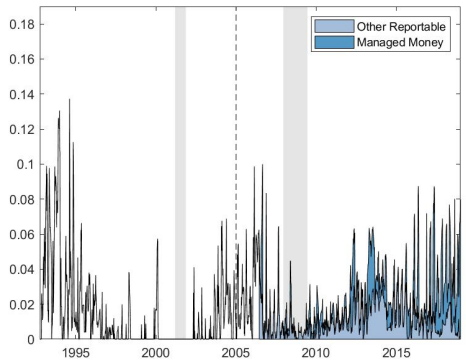

(f) **Oats**

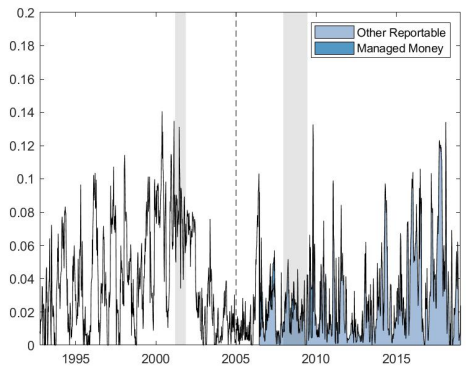

Figure 3.3: **Spreading Pressure by Week**

This figure presents the weekly average spreading pressure from non-commercials (black line) of palladium and WTI crude oil from October 6, 1992 through January 4, 2005 (left-hand side) and from January 4, 2005 through December 26, 2018 (right-hand side). The red dashed vertical line indicates the week of contract maturity, i.e., the first notice day or the last trading day, whichever comes first.

(a) **Palladium** ***(Pre-2005)***

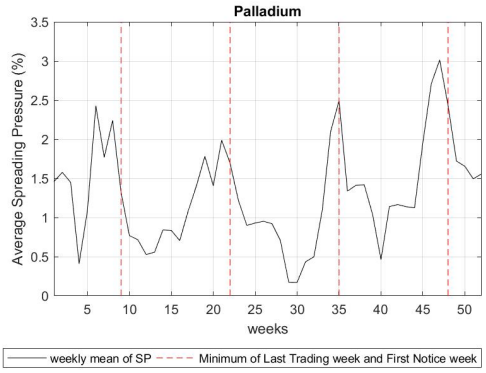

(b) **Palladium** ***(Post-2005)***

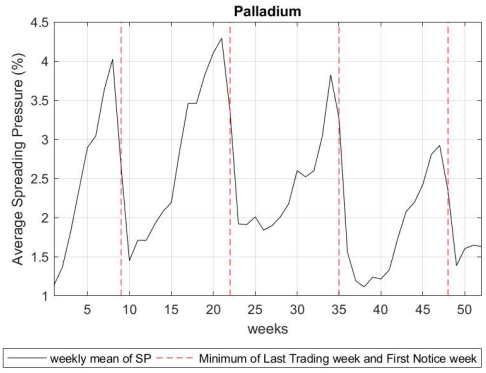

(c) **WTI Crude Oil** ***(Pre-2005)***

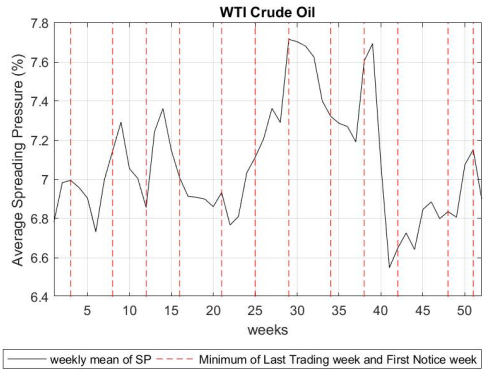

(d) **WTI Crude Oil** ***(Post-2005)***

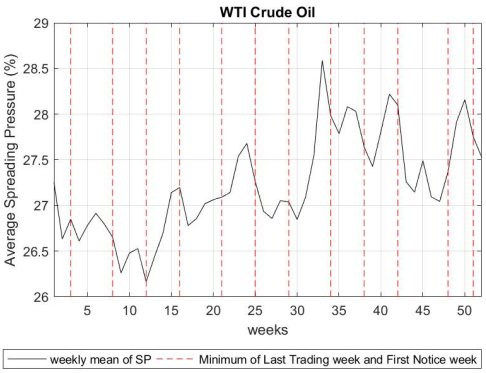

Figure 3.4: **Trader Positions and Futures Excess Returns: Full-Sample**

The figure presents scatter plots of average excess returns of commodity futures over trader position variables (or pressure) and fitted lines by cross-sectional regressions for each of four trader categories over the twenty-six sample commodities. The sample period is October 6, 1992 through December 26, 2018.

(a) **Commercials**

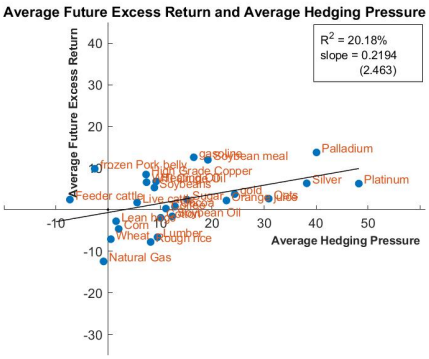

(b) **Non-Commercials with Spreading Positions**

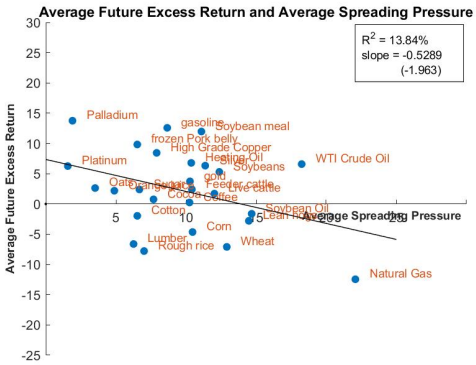

(c) **Non-Commercials without Spreading Positions**

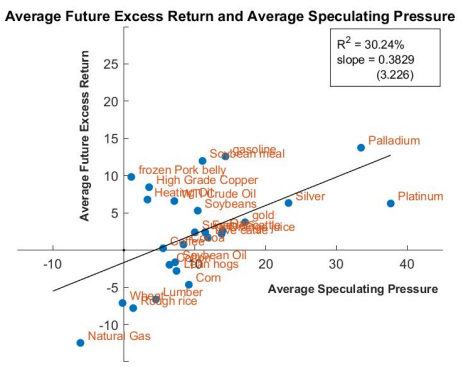

(d) **Non-Reportables**

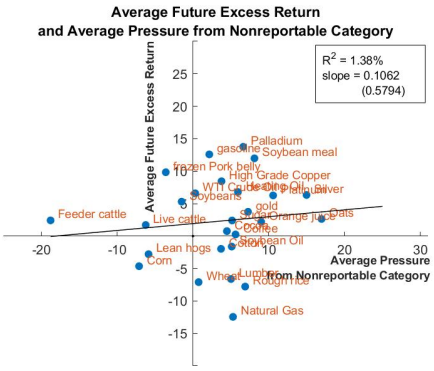

Figure 3.5: **Trader Positions and Futures Excess Returns: Post-2005**

This figure presents scatter-plots of average excess returns of commodity futures over traders position variables (or, pressure) and fitted lines by cross-sectional regressions for each of four trader categories over the twenty-six sample commodities. The sample period is January 4, 2005 throughs December 26, 2018.

(a) **Commercials**

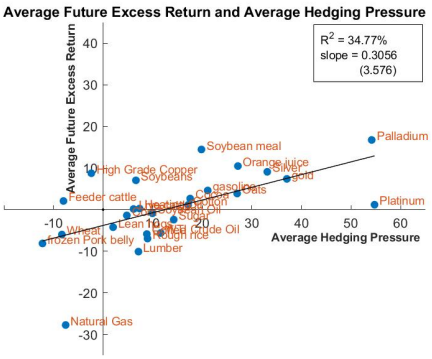

(b) **Non-Commercials with Spreading Positions**

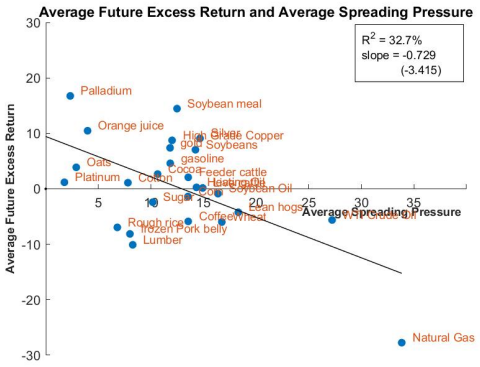

(c) **Non-Commercials without Spreading Positions**

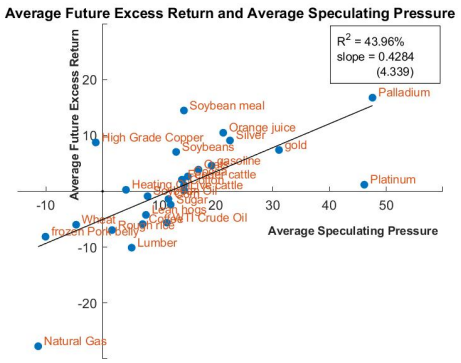

(d) **Non-Reportables**

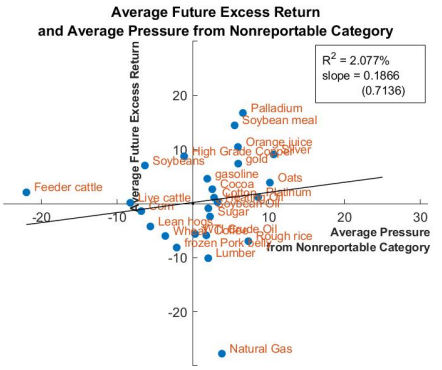

Figure 3.6: **Cumulative Excess Returns of Commodity Pricing Portfolios**

This figure presents the cumulative excess returns for commodity futures pricing portfolios; a long-short portfolio based on carry (basis), momentum, basis-momentum, or spreading pressure, along with an average commodity market factor. The sample period is October 6, 1992 through December 26, 2018 (for full sample at the top) and January 4, 2005 through December 26, 2018 (post-2005 at the bottom).

(a) **Full Sample**

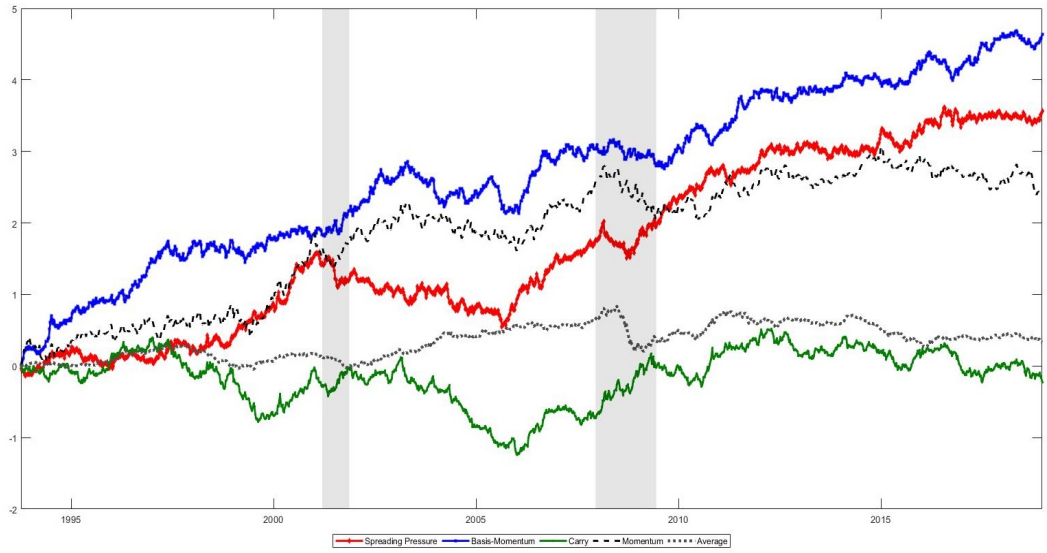

(b) **Post-2005**

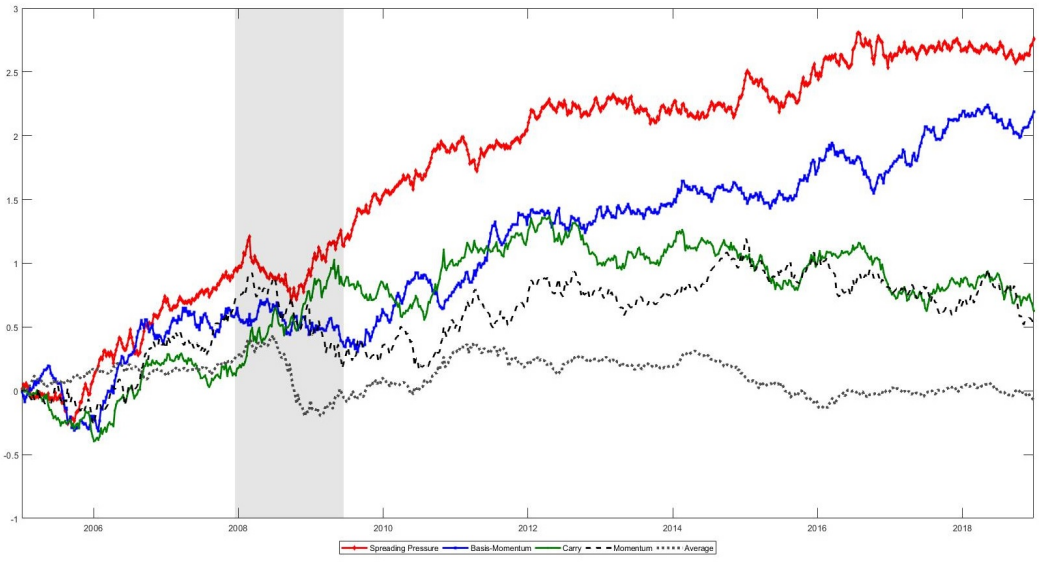

Figure 3.7: **Commodity Sensitivity to Real Economic Uncertainty**

This figure shows sensitivities of twenty-sixs commodities on real economic uncertainty shocks, and commodity turnover in spreading pressure portfolio long (top) and short (bottom) legs, respectively (monthly data from January 4, 2005 through December 26, 2018). We denote $\Delta RealUncertainty_t$ as normalized changes in real economic uncertainty, and we run the regression $R^e_{i,t} = \beta_{i,RealUncertainty}\Delta RealUncertainty_t + \varepsilon_{i,t}$. The coefficient $\beta_{i,RealUncertainty}$ (multiplied by -1 in the top panel) is a measurement of the sensitivity of commodity i on real economic uncertainty shocks. The left-side y-axis (blue) is the commodity turnover in spreading pressure portfolio long/short legs. Commodities that appear in either leg are in red on the x-axis. The right-side y-axis (orange) is the sensitivities of twenty-six commodities on real economic uncertainty shocks. Commodities with * on the x-axis are components of the S&P GSCI Index, and commodities with ** are components of the Bloomberg Commodity Index (DJ-UBSCI) but not components of the S&P GSCI Index.

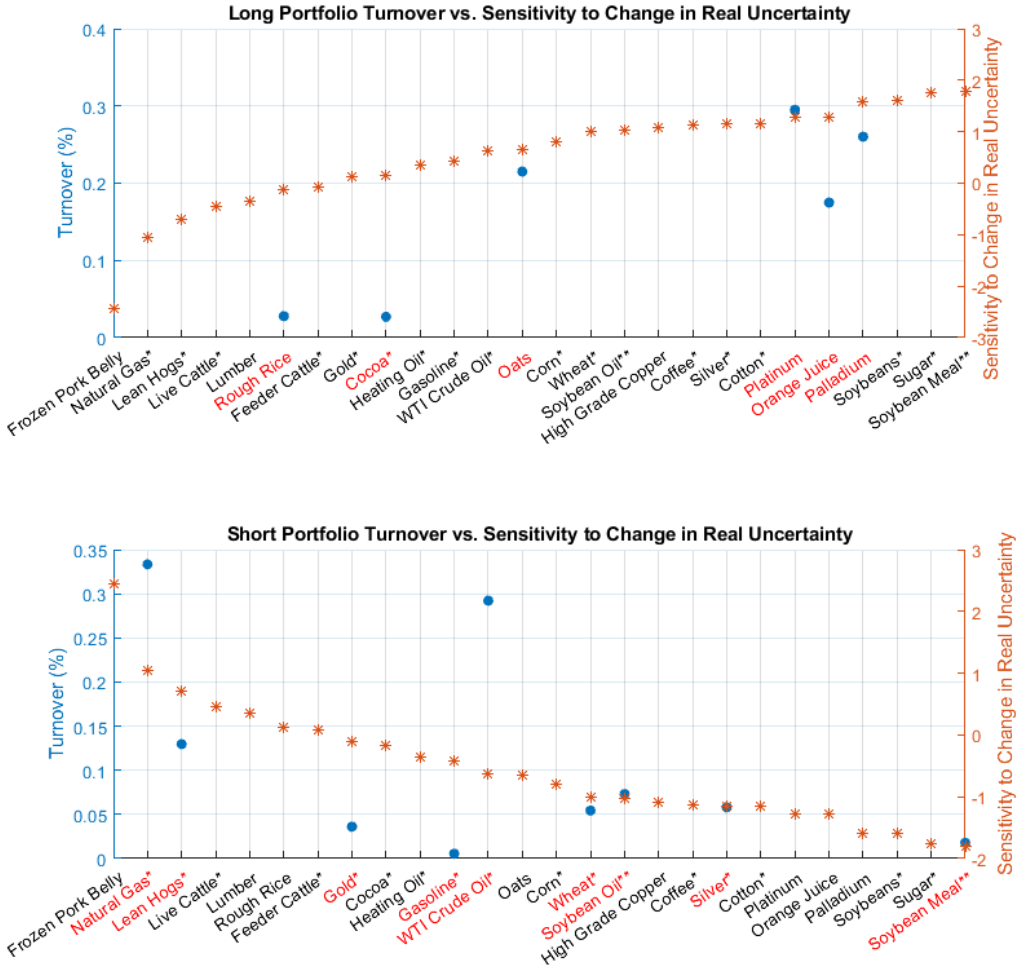

Appendix 3.A Tables

Table 3.A-1: **Spreading Position Portfolio: Transaction Cost**

This table presents the summary statistics of commodity futures weekly portfolio returns after accounting for transaction costs, where portfolios are constructed by sorting commodity futures on the fifty-two week average of spreading pressure or basis-momentum. Basis-momentum is calculated following Boons and Prado (2019) as $\prod_{s=t-11}^{t}\left(1+R^{(0)}_{long,s}\right)-\prod_{s=t-11}^{t}\left(1+R^{(1)}_{long,s}\right)$. *Low3* (*High3*) consists of commodity futures ranked in the bottom (top) three for spreading pressure or basis-momentum, and the rest of twenty commodities constitute the portfolio called *Mid*. *Low3-High3* represents a long-short portfolio strategy of buying Low3 and shorting High3. Following Paschke et al. (2020), we set the (round-trip) transaction cost of each commodity's contract as 0.033%. Portfolios' excess returns are calculated as equal-weighted average excess returns after accounting for transaction costs of portfolio constituents. Panel A presents results for the full sample from October 6, 1992 through December 26, 2018. Panels B and C show subsample results for October 6, 1992 through January 4, 2005, and for January 4, 2005 through December 26, 2018, respectively.

Panel A: Full Sample

	Spreading Pressure				Basis-Momentum			
	Low3	Mid	High3	Low3-High3	Low3	Mid	High3	High3-Low3
Mean	10.04	-2.53	-7.29	15.48	-8.74	-3.89	12.83	19.22
Std. Dev.	20.90	12.35	20.20	23.87	20.89	13.04	19.99	25.79
Sharpe	0.48	-0.20	-0.36	0.65	-0.42	-0.30	0.64	0.75
Skewness	-0.13	-0.09	-0.03	-0.01	0.10	-0.07	-0.09	-0.05
Kurtosis	5.15	4.86	4.02	3.90	3.82	5.23	4.34	3.48

Panel B: Pre-2005

	Spreading Pressure				Basis-Momentum			
	Low3	Mid	High3	Low3-High3	Low3	Mid	High3	High3-Low3
Mean	12.48	-2.00	2.25	8.63	-7.93	-2.29	17.46	22.83
Std. Dev.	18.91	10.56	16.39	23.88	20.14	10.26	21.22	27.11
Sharpe	0.66	-0.19	0.14	0.36	-0.39	-0.22	0.82	0.84
Skewness	-0.09	0.08	0.10	0.14	0.14	0.08	-0.07	-0.13
Kurtosis	4.10	3.23	3.68	4.13	3.24	2.97	4.06	3.45

Panel C: Post-2005

	Spreading Pressure				Basis-Momentum			
	Low3	Mid	High3	Low3-High3	Low3	Mid	High3	High3-Low3
Mean	8.09	-2.95	-14.96	21.00	-9.39	-5.18	9.10	16.31
Std. Dev.	22.37	13.62	22.77	23.84	21.49	14.92	18.93	24.68
Sharpe	0.36	-0.22	-0.66	0.88	-0.44	-0.35	0.48	0.66
Skewness	-0.14	-0.15	0.00	-0.12	0.08	-0.09	-0.15	0.03
Skewness	5.39	4.99	3.68	3.74	4.15	4.98	4.57	3.46

Table 3.A-2: **Spreading Pressure Portfolio (four commodities in each leg)**

This table presents the summary statistics of commodity futures weekly portfolios returns, where we construct the portfolios by sorting commodity futures on the fifty-two week average of spreading pressure or basis-momentum. Basis-momentum is calculated following Boons and Prado (2019) as $\prod_{s=t-11}^{t}\left(1+R_{long,s}^{(0)}\right)-\prod_{s=t-11}^{t}\left(1+R_{long,s}^{(1)}\right)$. *Low4* (*High4*) consists of commodity futures ranked in the bottom (top) four for spreading pressure or basis-momentum, and the remaining eighteen commodities constitute the portfolio called *Mid*. *Low4-High4* represents a long-short portfolio strategy of buying Low4 and shorting High4. Portfolios' excess returns are calculated as equal-weighted average excess returns of portfolio constituents. Panel A presents results for the full sample from October 6, 1992 through December 26, 2018. Panels B and C show the sub-sample results from October 6, 1992 through January 4, 2005, and from January 4, 2005 through December 26, 2018, respectively.

Panel A: Full Sample								
	Spreading Pressure				Basis-Momentum			
	Low4	Mid	High4	Low4-High4	Low4	Mid	High4	High4-Low4
Mean	8.87	1.82	-3.54	12.41	-5.29	1.22	13.11	18.41
Std. Dev.	18.47	12.53	18.37	20.5	19.09	13.26	18.09	22.34
Sharpe	0.48	0.15	-0.19	0.61	-0.28	0.09	0.73	0.82
Skewness	-0.14	-0.1	0.13	0.01	0.12	0.07	-0.13	-0.05
Kurtosis	4.81	4.98	4.38	3.79	4.14	5.68	4.14	3.57
Panel B: Sub-sample (pre-2005)								
	Spreading Pressure				Basis-Momentum			
	Low4	Mid	High4	Low4-High4	Low4	Mid	High4	High4-Low4
Mean	10.95	2.55	3.73	7.22	-3.57	2.49	18.49	22.06
Std. Dev.	16.2	10.86	14.95	20.49	17.93	10.28	18.55	23.27
Sharpe	0.68	0.24	0.25	0.35	-0.2	0.24	1	0.95
Skewness	-0.13	0.09	0.13	0.08	0.22	0.13	-0.07	-0.23
Kurtosis	3.4	3.39	3.68	3.59	4.18	3.14	3.75	3.57
Panel C: Sub-sample (post-2005)								
	Spreading Pressure				Basis-Momentum			
	Low4	Mid	High4	Low4-High4	Low4	Mid	High4	High4-Low4
Mean	7.2	1.24	-9.39	16.59	-6.68	0.2	8.8	15.47
Std. Dev.	20.12	13.73	20.7	20.5	19.98	15.24	17.7	21.58
Sharpe	0.36	0.09	-0.45	0.81	-0.33	0.01	0.5	0.72
Skewness	-0.13	-0.16	0.18	-0.05	0.07	0.06	-0.2	0.12
Skewness	5.01	5.16	4.12	3.97	4.04	5.35	4.5	3.56

Table 3.A-3: **Spreading Position Portfolio**

This table presents the summary statistics of commodity futures weekly portfolios returns, where we construct the portfolios by sorting commodity futures on the scaled spreading position, which is the fifty-two week average of speculators' spreading pressure scaled by its fifty-two week standard deviation. *Low3* (*High3*) consists of commodity futures ranked in the bottom (top) three for scaled spreading position, and the remaining twenty commodities constitute the portfolio called *Mid*. *Low3-High3* represents a long-short portfolio strategy of buying Low3 and shorting High3. Portfolio excess returns are calculated as equal-weighted average excess returns of portfolio constituents. Panel A presents results for the full sample from October 6, 1992 through December 26, 2018. Panels B and C show the sub-sample results from October 6, 1992 through January 4, 2005, and from January 4, 2005 through December 26, 2018, respectively.

Panel A: Full Sample				
	Low3	Mid	High3	Low3-High3
Mean	9.44	1.83	-3.69	13.13
Std. Dev.	20.62	12.15	21.43	24.41
Sharpe	0.46	0.15	-0.17	0.54
Skewness	0	-0.13	0.07	0.09
Kurtosis	5.39	4.96	4.58	3.68
Panel B: Sub-sample (pre-2005)				
	Low3	Mid	High3	Low3-High3
Mean	10.82	2.94	3.83	6.99
Std. Dev.	19.3	9.91	17.1	23.78
Sharpe	0.56	0.3	0.22	0.29
Skewness	0.3	0.03	-0.12	0.27
Kurtosis	4.39	3.11	3.91	3.99
Panel C: Sub-sample (post-2005)				
	Low3	Mid	High3	Low3-High3
Mean	8.34	0.94	-9.73	18.07
Std. Dev.	21.64	13.69	24.34	24.89
Sharpe	0.39	0.07	-0.4	0.73
Skewness	-0.17	-0.17	0.17	-0.05
Skewness	5.79	4.86	4.22	3.5

Table 3.A-4: **Spreading Pressure Portfolio within Each Sector**

This table presents the summary statistics of commodity futures weekly portfolios returns, where we construct the portfolios by sorting the commodity futures on the fifty-two week average of spreading pressure within five sectors: energy, grains, meats, metals, and soft. *Low1* (*High1*) consists of commodity futures ranked in the bottom (top) for spreading pressure in each sector, and the remaining commodities in each sector constitute the portfolio called *Mid*. *Low1-High1* represents a long-short portfolio strategy of buying Low1 and shorting High1. Portfolio excess returns are calculated as equal-weighted average excess returns of portfolio constituents. The sample period is from January 4, 2005 through December 26, 2018

	Energy Sector				Grain Sector			
	Low1	Mid	High1	Low1-High1	Low1	Mid	High1	Low1-High1
Mean	3.04	-2.09	-27.35	30.40	2.06	2.30	-3.36	5.42
Std. Dev.	33.76	29.34	42.63	41.49	33.40	20.17	30.19	34.87
Sharpe	0.09	-0.07	-0.64	0.73	0.06	0.11	-0.11	0.16
Skewness	0.25	0.19	0.26	-0.13	0.51	0.03	0.46	0.66
Kurtosis	5.75	5.28	3.84	4.42	7.60	4.13	4.65	7.55
	Meat Sector				Metal Sector			
	Low1	Mid	High1	Low1-High1	Low1	Mid	High1	Low1-High1
Mean	2.06	-4.00	-1.97	4.02	10.31	5.98	14.60	-4.29
Std. Dev.	19.75	17.18	23.22	25.01	24.72	21.04	29.74	23.91
Sharpe	0.10	-0.23	-0.08	0.16	0.42	0.28	0.49	-0.18
Skewness	-0.07	-0.23	-0.08	0.09	-0.39	-0.49	0.04	-0.17
Kurtosis	5.09	4.55	3.35	3.66	5.50	5.38	6.66	4.67
	Soft Sector							
	Low1	Mid	High1	Low1-High1				
Mean	9.07	-1.29	-8.00	17.07				
Std. Dev.	34.08	18.45	29.50	40.51				
Sharpe	0.27	-0.07	-0.27	0.42				
Skewness	0.40	0.14	0.20	0.14				
Skewness	4.48	4.05	3.91	3.18				

Table 3.A-5: **Fama-MacBeth Cross-Sectional Predictive Regressions**

This table presents the average coefficients by running Fama-MacBeth cross-sectional regressions of futures excess returns on the two-week (Panel A), three-week (Panel B), four-week (Panel C) lagged (fifty-two week average) spreading pressure ($\overline{SP}$). Included as control variables are basis-momentum (BM), hedgers' net position changes (Q_h) and/or speculators' net position changes (Q_s):

$$R_{i,t+k} = b_0 + b_{\overline{SP}}\overline{SP}_{i,t} + b_{BM}BM_{i,t} + b_Q^h Q_{i,t}^h + b_Q^s Q_{i,t}^s + \epsilon_{i,t+1}$$

Newey-West t-statistics with four lags and average R^2s are reported for each model specification. The sample period used in this table is between January 4, 2005 and December 26, 2018.

Model	(1)	(2)	(3)	(4)	(5)	(6)	(7)	(8)
Panel A: Return$(t+2)$								
$b_{\overline{SP}}$	-1.46				-1.34	-1.43	-1.38	-1.33
	(-2.81)				(-2.59)	(-2.69)	(-2.59)	(-2.49)
b_{BM}		1.03			1.09			1.28
		(1.57)			(1.71)			(1.89)
b_Q^h			2.47			2.14		0.57
			(2.61)			(2.20)		(0.20)
b_Q^s				-3.27			-2.91	-1.60
				(-3.19)			(-2.77)	(-0.54)
R^2	6.81%	6.42%	5.39%	5.34%	12.96%	12.16%	12.16%	22.84%
Panel B: Return$(t+3)$								
$b_{\overline{SP}}$	-1.42				-1.3	-1.28	-1.34	-1.2
	(-2.74)				(-2.55)	(-2.41)	(-2.52)	(-2.25)
b_{BM}		0.96			1.00			1.10
		(1.44)			(1.56)			(1.67)
b_Q^h			2.32			1.75		0.91
			(2.31)			(1.72)		(0.35)
b_Q^s				-1.94			-1.28	-0.62
				(-1.76)			(-1.12)	(-0.22)
R^2	6.81%	6.47%	5.25%	5.11%	12.98%	11.9%	11.82%	22.03%
Panel C: Return$(t+4)$								
$b_{\overline{SP}}$	-1.41				-1.24	-1.55	-1.56	-1.4
	(-2.73)				(-2.42)	(-2.93)	(-2.97)	(-2.68)
b_{BM}		0.92			0.93			0.95
		(1.35)			(1.43)			(1.35)
b_Q^h			3.18			2.91		5.43
			(2.97)			(2.72)		(2.07)
b_Q^s				-3.17			-2.94	3.12
				(-2.75)			(-2.54)	(1.05)
R^2	6.82%	6.47%	5.32%	5.28%	12.98%	12.06%	12.02%	22.41%

Table 3.A-6: **Spreading Pressure Factor versus the Szymanowska et al. (2014) Model: Spanning Regressions and GRS Tests**

This table presents a regression test to investigate whether the spreading pressure factor provides a significant intercept by using Szymanowska et al. (2014) three-factor model. This model has three factors constructed from a sort on the basis, the nearby return for the High3-minus-Low3 basis portfolio (R_{Basis}), the spreading return of the High3 portfolio ($R^{Spr}_{Basis_{high}}$), and the spreading return of the Low3 portfolio ($R^{Spr}_{Basis_{low}}$). t-statistics are calculated using Newey-West standard errors with a lag length of 1. This test uses the full sample from January 2, 1986 through June 30, 2018 and the two sub-samples (pre-2005 and post-2005)

	Full Sample	Pre-2005	Post-2005
α	15.52	8.81	20.36
	(3.19)	(1.19)	(3.19)
β_{Basis}	0.17	0.10	0.23
	(4.88)	(1.86)	(4.97)
$\beta^{Spr}_{Basis_{low}}$	-0.24	-0.22	-0.18
	(-1.71)	(-1.09)	(-0.92)
$\beta^{Spr}_{Basis_{high}}$	-0.04	0.10	-0.21
	(-0.31)	(0.55)	(-1.09)
R^2	3.55%	1.00%	7.13%
GRS-F	3.71	1.54	3.85
p-val	0.01	0.20	0.01

Table 3.A-7: **Cross-Sectional Asset Pricing Tests in Portfolio Level (nearby and spreading returns)**

This table presents the estimated risk premium on commodity futures risk factors by running Fama-MacBeth cross-sectional asset pricing tests. Six different model specifications are considered, and are nested in $R_{t,i} = \gamma_{t,0} + \lambda_{t,\overline{SP}}\beta_{t,\overline{SP}} + \lambda_{t,BM}\beta_{t,BM} + \lambda_{t,C}\beta_{t,C} + \lambda_{t,M}\beta_{t,M} + \lambda_{t,Avg}\beta_{t,Avg} + \epsilon_{t,i}$. We regresse the average returns of thirty-four commodity-sorted portfolios on their risk exposures. The portfolios include the nearby and spreading returns of twelve portfolios sorted on spreading pressure, basis momentum and basis-momentum (the High3, Mid, and Low3 portfolios sorted on each signal) and five sector portfolios (energy, grains, meats, metals and softs). Model (1) is a single-factor model that contains the spreading pressure factor only, Model (2) adds the basis-momentum factor, Model (3) is the Boons and Prado (2019) model, and Model (4) is the Bakshi et al. (2019) model. Models (5) and (6) add the spreading pressure factor to Models (3) and (4), respectively. Two versions of the t-statistics are reported following Shanken (1992) (in parentheses) and Kan et al. (2013) (in square brackets). OLS R^2 and GLS R^2 (in parentheses) are in the last column. Panel A presents results for the full sample from October 6, 1992 through December 26, 2018. Panels B and C show the subsample results for October 6, 1992 through January 4, 2005, and for January 4, 2005 through December 26, 2018, respectively.

Model	γ_0	λ_{SP}	λ_{BM}	λ_C	λ_M	λ_{Avg}	R^2
Panel A: Full Sample							
(1)	1.11	15.81					29.66%
	(0.72)	(2.87)					(11.58%)
	[0.65]	[2.78]					
(2)	1.19	12.52	20.35				57.80%
	(0.77)	(2.32)	(3.81)				(24.62%)
	[0.69]	[2.27]	[3.51]				
(3)	-1.09		23.80			3.27	61.67%
	(-2.13)		(4.28)			1.27	(17.44%)
	[-1.90]		[4.18]			1.04	
(4)	-0.87			5.27	17.33	2.79	37.01%
	(-1.72)			(0.99)	(2.90)	(1.09)	(6.22%)
	[-1.58]			[0.94]	[3.01]	[0.92]	
(5)	-1.16	13.64	21.03			3.58	74.92%
	(-2.26)	(2.56)	(3.94)			(1.40)	(25.84%)
	[-2.03]	[2.52]	[3.86]			[1.11]	
(6)	-1.04	15.04		3.67	15.66	3.35	56.68%
	(-2.06)	(2.82)		(0.69)	(2.64)	(1.32)	(16.42%)
	[-1.88]	[2.87]		[0.64]	[2.88]	[1.08]	

Table 3.A-7 - **Continued**

Model	γ_0	λ_{SP}	λ_{BM}	λ_C	λ_M	λ_{Avg}	R^2
Panel B: Pre-2005							
(1)	2.60	12.13					8.74%
	(1.31)	(1.57)					(2.95%)
	[1.39]	[1.37]					
(2)	2.24	8.67	24.17				37.90%
	(1.13)	(1.13)	(2.70)				(16.42%)
	[1.18]	[1.06]	[2.94]				
(3)	-1.23		23.60			5.60	55.09%
	(-1.42)		(2.64)			(1.72)	(17.87%)
	[-1.67]		[2.97]			[1.76]	
(4)	-1.09			-1.16	26.06	5.16	54.05%
	(-1.35)			(-0.14)	(2.73)	(1.63)	(15.24%)
	[-1.38]			[-0.14]	[3.03]	[1.73]	
(5)	-1.32	9.97	22.52			5.74	58.61%
	-1.55	1.32	2.54			1.77	(19.59%)
	[-1.84]	[1.24]	[2.85]			[1.79]	
(6)	-1.28	11.60		-1.66	25.63	5.44	61.80%
	(-1.62)	(1.51)		(-0.20)	(2.69)	(1.72)	(18.26%)
	[-1.71]	[1.55]		[-0.20]	[3.01]	[1.80]	
Panel C: Post-2005							
(1)	0.01	20.26					58.06%
	(0.00)	(2.74)					(15.99%)
	[0.00]	[2.66]					
(2)	0.34	18.21	16.33				72.05%
	(0.16)	(2.50)	(2.28)				(22.95%)
	[0.13]	[2.41]	[1.91]				
(3)	-1.16		23.52			1.54	46.24%
	(-1.76)		(3.32)			(0.40)	(10.58%)
	[-1.51]		[2.78]			[0.31]	
(4)	-0.89			13.72	12.01	0.96	28.65%
	(-1.35)			(1.91)	(1.54)	(0.25)	(2.25%)
	[-1.25]			[1.85]	[1.49]	[0.22]	
(5)	-1.25	19.04	18.23			2.19	80.18%
	(-1.90)	(2.65)	(2.73)			(0.57)	(23.25%)
	[-1.60]	[2.54]	[2.36]			[0.44]	
(6)	-1.13	20.38		9.01	6.94	1.90	63.02%
	(-1.71)	(2.93)		(1.30)	(0.92)	(0.49)	(16.18%)
	[-1.52]	[2.72]		[1.28]	[0.97]	[0.42]	

Table 3.A-8: **Cross-Sectional Asset Pricing Tests with Different Model Specifications in the Commodity Level**

This table presents cross-sectional tests for five asset pricing factor models in the commodity level, nested in $R_{t+1,i} = \gamma_{t,0} + \lambda_{t,SP}\beta_{t,SP} + \lambda_{t,BM}\beta_{t,BM} + \lambda_{t,C}\beta_{t,C} + \lambda_{t,M}\beta_{t,M} + \lambda_{t,Avg}\beta_{t,Avg} + \epsilon_{t,i}$. β is estimated over a one-year rolling window of weekly returns. Model (1) is a single-factor model that contains the spreading pressure factor only, Model (2) adds the basis-momentum factor, Model (3) is the Boons and Prado (2019) model, and Model (4) is the Bakshi et al. (2019) model. Models (5) and (6) add the spreading pressure factor to Models (3) and (4), respectively. t-statistics are reported following Fama and MacBeth (1973) (in parentheses), and we also present the cross-sectional R^2. Panel A presents results for the full sample from October 6, 1992 through December 26, 2018. Panels B and C show the subsample results for October 6, 1992 through January 4, 2005, and for January 4, 2005 through December 26, 2018.

Model	γ_0	λ_{SP}	λ_{BM}	λ_C	λ_M	λ_{Avg}	R^2
Panel A: Full Sample							
(1)	2.08	10.38					6.67%
	(0.84)	(2.13)					
(2)	2.38	11.55	2.65				27.30%
	(0.98)	(2.37)	(0.43)				
(3)	-1.49		5.88			3.65	31.96%
	(-0.60)		(0.97)			(1.22)	
(4)	1.30			15.65	0.64	0.86	38.29%
	(0.50)			(2.00)	(0.09)	(0.29)	
(5)	-1.84	12.59	5.72			4.01	34.20%
	(-0.73)	(2.59)	(0.93)			(1.33)	
(6)	0.80	14.35		11.41	-5.09	1.36	37.42%
	(0.30)	(2.94)		(1.45)	(-0.74)	(0.45)	
(7)	-1.67	14.73	11.50	7.57	-3.68	3.83	45.30%
	(-0.61)	(3.00)	(1.78)	(0.94)	(-0.53)	(1.20)	

Table 3.A-8 - **Continued**

Model	γ_0	λ_{SP}	λ_{BM}	λ_C	λ_M	λ_{Avg}	R^2
Panel B: Pre-2005							
(1)	4.10	3.49					1.00%
	(1.33)	(0.45)					
(2)	4.13	5.71	4.00				1.08%
	(1.33)	(0.74)	(0.38)				
(3)	-0.77		7.83			5.09	23.84%
	(-0.22)		(0.77)			(1.33)	
(4)	2.46			14.31	-10.22	1.86	24.78%
	(0.72)			(1.12)	(-0.93)	(0.50)	
(5)	-0.91	5.95	5.20			5.25	30.10%
	(-0.26)	(0.77)	(0.51)			(1.36)	
(6)	1.69	4.50		10.35	-16.40	2.66	27.38%
	(0.49)	(0.57)		(0.81)	(-1.53)	(0.70)	
(7)	-1.14	5.95	11.28	3.04	-11.92	5.49	27.83%
	(-0.31)	(0.76)	(1.04)	(0.23)	(-1.09)	(1.34)	
Panel C: Post-2005							
(1)	-0.81	17.67					56.87%
	(-0.21)	(2.78)					
(2)	-0.25	17.58	3.55				63.91%
	(-0.07)	(2.71)	(0.46)				
(3)	-3.23		5.91			2.47	43.89%
	(-0.88)		(0.78)			(0.54)	
(4)	-1.42			19.39	5.74	0.66	77.20%
	(-0.36)			(1.90)	(0.64)	(0.14)	
(5)	-3.83	18.99	7.40			3.10	68.43%
	(-1.04)	(2.94)	(0.94)			(0.67)	
(6)	-1.90	23.16		14.87	-0.31	1.13	75.96%
	(-0.49)	(3.62)		(1.43)	(-0.03)	(0.24)	
(7)	-4.08	22.51	13.09	13.83	-0.37	3.32	80.78%
	(-1.01)	(3.47)	(1.60)	(1.32)	(-0.04)	(0.68)	

Table 3.A-9: **Spreading Pressure and the Term Structure of Futures Prices**

This table reports the predictive regression of the one week-ahead slope and curvature of the commodity futures term structure on spreading pressure and hedging pressure:

$$\{Slope_{t+1}, Curvature_{t+1}\} = \alpha_{t+1} + \beta_{SP} SP_t + \beta_{HP} HP_t + \varepsilon_{i,t+1}.$$

We define the slope of the futures curves as $slope_t = \frac{\ln F_t^3 - \ln F_t^1}{T_3 - T_1}$, and the curvature as $curvature_t = \frac{\ln F_t^3 - \ln F_t^2}{T_3 - T_2} - \frac{\ln F_t^2 - \ln F_t^1}{T_2 - T_1}$. We report the results for four subgroups as well as the whole group. *Group* indicates the sub-sample depending on the shape of the term structure at time t, i.e., 1) positive slope, positive curvature, 2) positive slope, negative curvature, 3) negative slope, positive curvature, and 4) negative slope, negative curvature. *Percentage* (*Mean of SP*) denotes the proportion of the sample (average spreading pressure) for each group. The regression controls for both time- and commodity-fixed effects, as well as for time to earliest maturity date, for each commodity at each point in time. t-statistics, based on standard errors clustered at the time dimension, are in parentheses. The sample period is October 6, 1992 through January 4, 2005.

Group	Percentage	Mean of SP	$Slope_{t+1,i} \times 100$			$Curv_{t+1,i} \times 100$		
			$SP_{t,i}$	$HP_{t,i}$	R^2	$SP_{t,i}$	$HP_{t,i}$	R^2
(1) $+Slope$, $+Curv$	22.49%	6.39%	0.17	-0.05	46.22%	0.03	-0.05	18.43%
			(0.98)	(-2.42)		(0.12)	(-0.95)	
(2) $+Slope$,$-Curv$	40.32%	6.73%	0.04	-0.09	25.33%	-0.70	-0.11	26.18%
			(0.34)	(-4.90)		(-4.42)	(-4.80)	
(3) $-Slope$, $+Curv$	17.29%	5.56%	0.80	-0.10	28.66%	0.10	-0.04	30.21%
			(3.48)	(-2.16)		(0.35)	(-0.93)	
(4) $-Slope$, $-Curv$	19.89%	5.78%	-0.95	-0.07	38.53%	-0.93	-0.13	26.22%
			(-2.66)	(-1.45)		(-2.02)	(-1.87)	
(5) *All*	100%	6.27%	0.24	-0.13	14.17%	-0.67	-0.08	6.81%
			(1.96)	(-7.60)		(-4.44)	(-4.17)	

Table 3.A-10: **Commodity Portfolios Sorted on Spreading Pressure at the Trader Category Level (DCOT report)**

This table presents the summary statistics of commodity futures weekly portfolio returns, where we construct the portfolios by sorting commodity futures on the fifty-two week average of spreading pressure from money managers, other reportables, swap dealers, and all non-commercials. *Low3* (*High3*) consists of commodity futures ranked in the bottom (top) three for spreading pressure or basis-momentum, and the remaining twenty commodities constitute the portfolio called *Mid*. *Low3-High3* represents a long-short portfolio strategy of buying Low3 and shorting High3. Portfolios' excess returns are calculated as equal-weighted average excess returns of portfolio constituents. The sample period is June 13, 2006 through December 26, 2018.

	Spreading Pressure (Money Managers)				Spreading Pressure (Other Reportable)			
	Low3	Mid	High3	Low3-High3	Low3	Mid	High3	High3-Low3
Mean	0.55	0	-7.74	8.29	4.75	-0.47	-8.93	13.68
Std. Dev.	22.51	14.35	24.3	24.75	22.98	15.14	19.09	24.01
Sharpe	0.02	0	-0.32	0.34	0.21	-0.03	-0.47	0.57
Skewness	-0.12	-0.2	0.23	-0.02	-0.19	-0.05	-0.05	-0.1
Kurtosis	5.05	4.8	4.27	3.59	5.31	5.55	3.43	4.11
	Spreading Pressure (Swap Dealers)				Spreading Pressure			
	Low4	Mid	High4	Low4-High4	Low4	Mid	High4	High4-Low4
Mean	4.59	-0.32	-9.71	14.3	6.07	0.14	-14.1	20.17
Std. Dev.	20.14	14.61	25.65	25.9	23.54	14.19	22.89	23.79
Sharpe	0.23	-0.02	-0.38	0.55	0.26	0.01	-0.62	0.85
Skewness	0.08	-0.1	0.11	0.09	-0.12	-0.1	-0.01	-0.1
Kurtosis	3.36	4.67	5.25	3.54	5.16	5.06	3.77	3.93

Appendix 3.B Figures

Figure 3.A-1: **Information Efficiency of Both Legs of Spreading Pressure Portfolios**

This figure presents the price delay measure (inefficiency) for the long (low spreading pressure) and short (high spreading pressure) legs of the spreading pressure portfolio around 2005 (between 2001 and 2008). Following Hou and Moskowitz (2005) and Brogaard et al. (2019), we compute the ratio of R^2 from a regression of weekly portfolio returns on four lags of portfolio returns of each leg. The pre-2005 series is normalized to 1, and the post-2005 series is relative to the pre-2005 period.

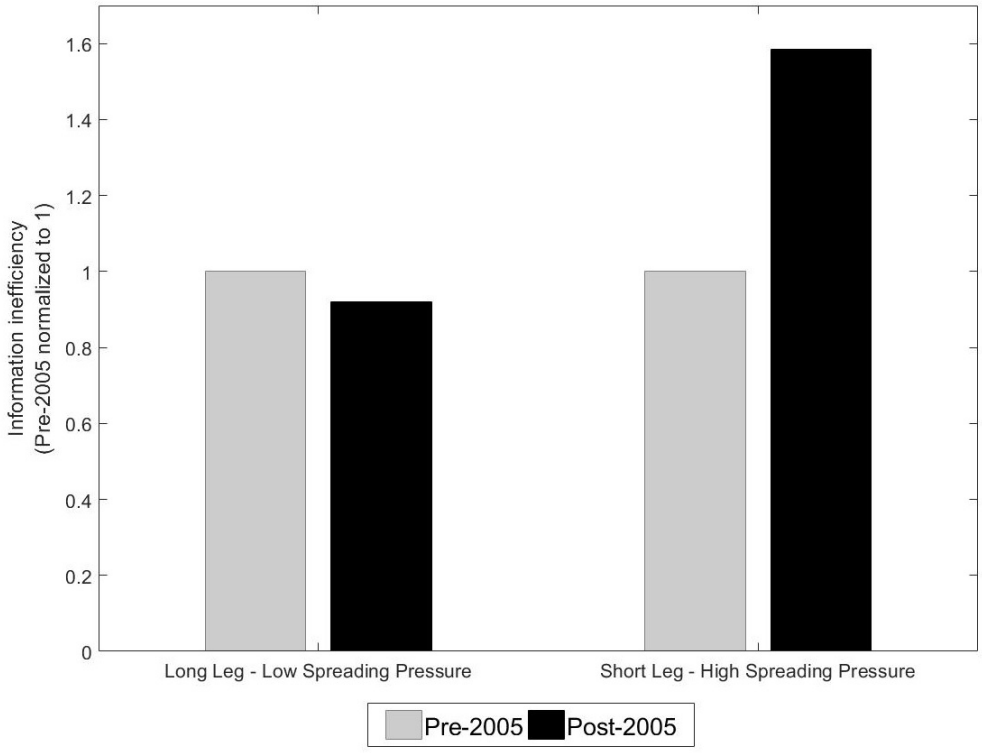

Figure 3.A-2: **Cumulative Excess Returns of Commodity Pricing Portfolios**

This figure presents cumulative exess returns for commodity futures pricing portfolios: a long-short portfolio based on basis-momentum, or spreading pressure, the short leg of the spreading pressure portfolio, a portfolio by shorting natural gas and WTI crude oil, and a portfolio constructed by going long on off-index commodities and shorting index commodities. The sample period is January 4, 2005 through December 26, 2018.

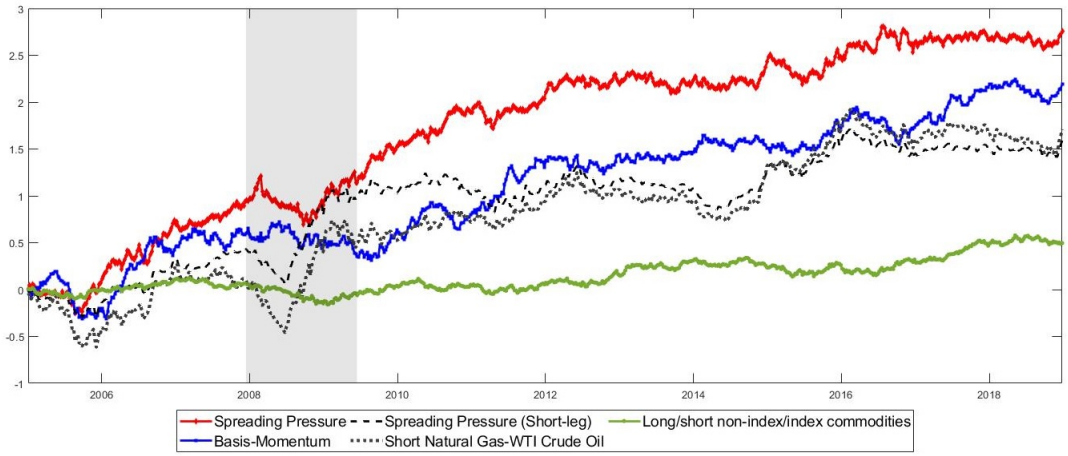

Figure 3.A-3: **Volatility and Liquidity of Both Legs of Spreading Pressure Portfolios**

This figure presents volatility and illiquidity for the long and short legs of the spreading pressure portfolio. Volatility of a portfolio is measured by equally weighted average of sum of squared daily returns of each commodity in each week. Illiquidity of a portfolio is the equally weighted average of Amihud measure (scaled by a billion) of each commodity in the portfolio. The sample period is January 4, 2005 through December 26, 2018.

(a) **Volatility**

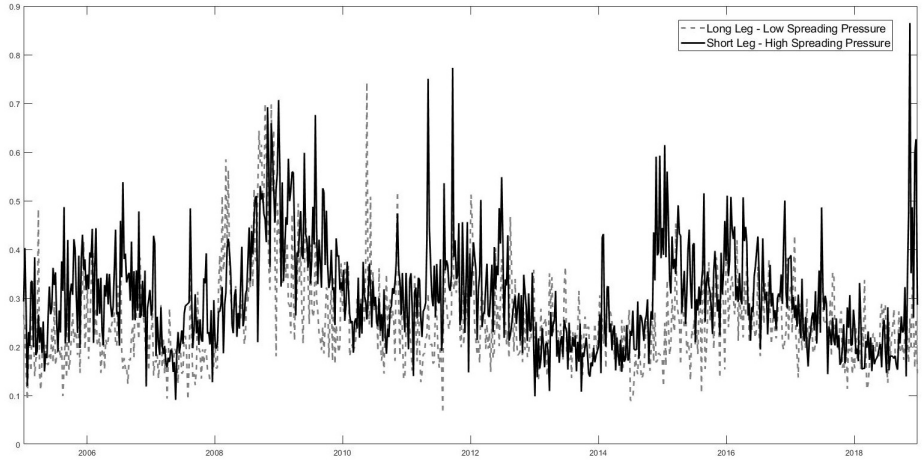

(b) **Liquidity**

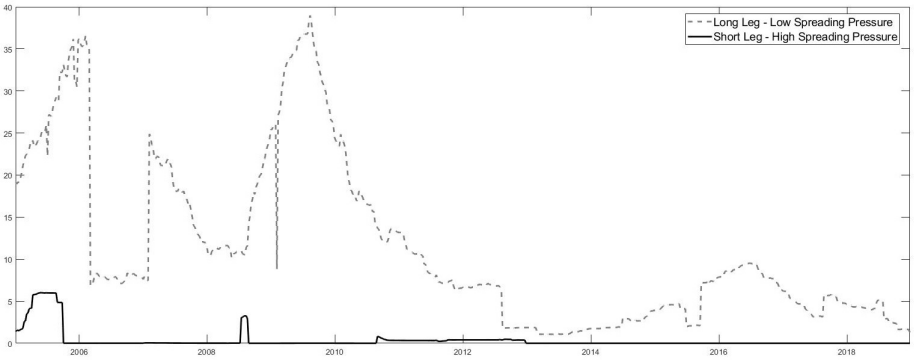

Figure 3.A-4: **Spreading Pressure and Commodity Turnover**

This figure presents commodity annualized turnover and the annual average of spreading pressure from all speculators, for managed money only, and for other reportable only. The figure includes two commodities, natural gas and platinum. The sample period is 1993 through 2018.

(a) **Natural Gas**

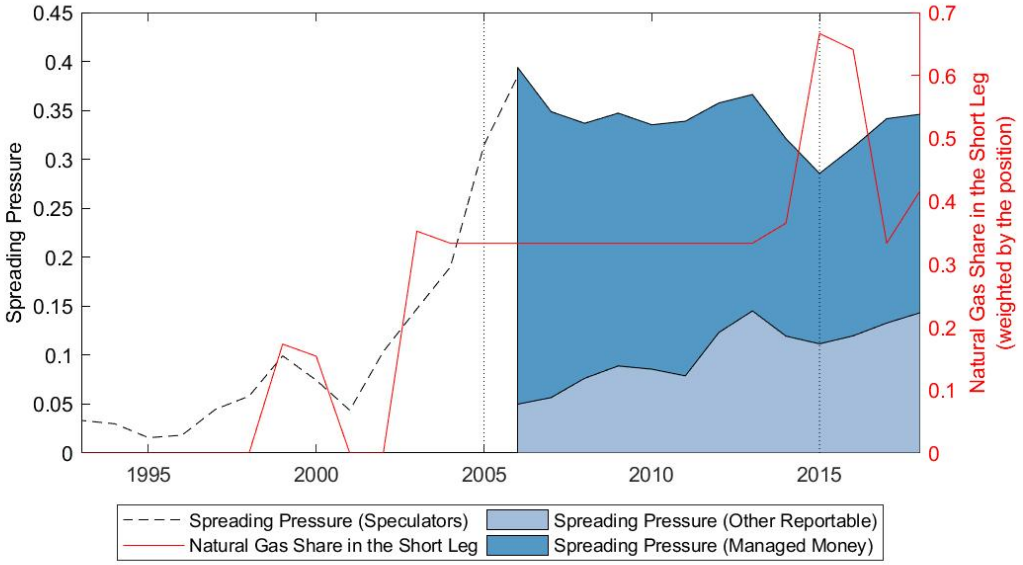

(b) **Platinum**

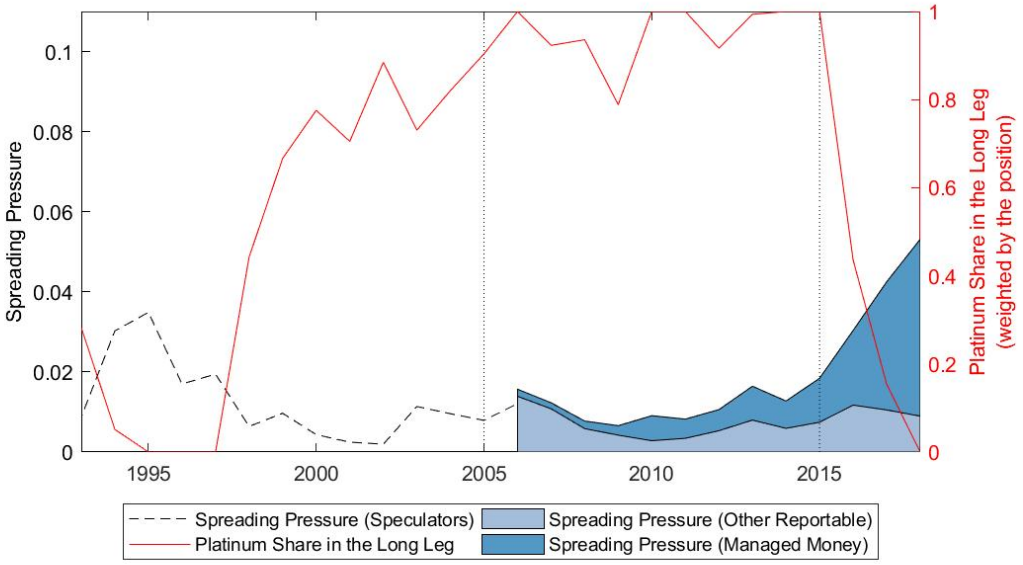

Chapter 4

Risk-Corrected Probabilities of Binary Events

4.1 Introduction

Knowledge of the ex ante physical probabilities of future infrequent but extreme events is crucial to asset pricing. These events may significantly affect asset prices, for instance, states of the world with large negative payoffs can distort prices even when their probabilities are very small. Under the "rare disasters" view, the change of event-related asset return is due to the event risk, which carries a significant risk premia (Barro, 2009; Farhi and Gabaix, 2015; Seo and Wachter, 2019). However, under the "peso problem" view, the return change of any asset is due to an expectation of a discrete shift in the return distribution (Rogoff, 1977, 1980; Lewis, 2016). Specifically, before the event outcomes' occurrence, financial market participants may speculate the potential outcomes via the event-related assets. The speculative activities and market participants' belief of future outcome have impacts on the shape of forward-looking return distributions. The degree of which the prices absorb the impact of the event before the event's actual occurrence depends on the extent market participants anticipate the event's actual outcome.

Building upon the latter standpoint, our work aims at retrieving, from market prices (options and prediction markets) and past opinion polls, a proxy for physical probability of a particular binary political event: the European Union (EU) withdrawal referendum held by the United Kingdom (UK) on the 23 June 2016 (Brexit). This event represented the possibility of a significant change in the country's international trade and immigration policy. The UK would cease to participate in that free trade area, becoming a more closed economy, at least in the short run. Agents would thus be expecting that the sterling (British pound or GBP) value to the other currencies, especially to the United States dollar (USD) would be negatively impacted. Figure 4.1a shows that there was a sharp depreciation of the GBP to the USD on the day after the referendum. On the same day, the change in out-of-the-money put option prices was also extreme relative to normal daily changes in option prices (Figure 4.1b). Does this suggest that the Brexit probability was negligible or substantially underestimated in the foreign exchange (FX) spot and option markets?

To answer this question, we first investigate the risk-neutral density (RND) extracted from British Pound options. We find that RNDs from short maturities options have a bimodal distribution one week before the referendum, in line with the evidence provided by Kostakis et al. (2020), and risk-neutral tail risk of GBP/USD deviates from its normal level since the beginning of 2016. Therefore, it is reasonable to suppose that agents attached a probability that a discrete change in the economic fundamentals that govern the dynamics of the GBP exchange rate would occur, which is the typical description of a "Peso Problem".

Under the risk-neutral assumption, several proxies of the Brexit probability were created in the financial market, including prediction and option markets. The reciprocal of odds from prediction markets are common as probabilities of event outcomes under risk neutrality (for example, Belke et al. (2018) and Hanke et al. (2018)). More recently, Kostakis et al. (2020) estimate Brexit probabilities from the British Pounds

options market, following the model-based methodology of Borochin and Golec (2016). They argue that option markets provide a good alternative to prediction markets for event probability extraction, since only some major events are considered in prediction markets. Following the literature, we also extract daily risk-neutral Brexit probabilities from both prediction and option markets, but different from Kostakis et al. (2020), we use both model-based (Borochin and Golec, 2016) and model-free (Langer and Lemoine, 2020) methods to obtain option-implied probabilities. We find that cheap out-of-the-money options carry more information about the probability of the 'Brexit' outcome. On average, the options market reveals a higher "Leave" probability by comparison to the prediction market. However, the question remains whether the attached probability implied in the financial markets is close to the physical probability of the peso event?

In this case, better estimates of physical probabilities are essential to understanding how well the financial markets anticipate the probability of binary political events such as Brexit, even though estimation of the physical probability of any event is very challenging. Sayers (2016) claims that internet polls were the closest to the Brexit physical probabilities. The underlying reasoning is that intention to vote leave was around 50% during most of the sample period, such that the actual result was within the margin of error. While Cesar et al. (2017) document a correlation between telephone and internet polls, they also show that the voting intention (constructed using 23 million tweeter hashtags) is not higher than 71%. Assuming that polls are independent referendum experiments and the market participants form a belief about the referendum outcome by learning from available polls' outcomes, we construct subjective physical probability proxy by considering a set of telephone and internet polls. On one hand, we find that past political opinion poll results capture well how market participants *learn* about the "Leave" probability. On the other hand, our findings also reveal that the probability estimates under risk neutrality from both option and prediction markets fail to match the likelihood of a Brexit outcome suggested by political opinion polls data.

The limitations of the risk-neutral Brexit probabilities extracted from prediction and options markets may cause it to deviate from the subjective probabilities from polls. One limitation is that state prices reflect agents' perception of wealth in both states of the world: with and without Brexit. Another limitation is that participants in both of these markets may have different attitudes towards risk. To eliminate these limitations, our paper thus provides both non-parametric (using the Ross-Recovery theorem - Ross (2015)) and parametric corrections (calibrating stochastic discount factors) of the risk-neutral probabilities obtained from these two markets. We argue that this risk correction is important in bringing probabilities closer to their perceived (subjective) physical measure estimated from past polls. To minimize the distance between risk-corrected probabilities and subjective probabilities, under the assumption that the agents in both markets have same expectation on the relative wealth between these two states, the average agent in prediction markets has always a stronger risk preference than the average agent in option markets. Specifically, average agents in both markets are risk seeking if they expect lower wealth in the "Leave" state compared to the "Remain" state.

Although polls reveal the proportion of "remain" and "leave" votes, there are still the crucial indecisive poll participants. Therefore, extracting physical probabilities of the future state of the world from polls could be more informative by attributing a probability that the indecisive will vote either in favor or against Brexit. This can only be reasonably done if the disaggregated Survey data is available, in addition to at least some personal characteristics of the respondents.[1] In this paper, we use the British Election Study (BES) survey data with individual-level information as an example and obtain the intention to vote "leave" as 51.07%. Daily estimates from the Survey data suggest that the survey-based estimates are less sensitive to the new information about the event compared to prediction and financial markets. Or put differently, the markets

[1]Venturi et al. (2021), for instance, attribute a probability, by estimating a Probit model, that the indecisive deputy would vote in favor of the impeachment of the Brazilian President in 2016.

react to news (e.g., Murder of MP Cox on 16 June 2016) about a binary event outcome, while the voting intention is primarily driven by persistent characteristics (e.g., age, income, education, views about immigration and risk preferences) of the voters.

The remainder of the paper is organized as follows. Section 4.2 shows the methodology employed to retrieve risk neutral probabilities from the option markets and the theory underlying the correction for risk. Section 4.3 explains the data we used in this paper. Section 4.4 recovers risk-neutral probabilities for the Brexit referendum, probabilities with risk-correction, subjective probabilities calculated from opinion polls and voting intention estimated from the BES Survey data. In the last section, we present our concluding remarks.

4.2 Methodology

4.2.1 Option-Implied Risk-Neutral Distributions

The risk-neutral probability distribution of financial assets contains information about investors' beliefs about the future performance of the underlying asset, and reflects investors' attitudes towards risk. Benefiting from options with a wide range of strike prices, we can use option prices to derive the risk-neutral probability distribution of the underlying asset.

To extract the risk-neutral probability distribution (RND) of the underlying asset prices, we follow the non-parametric method proposed by Figlewski (2009). This model-free method with flexible extreme value tails allows for some non-standard features in approximated RNDs, like fat tails, bimodality and so on. It is particularly useful in a binary world, like the Brexit period. We believe that this method is sufficient to infer a well-performing RND function from European options. However, the options we use in this paper are currency options listed on the Chicago Mercantile Exchange (CME), which are American options prior to 2017. Therefore, to make our data fit into this

non-parametric methodology, we convert American option prices into European option prices in the RND extraction steps. The steps about how to extract a well-behaved RND is in Appendix Appendix 4.A.

4.2.2 Forward-Looking Tail Risk

Apart from analysing the moments from RNDs we are also interested in exploring the information from option-implied measures of tail risk (Ait-Sahalia and Lo, 2000; Leiss and Nax, 2018). Tail risk measures under the risk-neutral probability capture the investors' forward-looking assessment of the likelihood of the adverse market state, the probability of the 'tail event' occurring, and the evolution of their belief over time.

In order to capture changes in market expectations, we focus on changes in the quantiles of RNDs (Bevilacqua et al., 2021). We denote the $\alpha\%$ quantiles of the RND extracted from prices of contracts expiring on time T_o as $\Pi^{\leftarrow}_{t,T_o}$ and define it as

$$\Pi^{\leftarrow}_{t,T_o}(x) := R^* \quad \text{where} \quad \Pi^{\leftarrow}_{t,T_o}(R^*) := Prob(R_{t,T_o} \leq \ R^*) = \alpha, \tag{4.1}$$

where $R_{t,T_o} = \ln \frac{S_{T_o}}{S_t}$ and S_t is the FX spot rate at time t (GBP/USD in our case). This measure is similar as option-implied Value-at-Risk (VaR) and the difference is these two measures have the opposite sign.

However, we cannot extract the RND of FX spot rate directly, since CME monthly currency options are written on the nearest futures contracts with March-quarterly maturity.[2] Thus, we make adjustment for the difference between the option and its underlying future expiry days (Cincibuch, 2004; Huchede and Wang, 2020). The price of a CME call option at time t is $C(t, K, T_f, T_o)$, with strike price K, maturity T_o and underlying future contract that expires at T_f. The time t price of a CME future with maturity T_f

[2]For example, an option expiring on January is written on a future expiring on the nearest March. Even for an option expiring in March, the difference between the option expiry day and the underlying future expiry day is about two weeks.

is F_{t,T_f}. The aim of this transform is to an option written on a future that also expires on the option expiry day, which is equivalent to an option on spot. We denote the US and UK interest rates as $r^{US}_{T_o,T_f}$ and $r^{UK}_{T_o,T_f}$, respectively. According to the no-arbitrage relationship,

$$F_{T_o,T_f} = F_{T_o,T_o} e^{(r^{US}_{T_o,T_f} - r^{UK}_{T_o,T_f})(T_f - T_o)}. \tag{4.2}$$

Then, we can rewrite the call option price as

$$\begin{aligned}
C(t,K,T_f,T_o) &= e^{-r_t(T_o-t)}\mathbb{E}_t[\max(F_{T_o,T_f} - K, 0)], \\
&= e^{-r_t(T_o-t)}\mathbb{E}_t[\max(F_{T_o,T_o} e^{(r^{US}_{T_o,T_f} - r^{UK}_{T_o,T_f})(T_f-T_o)} - K, 0)], \\
&= e^{(r^{US}_{T_o,T_f} - r^{UK}_{T_o,T_f})(T_f-T_o)} e^{-r_t(T_o-t)}\mathbb{E}_t[\max(F_{T_o,T_o} - \bar{K}, 0)], \\
&= e^{(r^{US}_{T_o,T_f} - r^{UK}_{T_o,T_f})(T_f-T_o)} e^{-r_t(T_o-t)}\mathbb{E}_t[\max(S_{T_o} - \bar{K}, 0)], \\
&= e^{(r^{US}_{T_o,T_f} - r^{UK}_{T_o,T_f})(T_f-T_o)} C(t,\bar{K},T_o),
\end{aligned} \tag{4.3}$$

where

$$\bar{K} = K e^{-(r^{US}_{T_o,T_f} - r^{UK}_{T_o,T_f})(T_f-T_o)}. \tag{4.4}$$

Similarly, we can convert the put price from the option on the future to an option on the spot. Then, we can extract RNDs of FX spot rates from spot option prices and calculate market expectations in different horizons.

4.2.3 Option-Implied Risk-Neutral Event Probability

4.2.3.1 Model-Based Estimation

To analyze the evolution of the uncertainty about Brexit outcome, we infer a time-series of pre-Brexit probabilities by following the methodology of Borochin and Golec (2016). This methodology uses options to estimate risk-neutral probabilities and to identify state-contingent underlying asset prices and volatilities. Following the same framework, our world is binary with two limiting future states: one in which the UK

leaves the European Union ("Leave" state) and the other in which the UK remains in the European Union ("Remain" state). Then, using the information from futures and options markets, we estimate five latent variables, which correspond to the futures prices and volatilities in each state of the world and the risk-neutral probability in one of the states.

Consider that the USD price of one unit of a GBP in a future contract at time t is given by F^L_{t,T_f} in the "Leave" state, and F^R_{t,T_f} in the "Remain" state, where T_f is the maturity of the future contract and t is a time point before the Brexit referendum, which was held on 23 June, 2016. In the absence of arbitrage, the future price observed at time t must be the probability weighted average of the future price in the "Leave" state and the future price in the "Remain" state:

$$F_{t,T_f} = p^L_t \times F^L_{t,T_f} + (1 - p^L_t) \times F^R_{t,T_f}, \tag{4.5}$$

where p^L_t is the time t risk-neutral probability that the UK leaves the European Union ("Leave" probability).

Consider a set of options on GBPUSD futures contracts with the expiry day T_o, where T_o is a time point after the Brexit referendum. In the absence of arbitrage, the European options price observed at time t ($O(F_{t,T_f}, K, \sigma_t, T_o)$) should be the probability weighted average of the theoretical option price in the "Leave" state ($\hat{O}(F^L_{t,T_f}, K, \sigma^L_t, T_o)$) and the theoretical option price in the "Remain" state ($\hat{O}(F^R_{t,T_f}, K, \sigma^R_t, T_o)$):

$$O(F_{t,T_f}, K, \sigma_t, T_o) = p^L_t \times \hat{O}(F^L_{t,T_f}, K, \sigma^L_t, T_o) + (1 - p^L_t) \times \hat{O}(F^R_{t,T_f}, K, \sigma^R_t, T_o), \tag{4.6}$$

where K is the strike price, σ^L_t and σ^R_t are return volatilities in the "Leave" state and "Remain" state, respectively.

We use the Black model (Black, 1976) to calculate theoretical prices for European futures options. Since the option contracts in our sample are American-style, to fit our

data into equation (4.6), we convert the American option prices into European option prices by following the same steps in Appendix Appendix 4.A. First, we obtain the implied volatility from the American option price by using Barone-Adesi-Whaley (BAW) American futures option pricing model (Barone-Adesi and Whaley, 1987). Then, we use the BAW implied volatility in the Black model (Black, 1976) to calculate the price of the corresponding European option.

According to equation (4.5) and (4.6), our aim now is to estimate the five parameters at each point in time t, $\Theta_t = \left\{p_t^L, F_{t,T_f}^L, F_{t,T_f}^R, \sigma_t^L, \sigma_t^R\right\}$. We proceed by constructing a system that includes a GBPUSD future contract and N traded options that are written on this future contract with a single expiry day T_o and a wide range of strike prices K_i, where $i = 1, 2, ..., N$.

We believe that both call and put options could bring information to the system. Borochin and Golec (2016) set $N = 8$ and select eight call options only to estimate these latent parameters from the system. They argue that put option price is less reliable to be incorporated in the system since the trade of stock put options is usually less frequent than stock call options. Note that a call on GBP/USD is a put on USD/GBP vice versa, this is not necessarily true for currency options. When we look at the open positions of options, the open interest of call options is significantly lower than the put options in our sample period, which guarantees the reliability and information content of put option prices. Also, the probability of Brexit may significantly reduce the British Pound's future price, so using put options in the system to recover the Brexit outcome probability is very useful (Langer and Lemoine, 2020). Due to the reasons mentioned above, our system incorporates both put and call options with positive open interest.

Different from Borochin and Golec (2016)'s method with ATM options only, we use all observed (deep) out-of-the-money (OTM) and at-the-money (ATM) options. We believe that options with different strike prices could bring additional information to the system, for example, cheap out-of-the-money options might carry important information

about tail risk (Kelly and Jiang, 2014). Following Borochin and Golec (2016), we use options with short maturity (maturity date is still after the event day), since their prices are more sensitive to changes in underlying asset price.

We denote observed asset prices in the left-hand side of equations (4.5) and (4.6) as M_t, and theoretical asset price in the right-hand side as $\hat{M}_t$. The non-linear least squares estimation of Θ_t involves numerically solving of a optimization problem with objective function

$$\Theta_t = \arg\min_{\Theta_t} \sum_{i=1}^{N+1} \omega_{t,i} \{M_{t,K_i} - \hat{M}_{t,K_i}(\Theta_t)\}^2, \tag{4.7}$$

and constraints

$$s.t. \begin{cases} 0 < F^L_{t,T_f} \leqslant F_{t,T_f} \leqslant F^R_{t,T_f}, \\ \sigma^R_t, \sigma^L_t > 0, \\ 0 < p^L_t < 1, \end{cases} \tag{4.8}$$

where $\omega_{t,i}$ is the weight on observation i at time t. Our baseline specification sets $\omega_{t,i}$ as a constant value 1 across i, a standard approach used in the literature. However, cheap out-of-the-money options might carry important information about potential extreme events, so, different from Kostakis et al. (2020), we also estimate the system by assigning a large weight to error terms for cheap options. Specifically, our second and third specifications set $\omega^2_{t,i} = \frac{1}{M_{t,K_i}}$ and $\omega^3_{t,i} = \frac{1}{M^2_{t,K_i}}$, respectively (Carvalho and Guimaraes, 2018).

4.2.3.2 Model-Free Estimation

Model-based estimation of option-implied probabilities provides valuable insights about the time-varying event probabilities. However, this method requires an option pricing model that is able to reconcile observed and theoretical option prices. The strict assumptions of the underlying return process in option pricing models are commonly violated

in the real world, e.g., the implied volatility smiles and smirks. In order to estimate the probability of an event using a model-free methodology, we follow Langer and Lemoine (2020). Following the same notation in the previous section, we re-write equation (4.6) as

$$\frac{O(F_{t,T_f}, K, T_o)}{\bar{O}(F^L_{t,T_f}, K, T_o)} = p^L_t + (1 - p^L_t)\frac{\bar{O}(F^R_{t,T_f}, K, T_o)}{\bar{O}(F^L_{t,T_f}, K, T_o)} \triangleq \bar{p}^L \tag{4.9}$$

The ratio of the observed option price and the counterfactual option price in the "Leave" state (labelled as $\bar{p}^L$) is equal to the risk-neutral probability of the "Leave" outcome in addition to a bias term, which depends on the unobserved counterfactual option prices in the "Leave" and 'Remain' states. Since option prices are non-negative, $\bar{p}^L$ must be higher than p^L. Thus, $\bar{p}^L$ is the upper bound of the actual risk-neutral probability of "Leave" outcome. In order to recover $\bar{p}^L$, we reduce the bias term by choosing options with maximum price difference in "Leave" and 'Remain' states ($\bar{O}(F^L_{t,T_f}, K, T_o) - \bar{O}(F^R_{t,T_f}, K, T_o)$). We know that the GBP/USD spot/future rate is lower in the "Leave" state than the 'Remain' state. Thus, put option price is higher in the "Leave" state than the 'Remain' state, while call option price is the opposite. So, employing put options to recover the upper bound of the actual "Leave" probability can minimize the bias and tight the upper bound.

Assume that time $t-1$ is one day before the event day and t is the event day that outcome L is realized. Since the interval between $t-1$ and t is small enough, we can re-write equation (4.9) as

$$\frac{P(F_{t-1,T_f}, K, T_o)}{P(F^L_{t,T_f}, K, T_o)} = p^L_{t-1} + (1 - p^L_{t-1})\frac{\bar{P}(F^R_{t,T_f}, K, T_o)}{P(F^L_{t,T_f}, K, T_o)}, \tag{4.10}$$

where $P(F^L_{t,T_f}, K, T_o)$ is the observed put option price in the "Leave" state after the Brexit outcome release.

Empirically, we can estimate $\bar{p}^L$ in each strike price K from the following regression,

$$\ln \frac{P(F_{t-1,T_f}, K, T_o)}{P(F^L_{t,T_f}, K, T_o)} = \alpha_K + \beta_K Event_t + \theta_K X_t + \varepsilon_{Kt}. \tag{4.11}$$

where $Event_t$ is a dummy variable to indicate the information releasing day and X_t is a set of control variables, including time-to-maturity and its squared term, dummy variables to control for the days before and after the event, and dummy variables to control for a three-day window around the releasing day of the event outcome. Then we can recover $\bar{p}^L_K$ as

$$\bar{p}^L_K = e^{\hat{\beta}_K}, \tag{4.12}$$

where $\hat{\beta}_K$ is the estimated β_K in equation (4.11). Our estimated $\bar{p}^L_K$ is a set of probabilities across a dense set of strike prices. In order to fit the estimated probabilities across strike prices using a spline, we adopt the following regression

$$\ln \frac{P(F_{t-1,T_f}, K, T_o)}{P(F^L_{t,T_f}, K, T_o)} = \beta_0 Event_t + \sum_{j=1}^{J} \beta_j \min(\mu_{j-1} - K, \mu_j - \mu_{j-1}) Event_t + \theta X_t + \varepsilon_t, \tag{4.13}$$

where μ_j are knots that evenly divide strike prices into J groups. We set $J = 20$, which means that twenty knots are used in this regression. Then we can recover $\bar{p}^L(\mu_i)$ as

$$\bar{p}^L(\mu_i) = \exp(\hat{\beta}_0 + \sum_{j=1}^{20} \hat{\beta}_j \min(\mu_{j-1} - \mu_i, \mu_j - \mu_{j-1})). \tag{4.14}$$

4.2.4 Correcting Risk-neutral Probabilities using Stochastic Discount Factors

In addition to the primitive security prices and risk-neutral probabilities that will be obtained in the options market, we will also use data from prediction markets. The latter is much simpler to analyse than the more complex derivative asset markets. The reason is that betting odds from prediction markets provide straightforward (public) Arrow-Debrew primitive prices. The shortcoming, however, is that these prices are

available (or traded) only for certain states of nature, notably those that raise public interest such as the Brexit referendum.

As suggested by macro-finance theory, there is a mapping between prices of state-contingent securities and their respective probabilities. Knowledge of Von Neumann-Morgenstern utility functions is key to unlock state or event physical probabilities that are embedded in these primitive prices. We employ two approaches to tackle this problem. The first one is based on Ross (2015)'s recovery theorem. The second assumes functional forms for investors' preferences and calibrates the model's crucial parameters.

Ross (2015) relies on a set of crucial assumptions regarding the structure of the economic environment that delivers a "non-parametric" recovery of these probabilities. The exact meaning of "non-parametric" is that the recovery is obtained without imposing any structure on the functional form of the utility function. Also, there is no need to perform any *a priori* parameterisation of the stochastic discount factor that describes the relevant economic system. In fact, the recovery does not require any knowledge of the underlying consumption, income, wealth or endowment processes that are crucial to saving decisions.

But all of this comes at a cost. Maybe the most contentious one is the assumption that both state prices and transition probability functions are time-homogenous. The theorem also considers transition independent pricing kernels, no-arbitrage and a finite state space under complete markets. A comprehensive review is provided by Carr and Yu (2012) and applications can be found in Martin and Ross (2019) and Schneider and Trojani (2019), for instance. For a criticism, see Borovička et al. (2016). We do not take a stand on the relative merit of each approach neither discuss their advantages and shortcomings in detail. However, we will point out some crucial differences between the risk correction approaches while presenting the methods and results.

4.2.4.1 General Recovery

The general set up of the model is given below. Consider the following Arrow-Debreu (AD) state price matrix

$$\mathbf{A_t} =: \begin{bmatrix} A_{11,t} & A_{12,t} & \dots & A_{1n,t} \\ A_{21,t} & A_{22,t} & \dots & A_{2n,t} \\ \vdots & \vdots & \vdots & \vdots \\ A_{n1,t} & A_{n2,t} & \dots & A_{nn,t} \end{bmatrix}, \tag{4.15}$$

where $A_{ij,t}$ is the price in state i of the AD primitive security that pays off one unit of the domestic currency if and only if state j materialises; $p(i,j)$ as the probability of occurrence of state j given the initial state i. Hence, $f(i,j)$ can be understood as a frequency or a mass function for discrete states, as in Carr and Yu (2012), for instance, or a density function for continuous states as in Ross (2015). There is a finite number of states of nature, n, in which the economy could make a transition from t to $t+1$: $i \in \{1, 2 \dots, n\}, \forall t$ and $t = 1, 2, \dots, T$, where T is the end of the sample period.

4.2.4.1.1 AD primal prices Starting from state $i \in \{1, 2, \dots, n\}$ at time t, write the following general Euler equation for a representative utility optimizer, solving it for the corresponding primitive price

$$A_{ij,t} = \beta \frac{u'(ij, t+1)}{u'(i,t)} p(ij,t), \tag{4.16}$$

where we consider a period utility function that is additively separable between time and states, twice continuously differentiable and follows the Inada conditions. For a risk averse agent, the function will be strictly concave; $\beta \in (0,1)$ is a subjective time-discount factor. Note that $\beta \frac{u'(ij,t+1)}{u'(i,t)}$ are pricing kernels.

The details about how to obtain the AD state price matrix from the betting and option markets is shown in Appendix Appendix 4.B.

4.2.4.2 Non-parametric Recovery

Define the inverse marginal utilities as $v(i,t) =: \frac{1}{u'(i,t)}$ and $v(ij,t) =: \frac{1}{u'(ij,t)}$. Assume that pricing kernels are transition independent, i.e. that $u'(ij,t+1) = u'(j,t)$, $\forall i$, $\forall j$ and $\forall t$ such that (4.16) can be simply rewritten as:

$$A_{ij,t} = \beta \frac{v(i,t)}{v(ij,t)} p(ij,t) = \frac{v(i,t)}{v(j,t)} p(ij,t). \tag{4.17}$$

One can stack all equations for each i, j and t in matrices, which allow us to write the system in the following compact way

$$\underset{(n\times n)}{\mathbf{A_t}} = \beta \underset{(n\times n)}{\mathbf{D_t}} \underset{(n\times n)}{\mathbf{P_t}} \underset{(n\times n)}{\mathbf{D_t}^{-1}}, \tag{4.18}$$

where

$$\mathbf{D_t} =: \begin{bmatrix} v_{11,t} & 0 & \dots & 0 \\ 0 & v_{22,t} & \dots & 0 \\ \vdots & \vdots & \vdots & \vdots \\ 0 & 0 & \dots & v_{nn,t} \end{bmatrix} \text{ and } \mathbf{P_t} =: \begin{bmatrix} p_{11,t} & p_{12,t} & \dots & p_{1n,t} \\ p_{21,t} & p_{22,t} & \dots & p_{2n,t} \\ \vdots & \vdots & \vdots & \vdots \\ p_{n1,t} & p_{n2,t} & \dots & p_{nn,t} \end{bmatrix}. \tag{4.19}$$

Assume that all other hypothesis put forward by Ross (2015), which were made clearly explicit in Martin and Ross (2019), are valid. Entries of $\mathbf{A_t}$ are all non-negative (due to non-arbitrage) and the matrix is irreducible (due to complete markets). Perron-Frobenius theorem then ensures that $\mathbf{A_t}$ has a unique largest (in absolute value) real eigenvalue and that all elements in the corresponding eigenvector are strictly positive. Let us consider that ϕ is the eigenvalue and $\mathbf{Z_t}$ the eigenvector such that

$$\mathbf{A_t Z_t} = \phi \mathbf{Z_t}, \tag{4.20}$$

where

$$\mathbf{Z_t} =: \mathbf{D_t e}, \tag{4.21}$$

and

$$\mathbf{e} =: \begin{bmatrix} 1 & 1 & \cdots & 1(n) \end{bmatrix}^{\top}. \tag{4.22}$$

The theorem guarantees that the solution is unique up to a scalar (ϕ). The decomposition in (4.20) thus gives ϕ and, by Gaussian elimination, $\mathbf{Z_t}$. In Appendix Appendix 4.C, we show how to obtain $\mathbf{P_t}$ with a simple example.

4.2.4.3 Parametric Recovery

The second approach is parametric where we need to make assumptions on the functional form of utility and risk preferences in equation 4.16 in order to obtain physical probability from AD prices. For example, we can define utility over wealth, and we have two representative agents with power utility functions given by

$$u^o(W_i) = \frac{W_i^{1-\gamma^o}}{1-\gamma^o}, u^p(W_i) = \frac{W_i^{1-\gamma^p}}{1-\gamma^p}, \tag{4.23}$$

where o and p stand for the agent in the option and prediction market, respectively. It follows, for instance, that γ^o (γ^p) is the constant relative risk aversion coefficient for the agent in the option (prediction) market; W_i is the level of wealth in state i. Notice that we are implicitly assuming that both markets are segmented. We will later show how the range of risk aversion parameter and changes in wealth for these states of nature, that is, remain vs. leave, affect the risk correction under parametric recovery.

4.3 Data Description

4.3.1 Exchange-listed British Pound Futures and Options

We obtain daily settlement prices and intraday trade and quote prices for American-style British pound monthly futures options. We also collect the data on the underlying assets of these options, GBP futures contracts. All these options and futures contracts are listed on the Chicago Mercantile Exchange (CME). Specifically, the CME GBP option is an option written on a future contract based on 62,500 GBPs, which is quoted in USD and cents per British pound increment. The expiration date of the monthly option is the two Fridays before the third Wednesday of each month. The expiry dates of CME British pound futures are available in quarterly frequency, that is, every Monday before the third Wednesday of March, June, September, and December. The underlying future contract of an option is the nearest future contract in March, also in a quarterly frequency. The sample period used in this paper runs from January 2, 2014, to August 30, 2016. To investigate whether there is a significant difference in the British pound RNDs before and after the Brexit referendum, which was held on June 23, 2016, we mainly focus on the period between May 3, 2016, and July 29, 2016. All futures and options data is obtained from Thomson Reuters Tick History (TRTH).

4.3.2 Betting Odds from Prediction Markets

Many researchers use information from the prediction market to extract underlying probabilities. This is because the odds of the event reflects investors' beliefs in the probability of its outcome (Roberts, 1990; Herron, 2000; Snowberg et al., 2007, 2011; Croxson and James Reade, 2014; Meng, 2017; Auld and Linton, 2019). As the largest betting exchange with high liquidity, Betfair's information can be a valuable source of recovering the probability of the outcome of a particular event. The *odds* (payouts) of *bets* (binary contracts) are driven by the supply and demand of buy and sell contracts.

There were two contracts listed on the Betfair website for consumers to bet on the outcome of the Brexit referendum: one with a payout in the Leave state and another with a payout in the Remain state. The normalized price of the bet is $\frac{1}{odds}$, which is the cost of winning \$1 if the consumer bets in the right direction. To avoid arbitrage opportunities, the sum of the normalized prices of two contracts betting on Brexit should be close to 1. Many authors use this price as a synonym of the market-implied probability of the event outcome (Snowberg and Wolfers (2010)). In order to analyse the implied probability of Brexit in the prediction market, we collect the 5-minute odds of these two contracts from May 3, 2016 until June 24, 2016. Then we calculate the market-implied probability of "Leave" outcome as

$$p_{p,t}^{L} = \frac{1}{LeaveOdds_t}, \tag{4.24}$$

Figure 4.2a shows daily "Leave" probabilities implied in the prediction market under risk neutrality. The prediction market consistently points to "Remain" as the most likely outcome. Specifically, the daily "Leave" probabilities is around 20% to 30% between the mid of May and the end of May, 2016. It reaches the highest point on 14 June, 2016, however, it is still lower than 50%. On the night of the referendum, the 'Leave' probability implied in the betting market decreases to 16.66%.

4.3.3 Political Opinion Polls

Political opinion polls are an important source of information on the expected outcome of a future binary political event. The option and prediction markets reveal the probabilities of future event's outcome, while polls reflect voters' voting intentions. We collect political opinion polls data between 10 January, 2016 and 23 June, 2016. In this period, 13 market search companies (including BMG Research, ComRes, GQR, ICM, Ipsos MORI, NATCEN, ORB, Opinium, Panelbase, Populus, Survation, TNS and YouGov)

published 128 polling results on whether the UK should be in or out of the EU.

Figure 4.2b shows that opinion polls from decided respondents favoured "Remain" majority of the time, 55% of 128 polls, though voting intentions to "Leave" that fluctuate around 50% from the opinion polls reflect the uncertainty around the Brexit outcome. In fact, several polls clustered around 14 June 2016 indicated a "Leave" outcome. In line with the polls' results, the betting market also consistently pointed to Remain as the most likely outcome (Figure 4.2a). However, the spike in leave probability around 14 June 2016 indicate that betting market participants take into consideration news about polling results when assessing the likelihood of Brexit outcome.

4.3.4 Survey Data

The British Election Study (BES) conducts a wide range of surveys for major political events in the UK, including the Brexit referendum. Respondents answer a wide range of questions designed to capture their risk preferences, demographic and socio-economic characteristics (e.g., gender, age, income), views on economy and politics, attitudes toward immigration, party identification and so on. This allows us to investigate the "Leave" voters' motivations at the micro-level, and estimate the voting intentions to "Leave" of *indecisive* voters.

We use the individual level data from waves 8 of the 2014–2017 BES Internet panel. This survey is conducted between 6/May/2016 and 22/June/2016 and covers 33,501 individuals. For the question *"If you do vote in the referendum on Britain's membership of the European Union, how do you think you will vote?"*, 15,215 respondents (45.42%) answer *"Stay in the EU"*, 15,793 respondents (47.14%) answer *"Leave the EU"*, 475 respondents (1.42%) answer *"I would not vote"* and 2,018 respondents (6.02%) answer *"Don't know"*. The latter group is of a particular interest since a large fraction of such voters are likely to determine the final Brexit outcome.

In order to investigate the "Leave" voters' motivations, we select a series of

explanatory variables, including risk preferences, personal annual gross income as well as the variables used in earlier studies (e.g., Goodwin and Milazzo (2017)). The details of these variables and corresponding BES questions are listed in Table 4.1. To keep sufficient number of observations, we use the median value of the explanatory variable to replace the "Don't Know" answers.[3]

4.3.5 Additional Data

In addition to the data from financial market, polls and survey, we also collect data for RND extraction and market fear measurement. In particular, we collect GBP/USD spot exchange rate between January 2, 2014 to August 30, 2016 from Bloomberg. For risk free rates, we use US and UK LIBOR rates obtained from Federal Reserve Bank of St. Louis website. In order to match futures and options maturities, we interpolate interest rates for specific horizons. Then we use the interpolated interest rate for further analysis.

To study the trading behavior of different type of traders in the CME British pounds derivative market, we obtain the publicly data from the Commodity Futures Trading Commission (CFTC). The weekly Commitment of Trader (COT) Reports contains the aggregate long and short positions for three types of traders: commercials, non-commercials and non-reportable, and spread positions for non-commercials. Following the literature, we view commercials as hedgers, non-commercials as speculators and non-reportable as small speculators.

[3]Our main results are not sensitive to this assumption, results of alternative specifications are available upon request.

4.4 Empirical Results

4.4.1 Implied Volatility and Risk-Neutral Density

To extract information about investors' beliefs on the performance of GBP/USD exchange rates and investors' attitudes towards risk before and after the Brexit referendum, we extract RNDs of GBP/USD futures from CME British pound monthly futures options.

Figure 4.3 display implied volatilities and RNDs inferred from CME British pound monthly futures options expiring on 8 July, 2016, which is the earliest expiry day after the referendum date. Specifically, Figure 4.3a and Figure 4.3c show implied volatility surface and its corresponding RND surface during June 2016. We select six specific days to plot their implied volatility curves and their corresponding RNDs in Figure 4.3b and Figure 4.3d, including 6-, 4-, 2-weeks before the referendum, the referendum day and 1-day and 1-week after the referendum.

Implied volatility surface of options expiring on 8 July, 2016 in Figure 4.3a shows the implied volatility change across a wide range of strike prices during June 2016. For a specific day before/at the referendum, the implied volatility decreases as the strike price increases, that is, the implied volatility curve of British Pound options exhibits a well-known 'smirk' shape. Fig. 4.3b shows that implied volatility curves in the shape of 'smirk' can be observed in the market at least from 12 May, 2016. It indicates that OTM puts are more expensive than ATM options and OTM calls. This option price differences across strike prices are driven by demand differences. That means, to avoid the possibility of a crash or tail risk, investors in British Pound option market have high demand of OTM puts before the Brexit outcome releases, and this demand become even higher as the outcome releasing day approaches. After the outcome released, the implied volatility curve gradually returns to the normal 'smile' shape.

Based on the fitted implied volatilities, we approximate the RND of GBP/USD

futures and append it into left and right tails. The RND surface in Figure 4.3c displays the RND movement from the beginning of June until the end of June in 2016. As we have seen, when the time approaches the referendum day, RND shows a more pronounced bimodal distribution, with a major mode towards the high price region and a minor mode towards the low price region. This suggests that a sharp rise or fall should be expected relative to the current level of GBP/USD futures once the Brexit outcome is realized. Taking the RND on the referendum day as an example, the red line in Figure 4.3d, we find that the major mode is 1.525 and the minor mode is 1.335, which represent the most likely GBP/USD futures prices if the Brexit outcome is 'Remain' or "Leave", respectively. After the Brexit outcome is realized, the market reaches a consensus and RND of GBP/USD futures go back to normal unimodal distributions.

After investigating the time-variation of RNDs during May and June in 2016 by using options expiring on 8 July, 2016, we examine the term structure of RNDs before and after the Brexit outcome is realized. In Figure 4.4, we display RNDs for all available horizons on the referendum day (Figure 4.4a) and the first day that after the result of the Brexit referendum (Figure 4.4b). On 23 June, 2016, the RND extracted from options expiring on 8 July, 2016 shows the strongest bimodal distribution. The RNDs extracted from options expiring in the following three months are slightly bimodally distributed. While RNDs for long horizons are more likely unimodally distributed. This implies that investor's expectations about short-term changes in the GBP/USD exchange rate are more divergent than their long-term forecasts. Similar to the pattern unveiled for changes in the RND that we observed from the option that expires on 8 July, 2016, RNDs from options that expire later also return to a normal unimodal distributions on the 24 June, 2016, as the result of the referendum is certain.

4.4.2 The Dynamic Behavior of the British Pound's Risk-Neutral Distribution

To study the dynamic behavior of the British Pound's RND, we extract risk-neutral moments from the RND of British Pound futures prices. Movements of risk-neutral moments can provide information about the daily changes in investors' expectations of the futures underlying prices and its associated uncertainty. Specifically, we focus on the risk-neutral second-, third- and fourth- moments, and the bi-modality coefficient measured by risk-neutral skewness and kurtosis. The time t bimodality coefficient (BC) of a RND from a contract expiring at T_o is

$$BC = \frac{Skewness^2 + 1}{ExcessKurtosis + \frac{3(n-1)^2}{(n-2)(n-3)}}, \tag{4.25}$$

where n is the sample size. The range of BC is from 0 to 1. $BC > \frac{5}{9}$ indicates that the distribution maybe bimodal or multimodal.

Figure 4.5 presents the annualized risk-neutral volatility, the risk-neutral skewness, the risk-neutral excess kurtosis and the bimodality coefficient from RNDs for five different horizons between 2 May, 2016 and 29 July, 2016. Since the prices of the GBP/USD futures expiring before the referendum day are not affected by the "Brexit" outcome, the risk-neutral moments of RNDs from an option that expires before the referendum are at normal levels, and RNDs have normal unimodal distribution. To further analyze the behavior of RNDs extracted from options expiring after the referendum, we use information in RNDs obtained from this option as a reference for normal levels.

The risk-neutral volatility (Figure 4.5a) represents the market's uncertainty around the expected value of GBP/USD futures. Risk-neutral volatilities obtained from options expiring within three-month after the referendum are higher than a normal level. Starting in early June 2016, risk-neutral volatilities from options expiring after the referendum increase significantly until the Brexit outcome is realized, especially for volatilities from

short maturity options. This means that the uncertainty of Brexit has a larger impact on the short-term value of the GBP/USD exchange rate than its long-term value. After the announcement on June 24, 2016, the risk-neutral volatility from options expiring in July and August drop back to their level in May within the next few days, but the risk-neutral volatility from longer maturity options take more time to recover to May levels. The change in risk-neutral volatility indicates the resolution of the uncertainty caused by the referendum. We can also use this change to infer how much information is provided by the announcement of the result. According to the empirical evidence presented above, agents use this information to settle short-term uncertainty, rather than long-term uncertainty. This finding is not surprising, since the procedures on how to leave the EU and the potential economic agreements between the EU and the UK would still be uncertain.

The risk-neutral skewness (Figure 4.5b) is a measure of asymmetry. Before the Brexit referendum, the risk-neutral skewness from options expiring after the referendum is more negative than the normal level, which indicates that RNDs have fat left tails. Specifically, risk-neutral skewness from options with short maturities is more negative than skewness from long maturities options. This is induced by the risk of "Leave". As the "Leave" result would represent a negative shock to GBP/USD exchange rate, especially in the short-horizon, the risk of "Leave" is shown as fat left tails in RNDs. As the day of the Brexit referendum approaches, risk-neutral skewness become even more negative, reflecting the market expectations of a negative shock (Hasler and Jeanneret, 2020). These unusual fat left tails that appeared a few days before the referendum are more likely to be prompted by bi-modally distributed RNDs. As the state of the world "Leave" is realized and the risk-neutral skewness goes back to a normal level, which is close to zero, RNDs return to normal symmetric distributions.

The risk-neutral excess kurtosis (Figure 4.5c) measures market expectations of extreme changes in the GBP/USD exchange rate. The higher the excess kurtosis, the

higher the probability concentrated in the tails of RNDs before the Brexit referendum. Similar to the third moment, the excess kurtosis also goes back to a normal level after the referendum.

Last, we examine the bi-modality coefficient (Figure 4.5d) calculated from the risk-neutral skewness and excess kurtosis. The time-varying BC indicates that bimodal RNDs from short maturity options can be observed within three days before the referendum, while RNDs from December contracts are consistently uni-modally distributed. After the referendum, the BC falls back to a normal level, which means that RNDs also return to normally unimodal distributions. Hence, regime switches of the moments of RNDs and changes of their shapes after the referendum are likely reflecting the fact that the outcome was not entirely unexpected.

4.4.3 The Tail Risk

To investigate the tail risk in the exchange rate, we calculate risk-neutral 10% quantiles of the GBP/USD spot rate return according to the definition in equation (4.1).

Figure 4.6a shows the term structure of tail risk of the GBP/USD exchange rate from January 2014 to August 2016. Apart from Brexit, this sample period covers two additional important events in the UK, namely the Scottish independence referendum on 18^{th} of September, 2014 and the UK general election on the 7^{th} of May, 2015. Since the available maturity for the options is up to one year in our sample and the trading in long maturity contracts is relatively thin, we calculate risk-neutral 10% quantiles for 1-month, 3-month and 6-month horizons. The stark declines in 10% quantiles before the event indicate that the uncertainty of the event outcome has triggered an increase in tail risk. Compared with the other two events, the tail risk caused by Brexit is much larger across all three horizons. In addition, for both the Scottish independence referendum and the United Kingdom general election, we can observe 10% quantiles steeply rises to the level of the no-event period on the day of the announcement of the results. The Brexit

referendum is different: the tail risk returns to normal levels more than 1-month after the binary event. This evidence suggests that the impact of the Brexit referendum on the level of tail risk is significantly different from the Scottish independence referendum and the 2015 United Kingdom's general election, at least for the GBP/USD foreign exchange market.

In Figure 4.6b provides a closer look at the period around the Brexit referendum, and shows that the tail risk deviates from its normal level since the beginning of 2016, especially after April 2016. It reflects the investors' forward-looking assessment of a higher likelihood of the "Leave" outcome. Using the sample period between 3 May, 2016 and 23 June, 2016, the correlation between the "Leave" probability implied in Betfair and the tail risk measure for 1-month, 3-month and 6-month horizons are -0.5123, -0.6024 and -0.6092, respectively. This result lends support to the view that the more likely the adverse state is, i.e. the "Leave" state, the higher is the degree of tail risk. Moreover, the tail risk is highest on 14 June, 2016, on the day when several poll results suggesting "Leave" outcome were released.

4.4.4 Option-Implied Event Probability: Model-Based Estimation

Information extracted from RNDs suggests that the CME British Pound option market contains investors' expectations for the Brexit result. To infer the investors' expected probability of the "Leave" outcome in the option market, we used the model-based methodology presented in section 4.2.3. This approach also allowed us to identify the implied futures prices and volatilities in "Leave" and 'Remain' states, respectively.

Figure 4.7 presents the daily option-implied probability of "Leave" using three different model specifications, together with the corresponding implied probability in the betting market. The option-implied probabilities from different model specifications are highly correlated (correlation greater than 0.85), but have different magnitudes, especially before 14 June, 2016. Compared with our baseline model, model specification II

and III attribute a large weight on cheap options, since cheap OTM options likely to carry important information about speculation related to tail events. These specifications reduce the level of estimated option-implied "Leave" probabilities (closer to risk-neutral probabilities from betting market), especially before the 14 June 2016. Apart from that, we find that daily "Leave" probabilities in the option market and the betting market mainly move together during this period. The correlation between probabilities from the betting market and option-implied probabilities under the three different specifications are 0.44, 0.42, and 0.47, respectively. In the betting market, the "Leave" probability reaches its highest on 14 June, 2016, which is consistent with the "Leave" probability from the poll of opinion polls (Wu et al., 2021). However, under model specification I and II, "Leave" probability from the option market reaches its highest on 16 June 2016. If we switch to the model specification III, the "Leave" probabilities on 14 and 16 June, 2016 are almost in the same magnitude. This suggests that the reaction of the option market to the murder of the pro-Remain MP Jo Cox on 16 June, 2016 is stronger than the betting market. Overall, the average probability of a "Leave" outcome provided by the options market (35.98%, 32.89% and 29.25% under the three model specifications, respectively) is higher than that of the betting market (27.43%).

We also plot the futures prices and their corresponding volatilities in the "Remain" and "Leave" states estimated under the different model specifications in Figure 4.8. The futures prices in these two states seem to move together in May 2016, and then start to diverge. This maybe indicate that investors in the CME British pound option market starts to pay more attention to Brexit news in June. In addition, the futures prices in the 'Leave' state reach the lowest value on 13 June, 2016 under model specifications II and III, and on 14 June, 2016 under model specification I. This pattern matches the pattern of tail risk. Tail risk for 1-month horizon reaches its peak on 13 June, 2016 and for 3- and 6-month horizons peaked on 14 June, 2016. Moreover, the futures volatilities in two states show that the volatilities in the "Remain" state are

much lower than "Remain" state.

4.4.5 Option-Implied Probability: Model-Free Method

Option-implied probability of the Brexit outcome varies across different model specifications. To evaluate the time-varying "Leave" probability estimated from the model-based method, we extract a upper bound for the "Leave" probability by using the model-free method demonstrated in Section 4.2.3.2. For this regression, we use all available put option data between 2 May, 2016 and 29 July, 2016. We indicate event date as 24 June, 2016, since it is the date that the Brexit outcome was released.

Figure 4.9 shows estimated "Leave" probability upper bounds. The red circles represent the estimated probability by using strike-price-by-strike-price regressions in equation (4.11). The black line is the fitted spline with 20 knots by using the regression specified in equation (4.13). The vertical black dashed line represents the GBP/USD exchange rate on the day of the event, so the left side of the line are strike prices of OTM put options. The minimum probability on the fitted spline line is 33.69%, which is our preferred estimate of the "Leave" probability's upper bound. Ideally, the tightest bound should occur on a strike price of an OTM option. However, OTM put options usually carry a crash risk premium. Even if the realized Brexit outcome is "Leave", OTM put option prices may retain most of its value. Then the bias term in equation (4.11) does not converge to zero. The probability estimated from OTM put options provide a relatively loose bound. In our results, the minimum probability, 33.69%, occurs on the right side of the vertical line. This means that 33.69% from in-the-money (ITM) put options is not the tightest bound for the "Leave" probability. But it is sufficient for us to rule out the model specification I from our model-based estimation, because the average probability estimated from this specification is higher than the upper bound. The average probability from model specification II is very close to the upper bound, but our estimated upper bound is a relatively loose upper bound, so we believe that the

estimation of the model specification III is likely to be more accurate.

4.4.6 Learning from the Opinion Polls

We use the "Leave" voting intention from political opinion polls to extract a proxy of *subjective* "Leave" probability. First, we convert the voting intention into a binary Brexit outcome. If the voting intention to "Leave" is higher than "Remain" from the political opinion poll i at day t, we consider the outcome as "Leave", and vice versa. We use value 1 to indicate "Leave" outcome, and 0 to indicate "Remain" outcome, which is labelled as $\mathbb{1}^L_{i,t}$. Second, we assume that different polls independent observations, and if there are several polls on a day, we assign the average of all available polls' outcomes at day t as the outcome at day t, $\frac{1}{K}\sum_{i=1}^{K}\mathbb{1}^L_{i,t}$, where K is the number of available polls at day t. However, the probability of the "Leave" outcome from individuals perspective is not only based on the polls' outcome on a single day, the past polls results also contribute to individuals' belief formation on the "Leave" outcome. Thus, in the third step, we allow for a learning mechanism from the past N days polls' results, and the weight for day-j information is $\omega_{j,t,N}$, where $t-N+1 \leq j \leq t$, then the *subjective* probability of "Leave" outcome from polls is

$$p^L_{poll,t} = \frac{\sum_{j=t-N+1}^{t}\omega_{j,t,N}\frac{1}{K}\sum_{i=1}^{K}\mathbb{1}^L_{i,j}}{\sum, m^t_{j=t-N}\omega_{j,N}}, \tag{4.26}$$

We consider 18 (2x3x3) different learning mechanisms, varying the estimation window, weights for past observations and number of past days. First, we consider both expanding (N is increasing) and rolling window (N is constant) estimation. Second, we use three different weight functions, since individuals may process past information differently. The first function is the equal-weighted average of past polls outcomes $\omega_{j,t,N} = \frac{1}{N}$, which assumes individuals gives equal importance to all past opinion polls. The second function is the liner decay weight function $\omega_{j,t,N} = \frac{N-(j-t)}{N}$, which assume that individuals treat

the past information less important than the new information. The last weight function is the exponential decay weight function $\omega_{j,t,N} = (\frac{N-(j-t)}{N})^3$, which gives even lower weight to the past information compared to the linear decay function. Finally, we use three different window lengths, 30, 60 and 90 days, respectively. For the expending window method, window lengths means the number of days that we start the probability calculation before the beginning day of our sample.

Table 4.3 shows the correlations between the daily change of subjected probabilities estimated from past opinion polls and the daily change of risk-neutral probabilities from option and prediction markets. We note that the subjective probabilities using the linear decay function with a 90-day rolling window best describes the learning mechanism of both option and prediction market participants, which we exhibit in Figure 4.10. The correlations between daily changes in Leave probabilities from polls and option (prediction) markets, is 0.3 (0.43). Using 18 different methods to calculate subjective probability, the average correlations between the subjective and option (prediction) market-implied risk-neutral probabilities is 0.21 (0.33). This indicates that the option and prediction markets incorporate the information from polls to a large extent.

4.4.7 Correcting the Risk-neutral Probability

Because the referendum is a binary event, we assume that the Arrow-Debreu (AD) state price matrix, $\mathbf{A_t}$ shown in equation (4.15), is 2×2. State two represents the UK leaving the EU in the referendum (leave), whereas the current (remain) state is one. We make two other assumptions to complete the second row of $\mathbf{A_t}$ in the non-parametric recovery. They are not necessary for the parametric risk-adjustment. The first assumption is of "high uncertainty" state 2 as embedded in the following prices: $A_{21} = A_{22} = 0.5$. The second corresponds to an (almost) absorbing state 2: $A_{21} = 0.01$ and $A_{22} = 0.99$.

For the parametric recovery, we experiment with several plausible values of the deep parameters assuming standard power utility. Start with $\beta = 0.99$, which is a

standard value in the RBC/DSGE literature for annual data and that is also consistent with our previous findings using the recovery theorem. We need to make an assumption about relative wealth change between the remain and leave states. According to a poll conducted by Ipsos Mori before referendum in 2016 (The Guardian, 2016), 25% of the voters except a decline in their living standards due to Brexit, while 14% of voters believe in an improvement in living standards, with 51% expecting no change. Hence, in our baseline setting, we assume that there will be a 10% decline in aggregate wealth if we move from "Remain" to "Leave" state and also analyze the impact of more drastic wealth changes. In our parametric risk correction, we consider both risk-averse and risk loving preferences with a constant relative risk aversion γ ranging from -6 and to 6.

Non-parametric recovery. Figure 4.11 presents the results using the non-parametric approach, which are shown in Figure 4.11a for the prediction and in Figure 4.11b for the option markets. While the non-parametric recovery is fairly general without imposing much structure, it generates only a very small upward correction of the leave probabilities. Notice that the "uncertain" case presents a smaller difference in the corrected probabilities than the "absorbing" case, however, the differences are minor. Thus, we next move to the parametric correction to check whether the level of leave probability could be larger under additional parametric assumptions to pin down the stochastic discount factor (SDF).

Parametric correction. Figure 4.12 shows risk-corrected leave probabilities from both markets under different parametric assumptions for risk preferences and relative wealth changes from remain to leave state. In the upper panels, we assume the wealth in "Leave" state is 10% (W^L) lower than the "Remain" state (W^R), which means $\frac{W^L}{W_R} = 0.90$, we calibrate risk-corrected probabilities with a set of relative risk aversion coefficients, $\gamma = \{-6, -4, -2, 0, 2, 4, 6\}$, where positive γ represents risk averse and negative γ represents risk loving behaviour. Results for prediction and option markets are displayed in Figure 4.12a and 4.12b, respectively. As can be seen, the assumption of risk

averse agents decreases the probabilities of the leave state. A possible explanation is that primitive prices already reflect higher relative demand for that worse - by assumption - state of nature. On the other hand, the assumption of risk loving agents increase leave probabilities.

Speculative Markets? Is it plausible to assume that market participants on aggregate are risk-seeking? While it is conceivable that the prediction markets are populated by risk-seeking agents, derivative markets are often used both for hedging (by risk-averse agents) and speculative (by risk-seeking agents) purposes, especially around rare events (Bond and Dow, 2021). Whether one trading motive dominates the other remains to be an empirical question.

First, we note in Figure 4.13a, the trading activity in the option market proxied by the put-call ratio, is closely linked to the uncertainty of opinion poll results about Brexit outcome. The latter is measured by the standard deviation of the expected "Leave" outcome under the assumption of binomial distribution. Both the uncertainty and the put-call ratio jump on 9 June, 2016. Clearly, relative high demand for put contracts on GBP could originate both from bearish speculative bets on the British pound and/or hedging needs to protect against a large drop in GBP (Hanke et al., 2018).

Figure 4.13b shows speculative versus hedging behaviour in the CME British pounds derivatives markets around the Brexit event. We measure the speculative versus hedging behaviour as total CME British pounds futures' and options' positions held by speculators (non-commercial traders) relative to the total positions held by hedgers (commercial traders). To eliminate potential maturity effects, we scaled it by the values in the previous year. We notice that relative speculative activity is abnormally high around mid-June (7 June and 14 June) which coincides with poll results suggesting a leave outcome together with heightened uncertainty, and higher leave probabilities estimated both from prediction and option markets. The level of relative speculative position is lower in the last week before the referendum after the murder of the pro-

remain MP Jo Cox and Bank of England's warning about the potential catastrophic implications of Brexit outcome.

Relative Wealth. We next assume mild risk seeking behaviour in both prediction and option markets ($\gamma = -2$), we obtain the risk-adjusted probabilities by using a wide range of relative wealth in "Remain" and "Leave" states, $\frac{W^L}{W_R} = \{0.75, 0.90, 0.95, 1.00, 1.05, 1.10, 1.25\}$. The figures 4.12c and 4.12d show the results for prediction and option markets, respectively. We see that only a large wealth decline (about 25%) from "Remain" to "Leave" state brings the risk-corrected leave probabilities closer to the physical probabilities estimated from the BES survey.

4.4.7.1 Risk-Corrected versus Subjective Probabilities

Using the subjective probabilities inferred from past opinion polls as the benchmark, we search for the corresponding relative risk reversion coefficient that minimizes the distance between risk-corrected probabilities and subjective probabilities. Assume $\beta = 0.99$ and the relative wealth $\frac{W^L}{W^R} = 0.90$, we can calibrate relative risk reversion coefficient, γ^{i*}, as

$$\gamma^{i*} \equiv \arg\min_{\gamma} \sum_{t=1}^{T} (\tilde{\pi}_t^i - \hat{\pi}_t)^2, \tag{4.27}$$

where $i = \{p, o\}$, p and o represent prediction and option markets, respectively. T is the sample size, $\tilde{\pi}_t^i$ is the risk-corrected probability by using by date from option or prediction markets, and $\hat{\pi}_t$ is the physical probabilities inferred from BES survey.

Figure 4.14 shows the risk-corrected probabilities by using data from both prediction and betting markets. The resulting risk aversion coefficient equals -1.83 in the prediction market ($\gamma^{p*} = -5.47$), and equals -1.01 in the option market ($\gamma^{o*} = -4.11$). Hence, by assuming that wealth in the "Leave" state would be 10% lower than the "Remain" state (baseline setting) and that risk-corrected probabilities are the closest to agent's perception of the physical probabilities, we find that the average agent in

both prediction and option markets are mildly risk seeking, with stronger risk seeking preferences in prediction markets as one would expect.

Then, we relax the assumption about the relative wealth in the "Leave" and "Remain" state, which was $\frac{W^L}{W^R} = 0.90$ and allow the relative wealth to be in a wider range, between 0.5 and 1.5, which means the wealth in the "Leave" state could be maximum 50% lower or higher than the "Remain" state. Then we calibrate the corresponding relative risk reversion coefficients by minimizing the squared difference between risk-corrected probabilities and subjective probabilities.

Figure 4.15 shows the corresponding relative risk reversion coefficients in both prediction and option markets with respect to the relative wealth. If the agents on average expect lower wealth in the "Leave" state than the "Remain" state ($\frac{W^L}{W^R} < 1$), the average agent in both prediction and option markets are risk loving as in the baseline case. Expectation of a mild decrease in wealth in the "Leave" state can only be rationalized by extreme risk-seeking behavior. If we assume that the agents on average expect a higher wealth in the "Leave" state than the "Remain" state ($\frac{W^L}{W^R} > 1$), then average agent in both markets is risk averse. However, symmetrically, the average risk aversion is low only if the agents on average expect a large increase in wealth moving to the "Leave" state which is empirically less plausible given the survey results before the Brexit referendum and Bank of England warnings.[4] The average agent in prediction markets has always a stronger risk preference than the average agent in option markets.

4.4.8 What Do We Learn from the Individual-level Survey Data?

To obtain the voting intention to "Leave" from individual-level BES survey data, we conduct Probit models to understand "Leave" voters underlying motivations to change the status quo. The Models (1) specification is using risk preferences as the only ex-

[4]One could argue that the Brexiteers were very optimistic about their wealth improvement post-Brexit, however, the BES survey results suggest that leave voters are more risk-seeking compared to remain voters.

planatory variable. Then we add voters' demographic characteristics, like gender and income, in Model (2). After that, we add voters' political views as additional variables in Model (3). Furthermore, we add voters immigration attitudes in Model (4). Last, we use all potential explanatory variables in the regression as Model (5).

Table 4.2 shows that *Risk Taking Preference* is one of the key motivation of respondents' "Leave" votes. Specifically, voters with higher risk taking preferences would like to vote for "Leave", which is consistent across different model specifications suggesting that controlling for other factors, risk seeking attitude is one of the important drivers of "Leave" votes. The most comprehensive Model (5) shows that being Male, having lower income, having left school early, belonging to elderly group also increase the likelihood of "Leave" vote. Voters with more concerns about immigration and more pessimism about economy prefer to vote "Leave". Party Identification also plays an important role for voters' choice.

In the bottom part of this table, we show both the share of leave voters and estimated intention to "Leave". The vote intention of "Leave" based on "Leave" and "Remain" respondents is 50.93%. By employing the estimated coefficients and indecisive respondents' individual characteristics, we obtain "Leave" probably implied for indecisive voters, which is higher than the probability of "Leave" vote implied for "Leave" and "Remain" voters under specification (4) and (5). According to model (5), the total intention to "Leave" is 51.07% including indecisive respondents. Hence, taking into account the indecisive voters (about 6% of the sample) suggests even a higher likelihood of Brexit outcome.

We also provide daily estimates of intention to leave using the most comprehensive model (5). Figure 4.16 shows that the intention to "Leave" is more persistent than the polling results. Arguably, one could extract a better proxy of physical Brexit probability based on survey estimates of voting intentions. However, these survey results were not available to market participants before the Brexit referendum. Ex-post we learn that

individual characteristics that are persistent over time are a better leading indicator for the Brexit outcome.

4.5 Concluding Remarks

We find that risk-neutral density distributions extracted from British Pound options with short maturities are bimodally distributed one week before the Brexit referendum. The changes of the risk-neutral tail risk in GBPs are highly correlated with changes of "Leave" probabilities from the betting market. This empirical evidence shows that the GBP options market incorporates investors' beliefs about a potential Brexit outcome. We estimate the risk-neutral probabilities of the Brexit referendum from the options market by using both model-based and model-free methods. The risk-neutral probability from the option market on average is higher than the probability from the betting market in the month before the Brexit referendum, but both market participants seem to closely track opinion poll results when assessing event probabilities. While subjective probabilities extracted from polls rationalize the Brexit surprise, voting intentions estimated from surveys which are determined by persistent characteristics (age, education, income), political views and the risk preferences of the voters, are likely to be a better guide for physical probabilities.

We construct risk-neutral Arrow-Debrew prices from both markets and filter out risk-corrected probabilities from market prices using both a non-parametric (Ross Recovery Theorem) and a parametric (calibrating the stochastic discount factor) approach. Only parametric recovery is likely to have an impact on the level of Brexit probability estimates, albeit under strict parametric assumption. However, we argue that markets could have signalled higher Brexit outcome once we allow for speculative trading triggered by such binary political events in both prediction and option markets. Arguably, reliance on risk-neutral probabilities from both markets were misleading as an indicator

for “Leave” outcome.

Table 4.1: **Variables and Corresponding BES Questions**

Variables	BES Question and Variables Values
Risk Taking	Generally speaking, how willing are you to take risks? 0 - 'Very unwilling' to 3 - 'Very willing'
Female	Are you male or female?
Personal Annula Gross Income $\geq$ 20k	Gross PERSONAL income is an individual's total income received from all sources, including wages, salaries, or rents and before tax deductions...What is your gross personal income?
Education	At what age did you finish full-time education?
Age	What is your age?
Party Identification	Generally speaking, do you think of yourself as Labour, Conservative, Liberal Democrat or what?
Level of Immigration Increasing	Do you think that each of the following are getting higher, getting lower or staying about the same?(The level of immigration) 0 - 'Getting a lot lower' to 4 - 'Getting a lot higher'
Brexit Would Reduce Immigration	Do you think the following would be higher, lower or about the same if the UK leaves the European Union? (Immigration to the UK) 0 - 'Much higher' to 4 - 'Much lower'
Immigrants Burden on Welfare State	How much do you agree or disagree with the following statements? (Immigrants are a burden on the welfare state) 0 - 'Strongly disagree' to 4 - 'Strongly agree'
Immigration Bad for Economy	Do you think immigration is good or bad for Britain's economy? 0 - 'Good for economy' to 6 - 'Bad for economy'
Immigration Undermines Cultural Life	And do you think that immigration undermines or enriches Britain's cultural life? 0 - 'Enriches for Britain's cultural life' to 6 - 'Undermines for Britain's cultural life'
Eurosceptic Newspaper Reader	Which daily newspaper do you read most often? Eurosceptic newspaper are The Express, The Daily Mail / The Scottish Daily Mail, The Sun, The Daily Telegraph, and The Times.
British Identity	Where would you place yourself on these scales? 0 - 'Not at all British' to 6 - 'Very strongly British'
English Identity	Where would you place yourself on these scales? 0 - 'Not at all English' to 6 - 'Very strongly English'
European Identity	Where would you place yourself on these scales? 0 - 'Not at all European to 6 - 'Very strongly European'
Economic Pessimism	Do you think that each of the following are getting better, getting worse or staying about the same? (The economy) 0 - 'Getting a lot better' to 4 - 'Getting a lot worse'

Table 4.2: **Probit Regression Models of EU Referendum Vote Choice**

This table presents result of the Probit regressions under five model specifications, where the dependent variable is the self-reported preferred choice at the 2016 referendum. T-statistics are reported in the parentheses. The sample period is between 6 May, 2016 and 22 June, 2016.

Variable	**(1)**		**(2)**		**(3)**		**(4)**		**(5)**	
Risk Taking Preference	0.11	(10.77)	0.19	(17.94)	0.15	(13.65)	0.24	(17.99)	0.27	(18.78)
Female			-0.01	(-0.82)	0.01	(0.60)	-0.04	(-2.21)	-0.10	(-4.61)
Personal Annula Gross Income $\geq$ 20k			-0.18	(-11.44)	-0.20	(-11.74)	-0.13	(-6.72)	-0.12	(-5.78)
Education (ref: Left School After 18):										
Left School Before 16			0.81	(44.76)	0.75	(38.81)	0.31	(13.11)	0.19	(7.39)
Left School Before 17 and 18			0.51	(26.80)	0.44	(21.88)	0.18	(7.49)	0.12	(4.70)
Age (ref: Aged 18-34)										
Aged 35-54			0.35	(15.17)	0.37	(15.15)	0.19	(6.81)	0.20	(6.69)
Aged $\geq$ 55			0.46	(20.90)	0.46	(19.32)	0.28	(10.13)	0.32	(10.59)
Party Identification (ref: Other/None)										
Conservative					0.29	(13.44)	0.01	(0.29)	-0.10	(-3.51)
Labour					-0.55	(-25.93)	-0.36	(-14.28)	-0.35	(-12.63)
Liberal Democrat					-0.66	(-19.19)	-0.37	(-9.21)	-0.27	(-6.35)
Nationalist					-0.52	(-13.62)	-0.36	(-7.77)	-0.08	(-1.46)
UKIP					1.80	(30.84)	1.22	(17.55)	1.10	(14.62)
Personal View about Immigration:										
Level of Immigration Increasing							0.30	(24.54)	0.25	(18.60)
Brexit Would Reduce Immigration							0.42	(37.56)	0.38	(32.17)
Immigrants Burden on Welfare State							0.21	(19.11)	0.16	(13.49)
Immigration Bad for Economy							0.12	(13.99)	0.08	(8.31)
Immigration Undermines Cultural Life							0.14	(19.22)	0.09	(11.54)
Eurosceptic Newspaper Reader									0.25	(11.20)
Identity:										
British Identity									0.02	(2.89)
English Identity									0.07	(13.60)
European Identity									-0.31	(-50.21)
Economic Pessimism									0.09	(7.54)
Constant	-0.14	(-8.42)	-0.94	(-31.91)	-0.80	(-24.48)	-4.01	(-69.12)	-3.15	(-42.00)
Adj. Generalized R^2	0.50%		16.03%		32.53%		61.09%		67.99%	
N	31008		31008		31008		31008		31008	
Share of Leave Voters	50.93%		50.93%		50.93%		50.93%		50.93%	
Intention to Leave (excluding Indecisive Respondents)	50.93%		50.94%		50.87%		50.94%		50.95%	
Intention to Leave of Indecisive Respondents	50.11%		50.92%		50.16%		53.58%		52.85%	
Intention to Leave (Total)	50.88%		50.94%		50.83%		51.10%		51.07%	

Table 4.3: **Correlation between the Change of Physical and Risk-Neutral Probabilities**

This table presents the correlations between the change of physical probabilities and the change of risk-neutral probabilities from option and prediction markets, display in column "Correlation (with Option)" and "Correlation (with Prediction)", respectively. Physical probabilities are inferred from political opinion polls by using 18 different learning models, including two methods (expending and rolling windows), three type of weights (equal-weighted, exponential decay and linear decay), three window lengths (30, 60 and 90 days). The sample period is between 3 May, 2016 and 23 June, 2016.

Method	Weight	Windows (days)	Correlation (with Option)	Correlation (with Prediction)
Expanding	**Equal-weighted**	**30**	0.16	0.29
Expanding	**Exponential Decay**	**30**	0.10	0.24
Expanding	**Linear Decay**	**30**	0.13	0.28
Expanding	**Equal-weighted**	**60**	0.21	0.33
Expanding	**Exponential Decay**	**60**	0.17	0.31
Expanding	**Linear Decay**	**60**	0.20	0.33
Expanding	**Equal-weighted**	**90**	0.24	0.36
Expanding	**Exponential Decay**	**90**	0.21	0.34
Expanding	**Linear Decay**	**90**	0.23	0.36
Rolling	**Equal-weighted**	**30**	0.16	0.18
Rolling	**Exponential Decay**	**30**	0.16	0.30
Rolling	**Linear Decay**	**30**	0.24	0.39
Rolling	**Equal-weighted**	**60**	0.20	0.34
Rolling	**Exponential Decay**	**60**	0.22	0.36
Rolling	**Linear Decay**	**60**	0.29	0.42
Rolling	**Equal-weighted**	**90**	0.25	0.34
Rolling	**Exponential Decay**	**90**	0.26	0.39
Rolling	**Linear Decay**	**90**	**0.30**	**0.43**
	Min		0.10	0.18
	Max		0.30	0.43
	Average		0.21	0.33
	Standard Deviation		0.05	0.06

Figure 4.1: **GBP/USD Exchange Rate and Put Option Price**

This figure presents the GBP/USD spot exchange rate and the CME British Pound put options price change around the Brexit referendum. Figure 4.1a displays the GBP/USD spot exchange rate between May and July, 2016. Figure 4.1b displays price changes of the CME British Pound put options on the event day and also non-event days.

(a) **GBP/USD Exchange Rate**

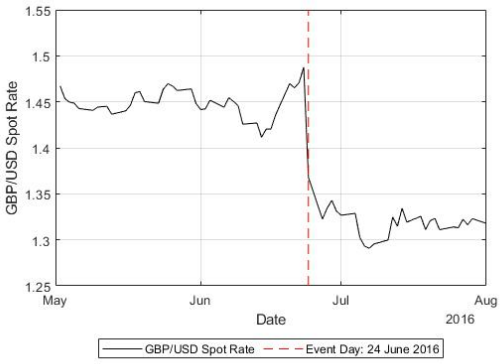

(b) **Put Option Price Changes**

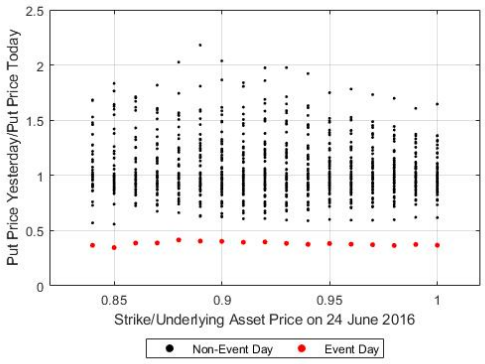

Figure 4.2: **Prediction Markets versus Political Opinion Polls**

This figure presents the implied probability of "Leave" obtained from prediction market and the percentage of Leave voters in several polls. Figure 4.2a shows the "Leave" probability recovered from predication market by using Betfair "Leave" odds between 3 May, 2016 and the 23 June, 2016. Figure 4.2b shows the voting intentions of "Leave' from thirteen market research companies (see legend below for dots, triangles and squares, n=128) between 10 January, 2016 and the 23 June, 2016. The voting intentions of "Leave' are measured as "Leave" percentage of decided respondents from political opinion polls.

(a) **Leave Probabilities from Prediction Market**

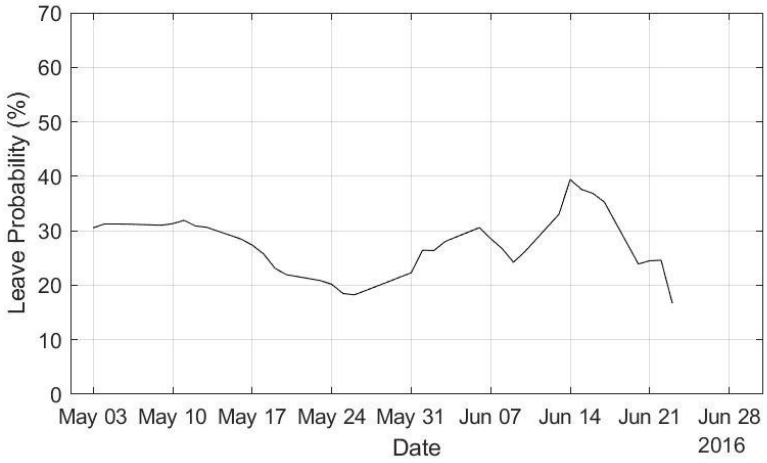

(b) **Voting Intention from Political Opinion Polls**

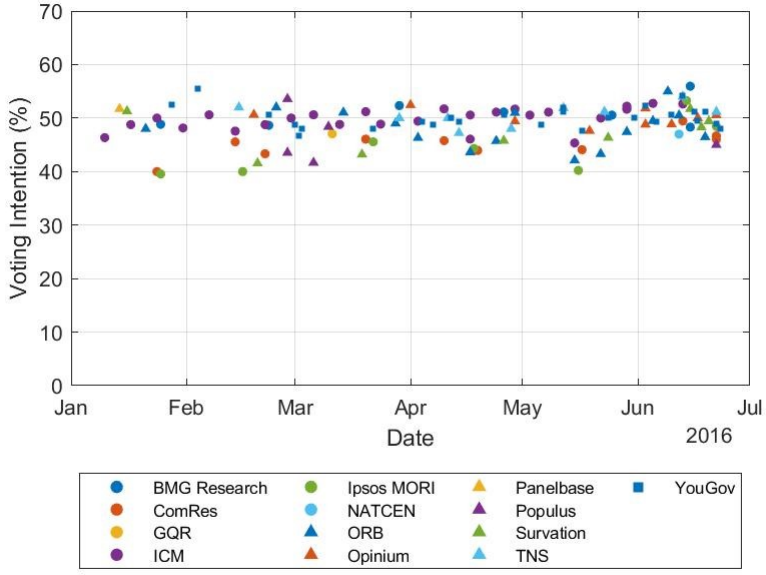

Figure 4.3: **IVs and RNDs Inferred from British Pound Options expiring on 8 July, 2016**

This figure presents fitted implied volatilities (Figure 4.3a and Figure 4.3b) and risk-neutral density distributions of GBP/USD futures (Figure 4.3c and Figure 4.3d) inferred from CME British Pound monthly futures options expiring on 8 July, 2016. Figure 4.3a and Figure 4.3c display the fitted implied volatility surface and RND surface of GBP/USD futures between 1 June, 2016 and 30 June 2016 across a wide range of strike prices. The red lines in these two figures indicates the Brexit referendum day (23 June, 2016). Figure 4.3b and Figure 4.3d are the fitted implied volatility curves and the corresponding RNDs of the six specific days, 6-, 4-, 2-weeks before the Brexit referendum (12 May, 2016, 26 May ,2016 and 09 June, 2016), the Brexit referendum day (23 June, 2016) and 1-day and 1-week after the Brexit referendum (24 June, 2016 and 30 June, 2016). In these two figures, black, red and blue lines represent the dates before, at and after the Brexit referendum, respectively.

(a) **Implied Volatility Surface**

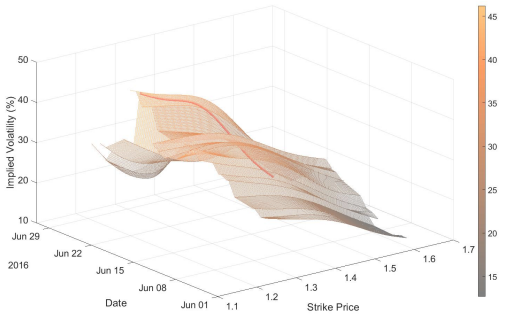

(b) **Implied Volatility in Different Days**

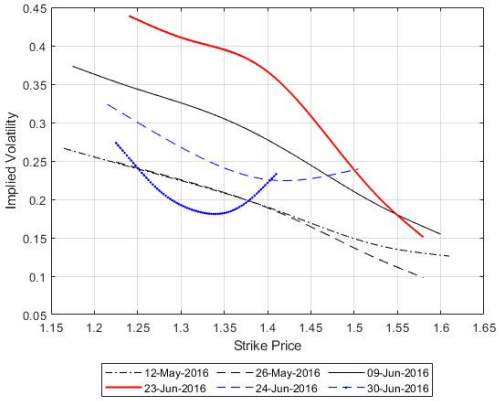

(c) **Risk-Neutral Density Surface**

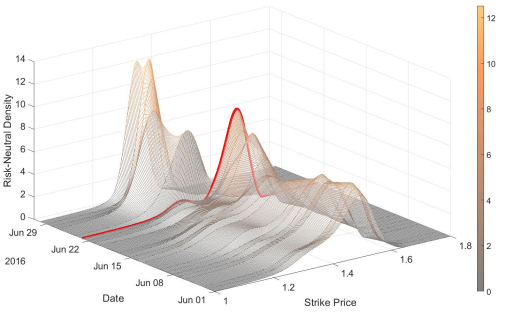

(d) **Risk-Neutral Densities in Different Days**

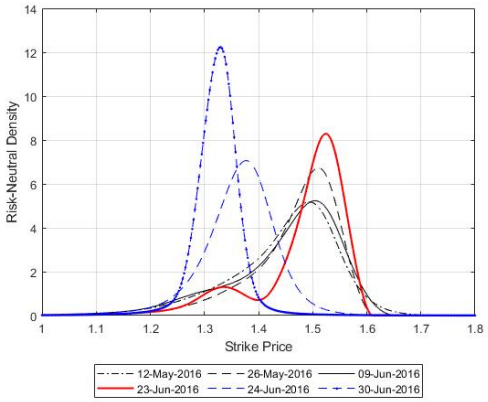

Figure 4.4: **RNDs Inferred from British Pound Options on 23 and 24 June, 2016**

This figure presents risk-neutral density distributions of GBP/USD futures inferred from British Pound options across all available maturities on 23 June, 2016 (Figure 4.4a) and 24 June, 2016 (Figure 4.4b). Red lines are RNDs extracted from options expiring on 8 July, 2016. Black/gray lines are RNDs extracted from options expiring after 8 July, 2016, between 5 August, 2016 and 9 July, 2017.

(a) **Risk-Neutral Densities on 23 June, 2016**

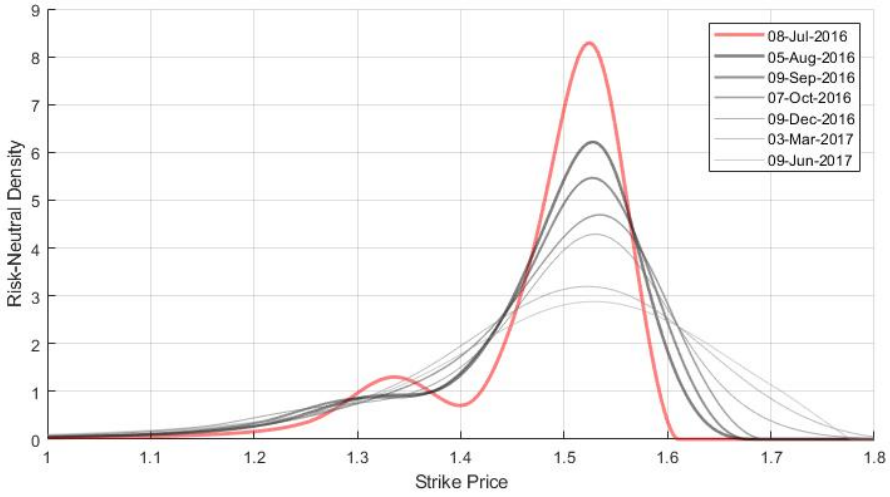

(b) **Risk-Neutral Densities on 24 June, 2016**

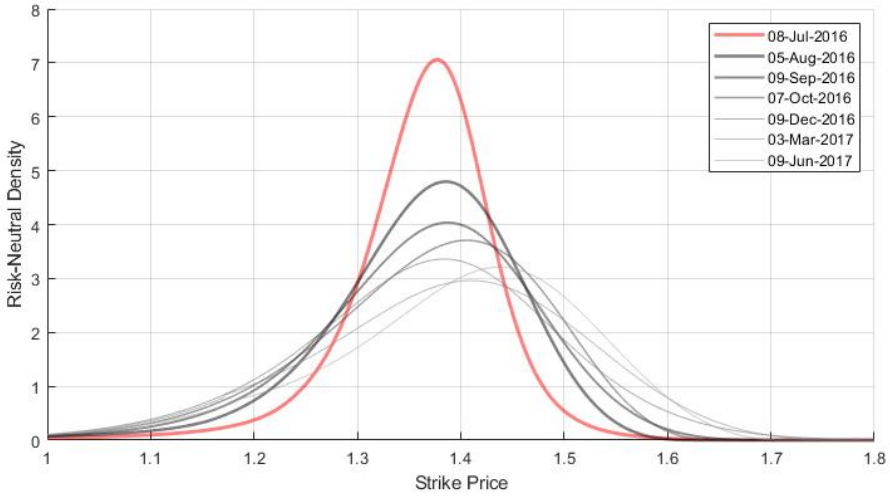

Figure 4.5: **Information in RNDs Inferred from British Pound Options**

This figure presents presents the annualized risk-neutral volatility (Figure 4.5a), the risk-neutral skewness (Figure 4.5b), the risk-neutral excess kurtosis (Figure 4.5c) and the Bimodality Coefficient (Figure 4.5d) of British Pound futures prices between 2 May, 2016 and 29 July, 2016. In this figure, we focus on RNDs from options with five different maturities, one maturity is before the Brexit referendum (3 June, 2016, blue line), three within the next following three months after the Brexit referendum (8 July, 2016 (red line), 5 August, 2016 (black line) and 9 September, 2016 (dark gray line)) and one six-month after the Brexit referendum (9 December, 2016, light gray line). The vertical line shows the day of the Brexit referendum on 23 June, 2016.

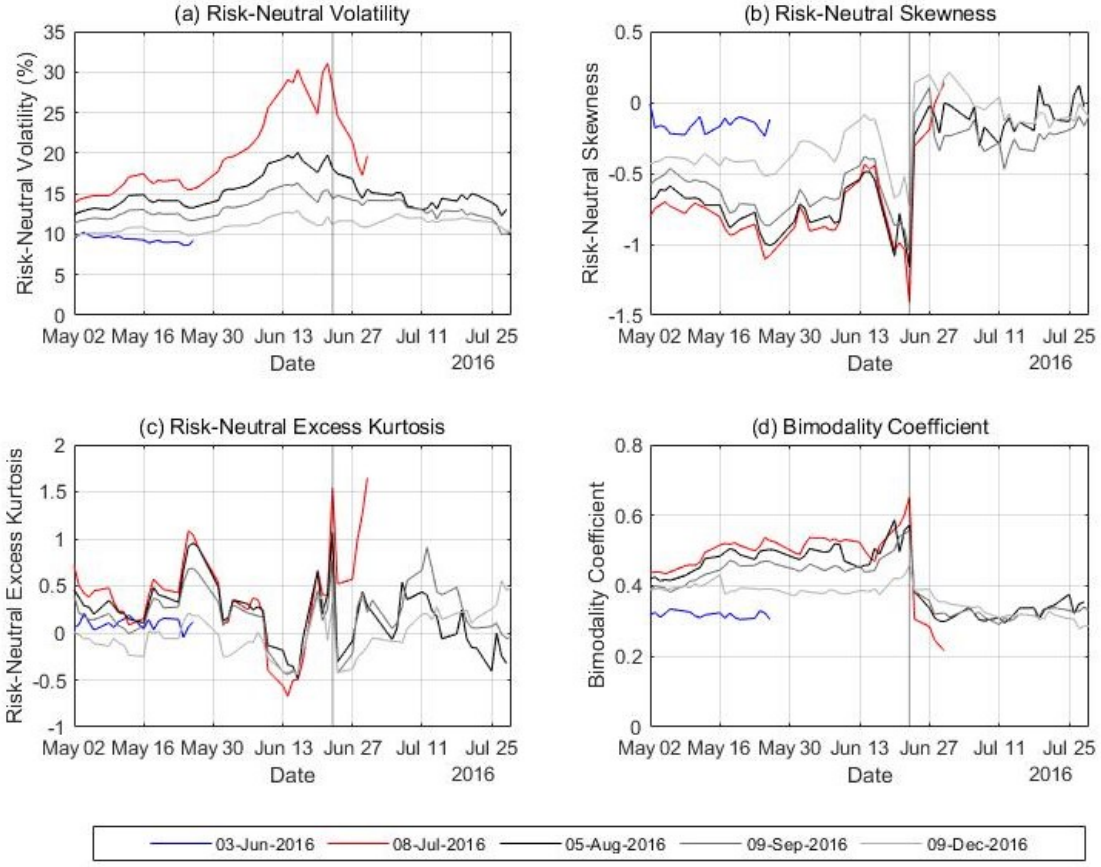

Figure 4.6: **British Pound Risk-Neutral 10% Quantiles**

This figure presents the British Pound Risk-Neutral 10% Quantiles for three horizons. The black, blue and red lines correspond to the variation of 10% quantile for the one-month, three-month and six-month horizons, respectively. Figure 4.6a display the 10% quantiles during the period between 2013 and 2016. Three vertical lines indicates Scottish independence referendum on 18 September 2014, United Kingdom general election on 7 May, 2015 and Brexit referendum on 23 June, 2016. In Fugure 4.6b, we zoom into the Brexit period.The vertical line shows the day of the Brexit referendum on 23 June, 2016.

(a) **Period from 2013 to 2016**

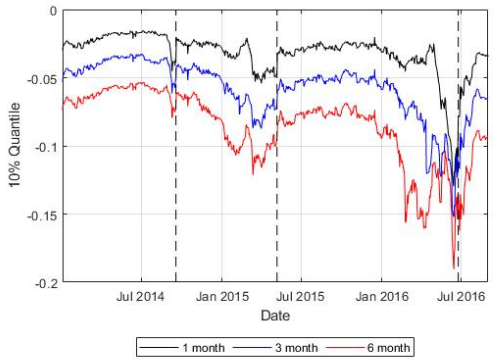

(b) **Brexit Period**

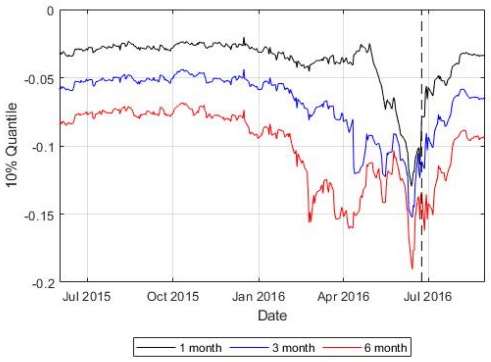

Figure 4.7: **Risk-Neutral Brexit Probabilities Implied by Option and Prediction Markets**

This figure presents the risk-neutral Brexit probabilities implied by option and prediction markets. The red line is the probability of Leave implied in the prediction market (Betfair) and the other three lines are risk-neutral probabilities of Leave implied in option market. Specifically, solid black, dash blue and dotted blue lines represent risk-neutral probabilities estimated from three different model specifications by setting $\omega_{t,i} = 1$, $\omega_{t,i} = \frac{1}{M_{t,K_i}}$ and $\omega_{t,i} = \frac{1}{M^2_{t,K_i}}$, respectively. The sample period used in this figure is from 3 May, 2016 to 23 June, 2016. The vertical lines show 14 and 16 June, 2016.

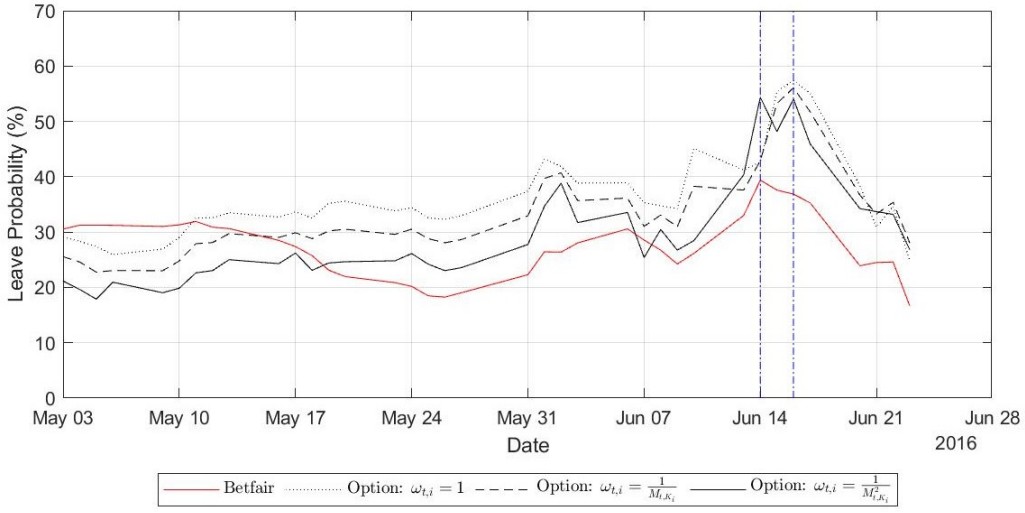

Figure 4.8: **State Prices and Volatility of GBP Futures**

This figure presents British Pound futures prices (Figure 4.8a) and corresponding volatilities (Figure 4.8b) in "Leave" and 'Remain' states. Blue line in Figure 4.8a is the actual British Pound futures price. Black and red lines in Figure 4.8a and Figure 4.8b represent British pound futures prices and corresponding volatilities in "Leave" and "Remain" state, receptively. Solid, dashed and dotted lines show state variables estimated from three different model specifications by setting $\omega_{t,i} = 1$, $\omega_{t,i} = \frac{1}{M_{t,K_i}}$ and $\omega_{t,i} = \frac{1}{M^2_{t,K_i}}$, respectively. The vertical lines show 14 and 16 June, 2016. The sample period used in this figure is from May 3, 2016 to June 23, 2016.

(a) **Option Implied State Prices**

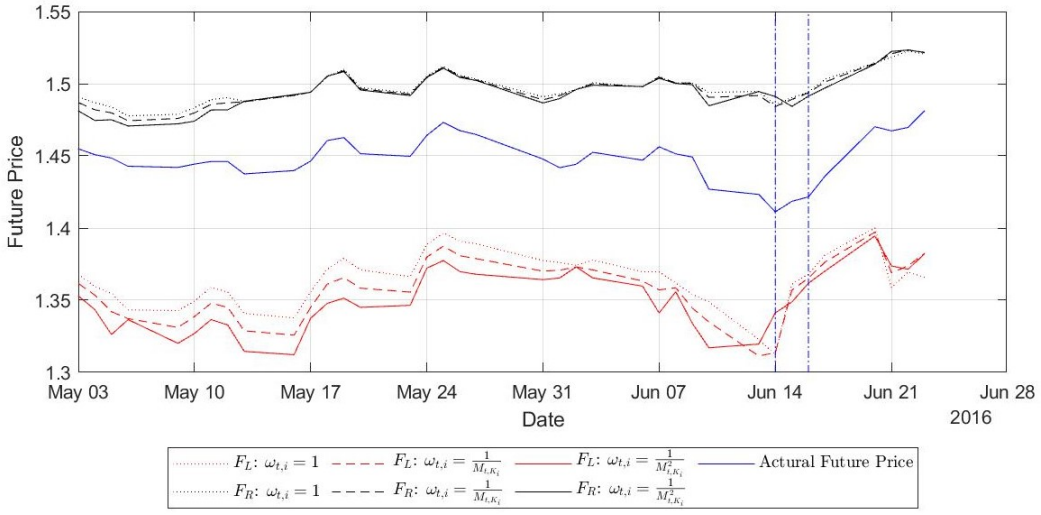

(b) **Option Implied State Volatility**

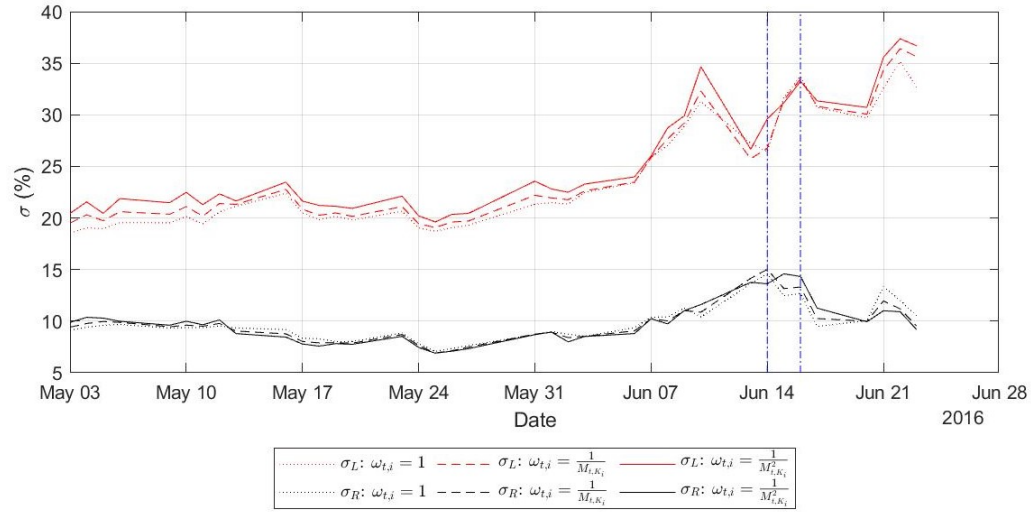

Figure 4.9: **Leave Probabilities Recovered from the Model-free Method**

This figure presents estimates of the "Leave" probability using a model-free method. Red circles represent the upper bounds of the estimated probability using the corresponding strike prices only. The black solid line is the fitted spline with 20 knots. The minimum of the spline is our preferred upper bound for the "Leave" probability. The sample period used in this estimation runs from the 2 May, 2016 and the 29 July, 2016.The dashed vertical line is the USD/GBP spot rate on the day of Brexit referendum, 23 June, 2016.

Figure 4.10: **Leave Probabilities from the Political Opinion Polls**

This figure presents the implied probability of "Leave" obtained from polls data (blue line), Betfair odds (red line) and option market (black line). The vertical lines show 14 June, 2016 and 16 June, 2016. The sample period is between 6 May, 2016 and 22 June, 2016.

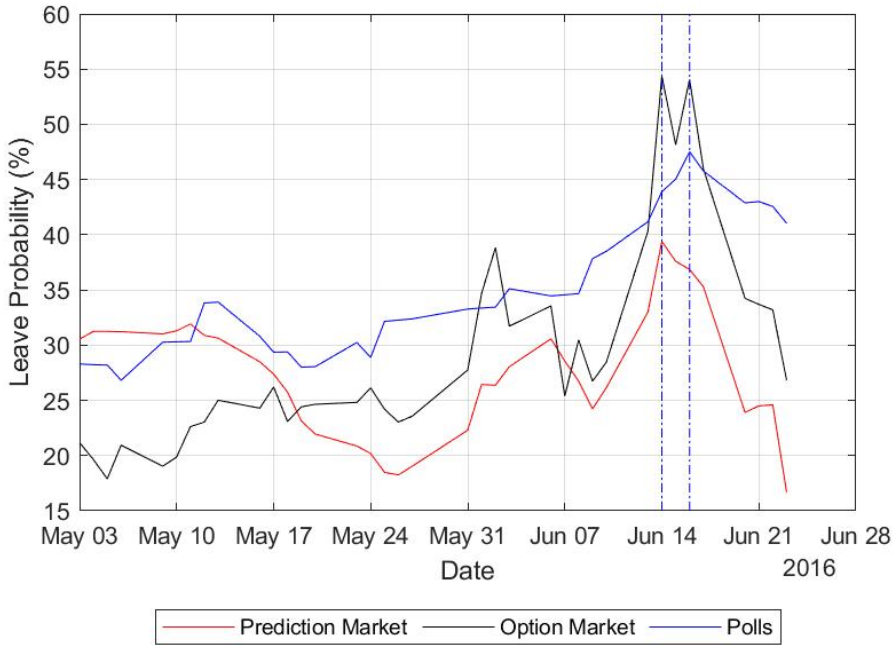

Figure 4.11: **Risk-Corrected Leave Probability (Non-Parametric)**

This figure presents the probabilities recovered using Ross (2015). Figure 4.11a and Figure 4.11b shows the non-corrected (risk-neutral) and risk-corrected probabilities in prediction markets and option markets, respectively. Red solid line is the non-corrected probabilities. Black dashed line is the risk-corrected probabilities corresponding to an (almost) absorbing state 2, where the Arrow-Debreu prices are $A_{21} = 0.01$ and $A_{22} = 0.99$. Black dotted line is the risk-corrected probabilities corresponding to "high uncertainty" state 2, where the Arrow-Debreu prices are $A_{21} = 0.5$ and $A_{22} = 0.5$. The sample period is between 3 May, 2016 and 23 June, 2016.

(a) **Prediction Markets**

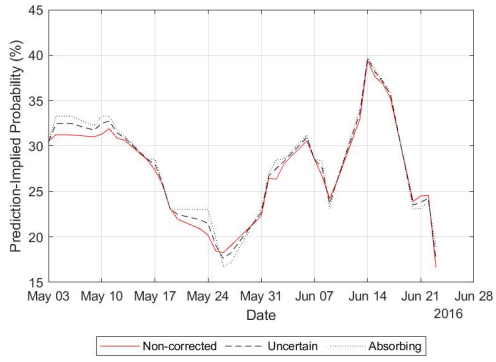

(b) **Option Markets**

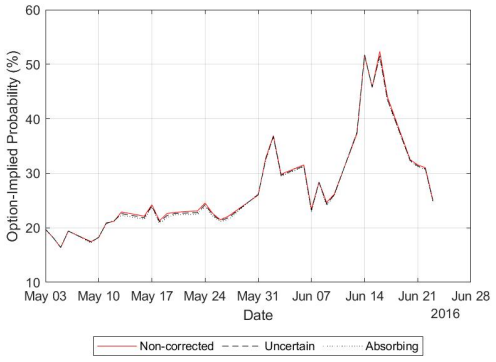

Figure 4.12: **Risk-Corrected Leave Probability (Parametric)**

This figure presents the probabilities recovered using the parametric approach. Figure 4.12a and 4.12c show the risk-corrected probabilities in prediction markets, and Figure 4.12b and 4.12d show the risk-corrected probabilities in option markets. In Figure 4.12a and 4.12b, assume the relative wealth in "Remain" and "Leave" states, $\frac{W^L}{W_R}$, is 0.90, we display the probabilities corrected using different value for the constant relative risk aversion coefficient ($\gamma = -6, -4, -2, 0, 2, 4, 6$). In Figure 4.12c and 4.12d, assume the constant relative risk aversion coefficient, γ, is -2, we display the probabilities corrected using different value for the relative wealth in "Remain" and "Leave" states ($\frac{W^L}{W_R} = 0.75, 0.90, 0.95, 1.00, 1.05, 1.10, 1.25$), where W^R is the wealth of the representative agent in the remain state and W^L the corresponding wealth in the leave state. The sample period is between 3 May, 2016 and 23 June, 2016.

(a) **Prediction Markets (γ)**

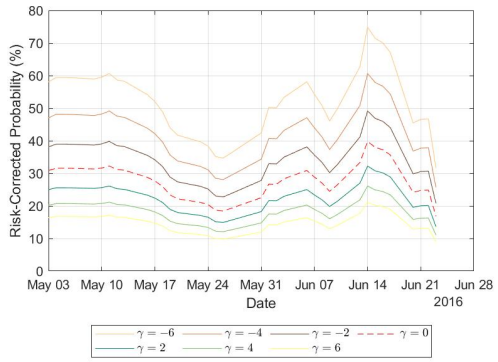

(b) **Option Markets (γ)**

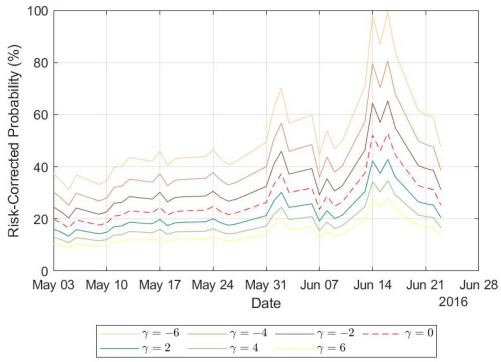

(c) **Prediction Markets (Relative Wealth)**

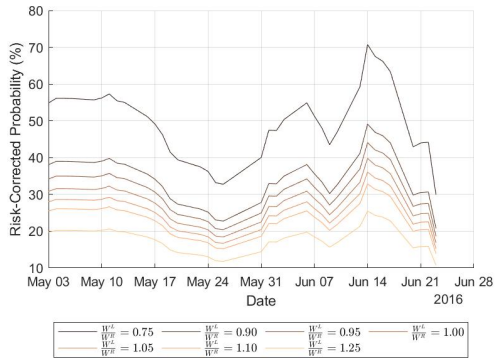

(d) **Option Markets (Relative Wealth)**

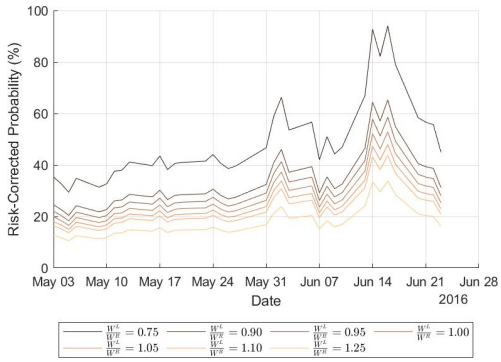

Figure 4.13: **Trading Behaviors on Derivative Markets**

This figure presents the trading behaviors on CME British pounds derivative markets. Figure 4.13a shows the put–call ratio (left axis) and the uncertainty of opinion polls outcomes (right axis). Put–call ratio is calculated from the open interest of CME British pounds options expiring on 8 July, 2016. The uncertainty of opinion polls outcomes is defined as the standard deviation of the expected "Leave" outcome under the assumption of binomial distribution, which is $\sqrt{\frac{p^L_{poll,t}(1-p_{poll,t})^L}{n}}$, and n is window length used for subjective "Leave" probability ($p_{poll,t}$) calculation. Figure 4.13b presents the total CME British pounds futures' and options' positions held by speculators (non-commercial) relative to the total positions held by hedgers (commercial), scaled by the values in the past period. The sample period in Figure 4.13a is between 3 May, 2016 and 23 June, 2016. The sample period in Figure 4.13b is between 3 May, 2016 and 28 June, 2016. The data is sampled weekly (Tuesday-to-Tuesday).

(a) **Put Call Ratio and Polls Uncertainty**

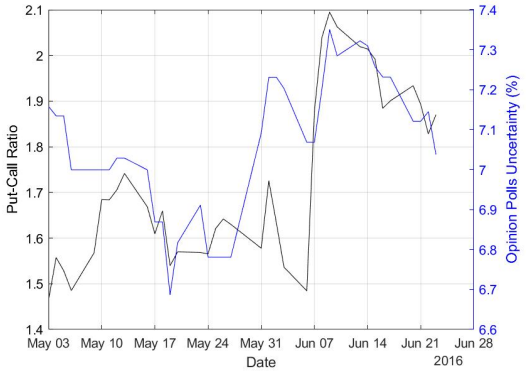

(b) **Speculative vs. Hedging Activity**

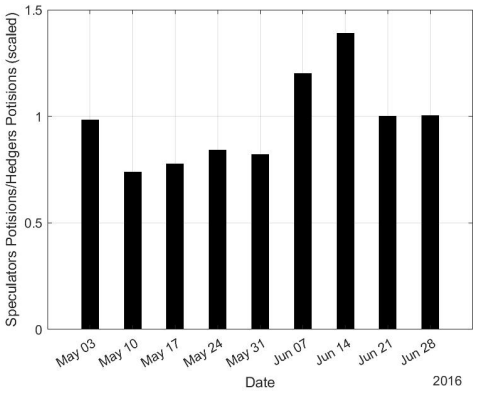

Figure 4.14: **Risk-Corrected versus Subjective Probabilities**

This figure presents the subjective probabilities extracted from opinion polls and risk-corrected probabilities by using data from the betting and option markets. Probabilities are corrected using the following parameterisation: (1) $\beta = 0.99$, (2) $\frac{W^L}{W^R} = 0.90$ where W^R is the level of wealth of the representative agent in the remain state and W^L the corresponding level of wealth in the leave state, (3)relative risk reversion coefficient, γ^{p*} and γ^{o*}, where p and o represent prediction and option markets respectively. Specifically, $\gamma^{i*} \equiv \arg\min_\gamma \sum_{t=1}^{T}(\tilde{\pi}_t^i - \hat{\pi}_t)^2$, where $i = p, o$, T is the sample size, $\tilde{\pi}_t^i$ is the risk-corrected probability by using date from option or prediction markets, and $\hat{\pi}_t$ is the subjective probabilities inferred from opinion polls; this gives $\gamma^{p*} = -1.83$ and $\gamma^{o*} = -1.01$.The sample period is between 6 May, 2016 and 22 June, 2016.

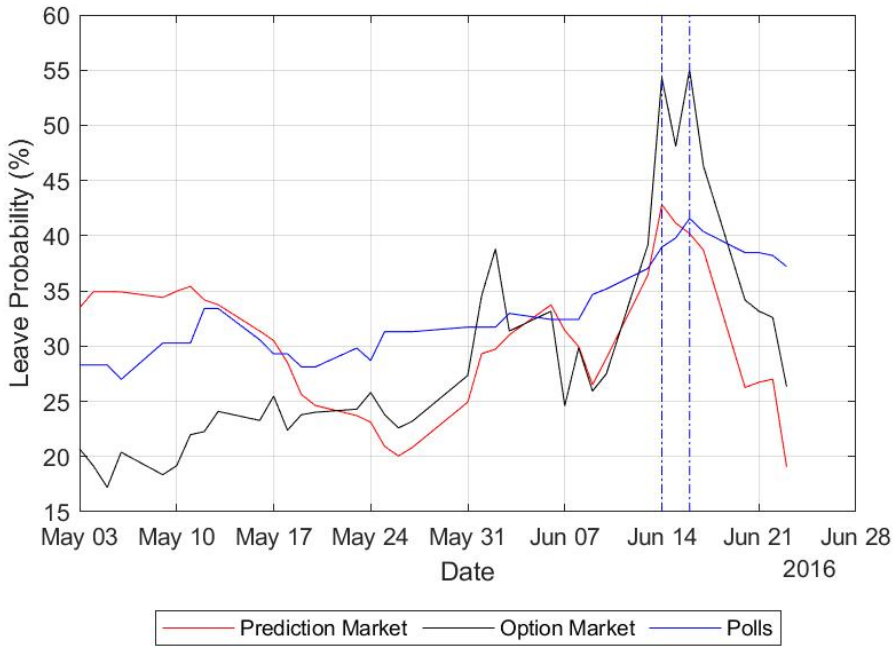

Figure 4.15: **Relative Risk Aversion Coefficient and Relative Wealth**

This figure presents the relative risk aversion coefficient used to minimize the distance between the risk-corrected probabilities and the physical probability from the BES data, with respect to different level of wealth in the "Leave" and "Remain" states. We use $\beta = 0.99$ and $\frac{W^L}{W^R}$ between 0.5 and 1.5, where W^R is the level of wealth of the representative agent in the "Remain" state and W^L the corresponding level of wealth in the "Leave" state. The red and black solid lines are the relative risk aversion coefficients for prediction and option markets, respectively. The dashed blue line represents the baseline case used in Figure 4.14. The sample period is between 6 May, 2016 and 22 June, 2016.

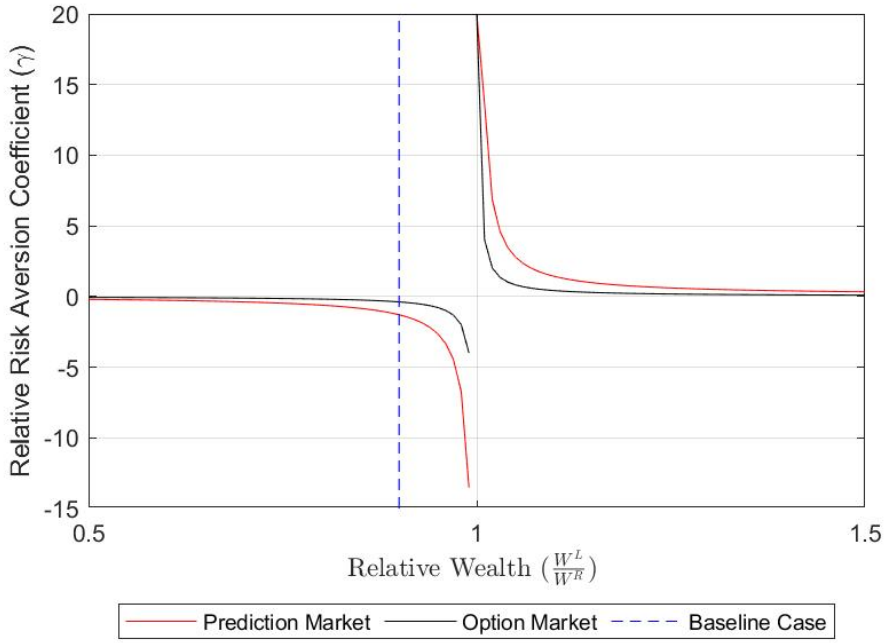

Figure 4.16: **Voting Intention from the BES Survey**

This figure presents the voting intention of "Leave" from the BES Survey (blue line, right y-axis) and implied probability of "Leave" obtained from Betfair odds (red line, left y-axis) and option market (black line, left y-axis). The vertical lines show 14 June, 2016 and 16 June, 2016. The sample period is between 6 May, 2016 and 22 June, 2016.

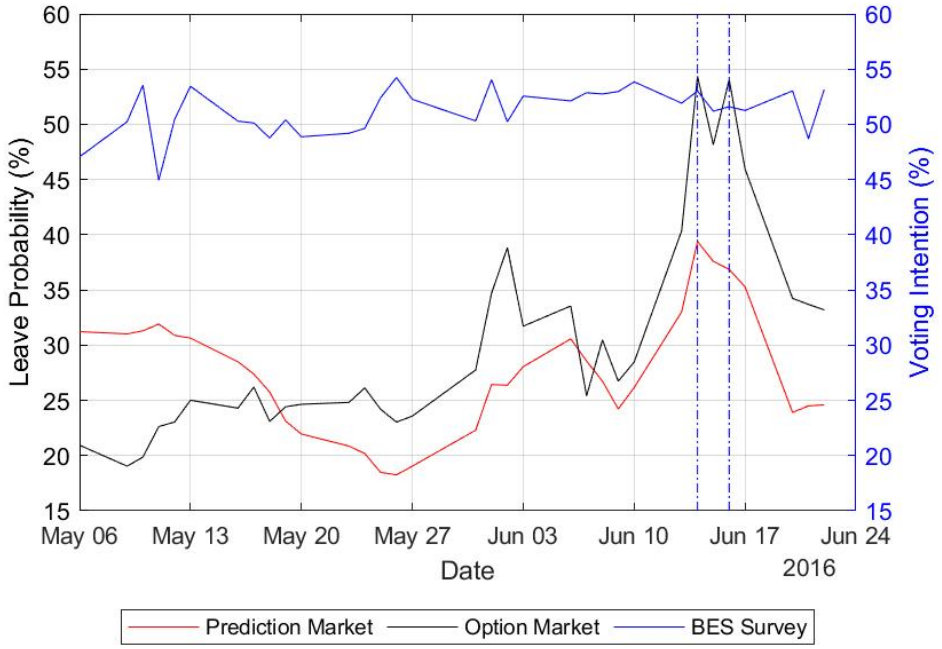

Appendix 4.A RNDs Extraction

First, we only use options with less noise and more informative prices for the RND extraction. Our selection is mainly based on options' trading volume and the open interest. Specifically, due to the thin trading volume of in-the-money (ITM) options and deep-out-of-the-money (deep OTM) options, we exclude them from our sample. We classify options with a price equal to $ 0.001 per pound and a price change less than $ 0.001 per pound increment as deep OTM. In addition, we discard options with zero open interest. Thus, we only use out-of-the-money (OTM) and at-the-money (ATM) options with positive open interest for the RND extraction.

Second, we covert option prices from price-strike space to volatility-strike space. Since options in our sample are American-style options written on futures, we use the Barone-Adesi-Whaley (BAW) American futures option pricing model (Barone-Adesi and Whaley, 1987) to obtain the implied volatility, which can eliminate the early exercise premium in the American option. Cincibuch (2004) studies the difference between the implied volatilities of CME American-style Japanese Yen futures options and OTC European-style Japanese Yen options. They find that there is no significant difference between BAW implied volatilities from American options and Black–Scholes (BS) implied volatilities from European options. Therefore, we use BAW implied volatilities to infer implied volatilities of European options and follow the standard procedure for extracting RND from European options.

Third, we smooth implied volatility curves. Previous studies adopt various methods to smooth implied volatility curves, for example, quadratic polynomial (Shimko, 1993) and cubic splines (Bates, 1991; Jiang and Tian, 2005; Monteiro et al., 2008). Due to the nature of the quadratic polynomial, the quadratic spline is not continuous in the second derivative. A standard cubic spline can avoid this issue, but it must pass the original data points, which brings noise from market microstructure frictions. To

avoid these issues, we fit the implied volatility curve by using a fourth-degree polynomial spline (Figlewski, 2009), which minimizes the sum of squared differences between the observed implied volatility curve and the fitted spline. Hence, implied volatilities can be interpolated as a dense set of fitted splines.

Fourth, we convert interpolated implied volatilities back to option prices. Because of the insignificant difference between BAW implied volatility and implied volatility from its corresponding European option, we use the interpolated BAW implied volatility in the Black model (Black, 1976) to calculate the price of the corresponding European option.

In the fifth step, we approximate the middle part of the RND by using interpolated European futures options prices. The middle part of RND at time t is between the second lowest and the second highest observed strike prices at time t. Let F_{t,T_f} denote the price of a future contract with maturity T_f at time t. Assume that T_o is an option's expiry date, then the time-T_o payoff of an European call option written on a future contract, with strike price K, is written $\max(F_{T_o,T_f} - K, 0)$. We denote $C(t, K, T_f, T_o)$ as the observed call option price at time t, with strike price K, maturity T_o and underlying future contract that expires at T_f. With the assumption of no arbitrage, the option price at time t is equal to the present value of the risk-neutral expected payoff at T_o,

$$\begin{aligned} C(t, K, T_f, T_o) &= e^{-r_t(T_o-t)}\mathbb{E}_t[\max(F_{T_o,T_f} - K, 0)] \\ &= e^{-r_t(T_o-t)} \int_K^\infty (F_{T_o,T_f} - K)\pi_t(F_{T_o,T_f})\, dF_{T_o,T_f}, \end{aligned} \tag{4.28}$$

where r_t is the risk-free interest rate at time t, $\pi_t(F_{T_o,T_f})$ is the risk-neutral probability density function of the underlying future price. Following the standard approach of Breeden and Litzenberger (1978),

$$\frac{\partial C(t,K,T_f,T_o)}{\partial K} = e^{-r_t(T_o-t)}[\int_0^K \pi_t(F_{T_o,T_f})\, dF_{T_o,T_f} - 1]. \tag{4.29}$$

Thus, the risk-neutral cumulative function of the underlying future price at time t is

$$\Pi_t(K) = Prob_t(F_{T_o,T_f} \leq K) = \int_0^K \pi_t(F_{T_o,T_f})\, dF_{T_o,T_f} = 1 + e^{r_t(T_o-t)} \frac{\partial C(t,K,T_f,T_o)}{\partial K}. \tag{4.30}$$

Taking the derivative with respect to K in equation (4.30), the risk-neutral probability density function is

$$\pi_t(K) = e^{r_t(T_o-t)} \frac{\partial^2 C(t,K,T_f,T_o)}{\partial K^2}. \tag{4.31}$$

Taking finite differences, we approximate the option-implied risk-neutral cumulative density function (CDF)

$$\Pi_t(K) \approx 1 + e^{r_t(T_o-t)} \frac{1}{\triangle}[C(t,K+\frac{\triangle}{2},T_f,T_o) - C(t,K-\frac{\triangle}{2},T_f,T_o)] \mid_{\triangle \to 0}, \tag{4.32}$$

and risk-neutral probability density function (PDF), which is also known as RND,

$$\pi_t(K) \approx e^{r_t(T_o-t)} \frac{1}{\triangle^2}[C(t,K+\triangle,T_f,T_o) + C(t,K-\triangle,T_f,T_o) - 2C(t,K,T_f,T_o)] \mid_{\triangle \to 0}. \tag{4.33}$$

Similar as the steps we extract RND from a set of call option prices, we can obtain the risk-neutral CDF from put option prices as the following,

$$\Pi_t(K) \approx e^{r_t(T_o-t)}\frac{1}{\triangle}[P(t,K+\frac{\triangle}{2},T_f,T_o)-P(t,K-\frac{\triangle}{2},T_f,T_o)]\mid_{\triangle\to 0}, \tag{4.34}$$

and its corresponding risk-neutral probability density function (PDF)

$$\pi_t(K) \approx e^{r_t(T_o-t)}\frac{1}{\triangle^2}[P(t,K+\triangle,T_f,T_o)+P(t,K-\triangle,T_f,T_o)-2P(t,K,T_f,T_o)]\mid_{\triangle\to 0}. \tag{4.35}$$

Then, $\pi_t(K)$ is the middle part of the RND. Finally, we append the RND into the left and right tails by fitting the generalized extreme value (GEV) distribution, which is a natural candidate to model the tails of an unknown distribution. GEV distribution has three parameters and its CDF is

$$\Pi_{GEV}(z) = e^{-(1+\xi z)^{-\frac{1}{\xi}}}, z = \frac{F_{t,T_1}-\mu}{\sigma}, \tag{4.36}$$

where ξ, μ and σ are used to control shape, location and scale of the tail distribution. $\xi > 0$ indicates a fat tail from the Frechet distribution, $\xi = 0$ determines a normal tail with the Gumbel distribution, and $\xi < 0$ means finite tails from the Weibull distribution. We define the strike price at α-quantile of the RND as $K(\alpha)$, which is equivalent to $\Pi_{GEV}(K(\alpha)) = \alpha$. $\Pi_{GEV}(z)$'s corresponding PDF can be written as $\pi_{GEV}(z)$. To estimate three parameters in GEV distribution, we set up three constraints for the right tail as the following:

$$\begin{aligned}
&\Pi_{GEV}(K(\alpha_{1R})) = \alpha_{1R},\\
&\pi_{GEV}(K(\alpha_{1R})) = \pi(K(\alpha_{1R})),\\
&\pi_{GEV}(K(\alpha_{2R})) = \pi(K(\alpha_{2R})),
\end{aligned} \tag{4.37}$$

where $\pi(K(\alpha))$ is the empirical RND function we estimated in the last step. The constraints used for left tail estimation are

$$\begin{aligned} &\Pi_{GEV}(-K(\alpha_{1L})) = 1 - \alpha_{1L}, \\ &\pi_{GEV}(-K(\alpha_{1L})) = \pi(K(\alpha_{1L})), \\ &\pi_{GEV}(-K(\alpha_{2L})) = \pi(K(\alpha_{2L})). \end{aligned} \tag{4.38}$$

Specifically, we set α_1 and α_2 as 5% and 2% for the left tail, and 92% and 95% for the right tail.

Appendix 4.B AD Prices for Risk Recovery

AD Prices from Betting Odds Consider the first observation in our sample. The timestamp is *25/02/2016 16:28:00*. Odds are 3.2 for leave and 1.5 for remain. The corresponding Arrow-Debrew prices for these states of nature are $\frac{1}{3.2}£$ and $\frac{1}{1.5}£$. This means that we can write

$$\mathbf{A_t} = \begin{pmatrix} \frac{1}{1.5} & \frac{1}{3.2} \\ A_{21,t} & A_{22,t} \end{pmatrix}. \tag{4.39}$$

We will use two assumptions to complete the second row of $\mathbf{A_t}$. The first assumption is of "high uncertainty" as embedded in the following AD prices

$$\mathbf{A_t} = \begin{pmatrix} \frac{1}{1.5} & \frac{1}{3.2} \\ 0.5 & 0.5 \end{pmatrix}, \tag{4.40}$$

and second, an (almost) absorbing state 2

$$\mathbf{A_t} = \begin{pmatrix} \frac{1}{1.5} & \frac{1}{3.2} \\ 0 & 1 \end{pmatrix}. \tag{4.41}$$

Note that, under risk neutrality and no discounting, the Arrow-Debrew pricing matrix is equivalent to the frequency matrix, i.e. $\mathbf{A_t} = \mathbf{P_t}$.

AD Prices from FX Derivatives The option price as well as the forward price in the left hand side of the system of equations (4.5) is expressed in USD. In other words, those contracts refer to the dollar price of a future pound (whatever state of nature, i.e leave or remain, realises). Hence, p_t^L refers to the probability that the GBP will reach a certain *dollar* value in each and respective state of nature. In order to calculate primitive or state prices we need the domestic (GBP) price of a future unit of domestic currency (GBP) in each state of nature. Let us maintain the hypothesis that there are

only two states: leave or remain. The time t GBP price of the AD securities are given by A_t^{R*} and A_t^{L*} whereas the time t USD price of the AD securities are written as A_t^R and A_t^L, for the remain and leave states, respectively. Calculating the asset return from the perspective of a US resident and assuming no-arbitrage results

$$\underbrace{\frac{1}{A_t^R + A_t^L}}_{\text{USD } T_f \text{ return of investing one USD at } t} = \underbrace{\frac{\overbrace{S_t^{-1}}^{\text{one USD in GBP}}}{\underbrace{A_t^{R*} + A_t^{L*}}_{\text{GBP } T_f \text{ return of investing one USD at } t}} \times F_{t,T_f}}_{\text{USD } T_f \text{ return of investing one USD at } t}, \tag{4.42}$$

or

$$A_t^{R*} + A_t^{L*} = \left(A_t^R + A_t^L\right) \frac{F_{t,T_f}}{S_t}. \tag{4.43}$$

Note also that $A_t^R + A_t^L = \frac{1}{1+i_t}$ and $A_t^{R*} + A_t^{L*} = \frac{1}{1+i_t^*}$, where i_t is the risk-free interest rate on a US bond which matures at T_f; the asterisk refers to the one in the UK economy. This gives

$$F_{t,T_f} = (1 + i_t) S_t \left(A_t^{R*} + A_t^{L*}\right). \tag{4.44}$$

Using the notation in the first section, recall that F_{t,T_f} is the USD price at time t of one unit of a future time, T_f, GBP. An agent that buys F_{t,T_f} will receive one GBP at T_f for certain, i.e. irrespective of the state of nature. It follows that $\frac{F_{t,T_f}}{S_t}$ is the GBP price at time t of one unit of a future GBP. This transformation is equivalent to the price of a risk free asset which can be divided into two primitive (theoretical) sterling prices, at t. The first is given by $\left(1 - p_t^L\right) \times \frac{F_{t,T_f}^L}{S_t}$ which can be seen as an asset that will pay one unit of GBP if (and only if) the leave state of nature realises, i.e., if $p_t^L = 0$. The second is $p_t^L \times \frac{F_{t,T_f}^R}{S_t}$ which has an analogous interpretation, however, for the remain

case. Given that S_t is the dollar price of a spot GBP and F_t is the dollar price of a future GBP, one can write (4.44) as

$$p_t^L F_{t,T_f}^L + (1 - p_t^L) F_{t,T_f}^R = (1 + i_t) S_t \left(A_t^{L*} + A_t^{R*} \right), \tag{4.45}$$

or

$$A_t^{L*} + A_t^{R*} = \underbrace{p_t^L \frac{F_{t,T_f}^L}{S_t(1+i_t)}}_{\text{which equals } A_t^{L*} \text{ by arbitrage}} + \underbrace{(1 - p_t^L) \frac{F_{t,T_f}^R}{S_t(1+i_t)}}_{\text{which equals } A_t^{R*} \text{ by arbitrage}} . \tag{4.46}$$

Appendix 4.C An Example for Non-parametric Recovery

Consider the symmetric case of AD prices in the betting market, in other words,

$$\mathbf{A_t} = \begin{pmatrix} \frac{1}{1.5} & \frac{1}{3.2} \\ \frac{1}{3.2} & \frac{1}{1.5} \end{pmatrix}. \tag{4.47}$$

Eigenvalues are $\phi_1 = 0.9791667$ and $\phi_2 = 0.3541667$; the corresponding eigenvectors are $Z_{1,t} = (0.7071068\ ,\ 0.7071068)^\top$ and $Z_{2,t} = (-0.7071068\ ,\ 0.7071068)^\top$. PF theorem guarantees that for square non-negative matrices, ϕ_1 is the highest in absolute value and all entries of the corresponding eigenvector are positive. This allow us to assume that $\phi_1 = \beta$ and

$$\mathbf{D_t} = \begin{pmatrix} 0.7071068 & 0 \\ 0 & 0.7071068 \end{pmatrix}, \tag{4.48}$$

which finally gives

$$\mathbf{P_t} = \begin{pmatrix} 0.6808511 & 0.3191489 \\ 0.3191489 & 0.6808511 \end{pmatrix}, \tag{4.49}$$

Bibliography

Abosedra, S. S. and Laopodis, N. T. (1996). Stochastic behavior of crude oil prices: A garch investigation. *The Journal of Energy and Development*, 21(2):283–291.

Ait-Sahalia, Y. and Lo, A. W. (2000). Nonparametric risk management and implied risk aversion. *Journal of Econometrics*, 94(1-2):9–51.

Alexander, C. (2004). Correlation in crude oil and natural gas markets. In Kaminski, V. V. and Jameson, R., editors, *Managing energy price risk: the new challenges and solutions. 3. ed*, pages 573–606. Risk Books, London.

Anderson, R. W. (1985). Some determinants of the volatility of futures prices. *The Journal of Futures Markets (pre-1986)*, 5(3):331.

Asness, C. S., Moskowitz, T. J., and Pedersen, L. H. (2013). Value and momentum everywhere. *The Journal of Finance*, 68(3):929–985.

Auld, T. and Linton, O. (2019). The behaviour of betting and currency markets on the night of the eu referendum. *International Journal of Forecasting*, 35(1):371–389.

Back, J., Prokopczuk, M., and Rudolf, M. (2013). Seasonality and the valuation of commodity options. *Journal of Banking & Finance*, 37(2):273–290.

Bakshi, G., Carr, P., and Wu, L. (2008). Stochastic risk premiums, stochastic skewness in

currency options, and stochastic discount factors in international economies. *Journal of Financial Economics*, 87(1):132–156.

Bakshi, G., Gao, X., and Rossi, A. G. (2019). Understanding the sources of risk underlying the cross section of commodity returns. *Management Science*, 65(2):619–641.

Barillas, F. and Shanken, J. (2017). Which alpha? *The Review of Financial Studies*, 30(4):1316–1338.

Barillas, F. and Shanken, J. (2018). Comparing asset pricing models. *The Journal of Finance*, 73(2):715–754.

Barone-Adesi, G. and Whaley, R. E. (1987). Efficient analytic approximation of american option values. *The Journal of Finance*, 42(2):301–320.

Barro, R. J. (2009). Rare Disasters, Asset Prices, and Welfare Costs. *American Economic Review*, 99(1):243–264.

Basak, S. and Pavlova, A. (2016). A model of financialization of commodities. *The Journal of Finance*, 71(4):1511–1556.

Basu, D. and Miffre, J. (2013). Capturing the risk premium of commodity futures: The role of hedging pressure. *Journal of Banking & Finance*, 37(7):2652–2664.

Bates, D. S. (1991). The crash of '87: was it expected? the evidence from options markets. *The Journal of Finance*, 46(3):1009–1044.

Belke, A., Dubova, I., and Osowski, T. (2018). Policy uncertainty and international financial markets: the case of Brexit. *Applied Economics*, 50(34-35):3752–3770.

Bessembinder, H. (1992). Systematic risk, hedging pressure, and risk premiums in futures markets. *The Review of Financial Studies*, 5(4):637–667.

Bevilacqua, M., Brandl-Cheng, L., Danielsson, J., Ergun, L. M., Uthemann, A., and Zigrand, J.-P. (2021). The calming of short-term market fears and its long-term consequences: The federal reserve's reaction to covid-19. Working paper, London School of Economics.

Black, F. (1976). The pricing of commodity contracts. *Journal of Financial Economics*, 3(1-2):167–179.

Bloom, N. (2009). The impact of uncertainty shocks. *Econometrica*, 77(3):623–685.

Bond, P. and Dow, J. (2021). Failing to forecast rare events. *Journal of Financial Economics*, 142(3):1001–1016.

Boons, M. and Prado, M. P. (2019). Basis-momentum. *The Journal of Finance*, 74(1):239–279.

Borochin, P. and Golec, J. (2016). Using options to measure the full value-effect of an event: Application to obamacare. *Journal of Financial Economics*, 120(1):169 – 193.

Borovička, J., Hansen, L. P., and Scheinkman, J. A. (2016). Misspecified recovery. *The Journal of Finance*, 71(6):2493–2544.

Breeden, D. T. and Litzenberger, R. H. (1978). Prices of state-contingent claims implicit in option prices. *The Journal of Business*, 51(4):621–651.

Broadie, M., Chernov, M., and Johannes, M. (2007). Model specification and risk premia: Evidence from futures options. *The Journal of Finance*, 62(3):1453–1490.

Brogaard, J., Ringgenberg, M. C., and Sovich, D. (2019). The economic impact of index investing. *The Review of Financial Studies*, 32(9):3461–3499.

Brooks, C. and Prokopczuk, M. (2013). The dynamics of commodity prices. *Quantitative Finance*, 13(4):527–542.

Brunetti, C., Büyükşahin, B., and Harris, J. H. (2016). Speculators, prices, and market volatility. *Journal of Financial and Quantitative Analysis*, 51(5):1545–1574.

Brunetti, C. and Reiffen, D. (2014). Commodity index trading and hedging costs. *Journal of Financial Markets*, 21:153–180.

Buyuksahin, B., Haigh, M. S., Harris, J. H., Overdahl, J. A., and Robe, M. A. (2008). Fundamentals, trader activity and derivative pricing. Working paper, Commodity Futures Trading Commission.

Carr, P., Geman, H., Madan, D. B., and Yor, M. (2002). The fine structure of asset returns: An empirical investigation. *The Journal of Business*, 75(2):305–332.

Carr, P. and Madan, D. (1999). Option valuation using the fast fourier transform. *Journal of Computational Finance*, 2(4):61–73.

Carr, P. and Wu, L. (2004). Time-changed lévy processes and option pricing. *Journal of Financial Economics*, 71(1):113–141.

Carr, P. and Wu, L. (2007). Stochastic skew in currency options. *Journal of Financial Economics*, 86(1):213–247.

Carr, P. and Yu, J. (2012). Risk, return, and ross recovery. *The Journal of Derivatives*, 20(1):38–59.

Carvalho, A. and Guimaraes, B. (2018). State-controlled companies and political risk: Evidence from the 2014 brazilian election. *Journal of Public Economics*, 159:66–78.

Cesar, A. D. L. J., Sofia, C.-D., Kenneth, B., and Akitaka, M. (2017). Predicting the Brexit Vote by Tracking and Classifying Public Opinion Using Twitter Data. *Statistics, Politics and Policy*, 8(1):85–104.

Chatrath, A., Miao, H., Ramchander, S., and Wang, T. (2015). The forecasting efficacy of risk-neutral moments for crude oil volatility. *Journal of Forecasting*, 34(3):177–190.

Cheng, I.-H., Kirilenko, A., and Xiong, W. (2015). Convective risk flows in commodity futures markets. *Review of Finance*, 19(5):1733–1781.

Cheng, I.-H. and Xiong, W. (2014). Financialization of commodity markets. *Annual Review of Financial Economics*, 6(1):419–441.

Cincibuch, M. (2004). Distributions implied by american currency futures options: A ghost's smile? *Journal of Futures Markets*, 24(2):147–178.

Croxson, K. and James Reade, J. (2014). Information and efficiency: Goal arrival in soccer betting. *The Economic Journal*, 124(575):62–91.

Dewally, M., Ederington, L. H., and Fernando, C. S. (2013). Determinants of trader profits in commodity futures markets. *The Review of Financial Studies*, 26(10):2648–2683.

Doran, J. S. and Ronn, E. I. (2005). The bias in black-scholes/black implied volatility: An analysis of equity and energy markets. *Review of Derivatives Research*, 8(3):177–198.

Doran, J. S. and Ronn, E. I. (2008). Computing the market price of volatility risk in the energy commodity markets. *Journal of Banking & Finance*, 32(12):2541–2552.

Duffie, D., Gray, S., and Hoang, P. (1999). Volatility in energy prices. In Kaminski, V. V. and Jameson, R., editors, *Managing Energy Price Risk: The New Challenges and Solutions. 2. ed.* Risk Books, London.

Ederington, L. H. and Guan, W. (2002). Measuring implied volatility: Is an average better? which average? *Journal of Futures Markets*, 22(9):811–837.

Fama, E. F. and MacBeth, J. D. (1973). Risk, return, and equilibrium: Empirical tests. *Journal of Political Economy*, 81(3):607–636.

Farhi, E. and Gabaix, X. (2015). Rare Disasters and Exchange Rates. *The Quarterly Journal of Economics*, 131(1):1–52.

Fernandez-Perez, A., Frijns, B., Fuertes, A.-M., and Miffre, J. (2018). The skewness of commodity futures returns. *Journal of Banking & Finance*, 86:143–158.

Figlewski, S. (2009). Estimating the implied risk neutral density for the us market portfolio. In Bollerslev, T., Russell, J. R., and Watson, M. W., editors, *Volatility and time series econometrics: essays in honor of Robert Engle*. Oxford University Press.

Geman, H. and Ohana, S. (2009). Forward curves, scarcity and price volatility in oil and natural gas markets. *Energy Economics*, 31(4):576–585.

Gibson, R. and Schwartz, E. S. (1990). Stochastic convenience yield and the pricing of oil contingent claims. *The Journal of Finance*, 45(3):959–976.

Goldstein, I., Li, Y., and Yang, L. (2014). Speculation and hedging in segmented markets. *The Review of Financial Studies*, 27(3):881–922.

Goldstein, I. and Yang, L. (2019). Commodity financialization and information transmission. AFA 2016 Annual Meeting.

Goodwin, M. and Milazzo, C. (2017). Taking back control? investigating the role of immigration in the 2016 vote for brexit. *The British Journal of Politics and International Relations*, 19(3):450–464.

Gorton, G. B., Hayashi, F., and Rouwenhorst, K. G. (2013). The fundamentals of commodity futures returns. *Review of Finance*, 17(1):35–105.

Hamilton, J. D. and Wu, J. C. (2014). Risk premia in crude oil futures prices. *Journal of International Money and Finance*, 42:9–37.

Hanke, M., Poulsen, R., and Weissensteiner, A. (2018). Event-related exchange-rate forecasts combining information from betting quotes and option prices. *Journal of Financial and Quantitative Analysis*, 53(6):2663–2683.

Harvey, C. R. and Siddique, A. (1999). Autoregressive conditional skewness. *Journal of Financial and Quantitative Analysis*, 34(4):465–487.

Hasler, M. and Jeanneret, A. (2020). A macro-finance model for option prices: A story of rare economic events. Working paper, University of Texas at Dallas.

He, Z., Kelly, B., and Manela, A. (2017). Intermediary asset pricing: New evidence from many asset classes. *Journal of Financial Economics*, 126(1):1–35.

Heidorn, T., Mokinski, F., Rühl, C., and Schmaltz, C. (2015). The impact of fundamental and financial traders on the term structure of oil. *Energy Economics*, 48:276–287.

Henderson, B. J., Pearson, N. D., and Wang, L. (2015). New evidence on the financialization of commodity markets. *The Review of Financial Studies*, 28(5):1285–1311.

Herron, M. C. (2000). Estimating the economic impact of political party competition in the 1992 british election. *American Journal of Political Science*, 44(2):326–337.

Hong, H. and Yogo, M. (2012). What does futures market interest tell us about the macroeconomy and asset prices? *Journal of Financial Economics*, 105(3):473–490.

Hou, K. and Moskowitz, T. J. (2005). Market frictions, price delay, and the cross-section of expected returns. *The Review of Financial Studies*, 18(3):981–1020.

Huchede, F. and Wang, X. (2020). An approach to compare exchange-traded and otc option valuations. *Available at CME Group*.

Jiang, G. J. and Tian, Y. S. (2005). The model-free implied volatility and its information content. *The Review of Financial Studies*, 18(4):1305–1342.

Kan, R., Robotti, C., and Shanken, J. (2013). Pricing model performance and the two-pass cross-sectional regression methodology. *The Journal of Finance*, 68(6):2617–2649.

Kang, W., Rouwenhorst, K. G., and Tang, K. (2020). A tale of two premiums: The role of hedgers and speculators in commodity futures markets. *The Journal of Finance*, 75(1):377–417.

Karstanje, D., Van Der Wel, M., and van Dijk, D. J. (2015). Common factors in commodity futures curves. Working paper, Erasmus School of Economics.

Kelly, B. and Jiang, H. (2014). Tail risk and asset prices. *The Review of Financial Studies*, 27(10):2841–2871.

Kilian, L. and Murphy, D. P. (2014). The role of inventories and speculative trading in the global market for crude oil. *Journal of Applied Econometrics*, 29(3):454–478.

Koijen, R. S., Moskowitz, T. J., Pedersen, L. H., and Vrugt, E. B. (2018). Carry. *Journal of Financial Economics*, 127(2):197–225.

Kostakis, A., Mu, L., and Otsubo, Y. (2020). Detecting political event risk in option market. Working paper.

Langer, A. and Lemoine, D. (2020). What were the odds? estimating the market's probability of uncertain events. Working Paper 28265, National Bureau of Economic Research.

Larsson, K. and Nossman, M. (2011). Jumps and stochastic volatility in oil prices: Time series evidence. *Energy Economics*, 33(3):504–514.

Leiss, M. and Nax, H. H. (2018). Option-implied objective measures of market risk. *Journal of Banking & Finance*, 88:241–249.

Lewellen, J., Nagel, S., and Shanken, J. (2010). A skeptical appraisal of asset pricing tests. *Journal of Financial Economics*, 96(2):175–194.

Lewis, K. K. (2016). *Peso Problem*, pages 1–6. Palgrave Macmillan UK, London.

Ludvigson, S., Ma, S., and Ng, S. (2019). Uncertainty and business cycles: Exogenous impulse or endogenous response? *American Economic Journal: Macroeconomics*. Forthcoming.

Marshall, B. R., Nguyen, N. H., and Visaltanachoti, N. (2012). Commodity liquidity measurement and transaction costs. *The Review of Financial Studies*, 25(2):599–638.

Martin, I. and Ross, S. A. (2019). Notes on the yield curve. *Journal of Financial Economics*, 134(3):689–702.

Masters, M. W. (2008). Testimony before the committee on homeland security and governmental affairs. *US Senate, Washington, May*, 20.

Meng, K. C. (2017). Using a free permit rule to forecast the marginal abatement cost of proposed climate policy. *American Economic Review*, 107(3):748–84.

Monteiro, A. M., Tutuncu, R. H., and Vicente, L. (2008). Recovering risk-neutral probability density functions from options prices using cubic splines and ensuring nonnegativity. *European Journal of Operational Research*, 187(2):525–542.

Mou, Y. (2011). Limits to arbitrage and commodity index investments: Front-running the goldman roll. Working Paper, Columbia Business School.

Paschke, R., Prokopczuk, M., and Simen, C. W. (2020). Curve momentum. *Journal of Banking & Finance*, 113:105718.

Pindyck, R. S. (2004). Volatility in natural gas and oil markets. *The Journal of Energy and Development*, 30(1):1–19.

Raman, V., Robe, M. A., and Yadav, P. K. (2017). The third dimension of financialization: Electronification, intraday institutional trading, and commodity market quality. WBS Finance Group Research Paper.

Regnier, E. (2007). Oil and energy price volatility. *Energy Economics*, 29(3):405–427.

Roberts, B. E. (1990). Political institutions, policy expectations, and the 1980 election: A financial market perspective. *American Journal of Political Science*, 34(2):289–310.

Rogoff, K. (1977). Rational expectations in the foreign exchange market revisited. Working paper, Massachusetts Institute of Technology.

Rogoff, K. S. (1980). *Essays on expectations and exchange rate volatility*. PhD thesis, Massachusetts Institute of Technology.

Ross, S. (2015). The recovery theorem. *The Journal of Finance*, 70(2):615–648.

Routledge, B. R., Seppi, D. J., and Spatt, C. S. (2000). Equilibrium forward curves for commodities. *The Journal of Finance*, 55(3):1297–1338.

Sayers, F. (2016). The online polls were right, and other lessons from the referendum. *Available at: https://yougov.co.uk/topics/politics/articles-reports/2016/06/28/online-polls-were-right*.

Schneider, P. and Trojani, F. (2019). (almost) model-free recovery. *The Journal of Finance*, 74(1):323–370.

Schwartz, E. S. (1997). The stochastic behavior of commodity prices: Implications for valuation and hedging. *The Journal of Finance*, 52(3):923–973.

Seo, S. B. and Wachter, J. A. (2019). Option prices in a model with stochastic disaster risk. *Management Science*, 65(8):3449–3469.

Shanken, J. (1992). On the estimation of beta-pricing models. *The Review of Financial Studies*, 5(1):1–33.

Shimko, D. (1993). Bounds of probability. *Risk*, 6(4):33–37.

Singleton, K. J. (2014). Investor flows and the 2008 boom/bust in oil prices. *Management Science*, 60(2):300–318.

Snowberg, E. and Wolfers, J. (2010). Explaining the favorite–long shot bias: Is it risk-love or misperceptions? *Journal of Political Economy*, 118(4):723–746.

Snowberg, E., Wolfers, J., and Zitzewitz, E. (2007). Partisan impacts on the economy: evidence from prediction markets and close elections. *The Quarterly Journal of Economics*, 122(2):807–829.

Snowberg, E., Wolfers, J., and Zitzewitz, E. (2011). How prediction markets can save event studies. Working Paper 16949, National Bureau of Economic Research.

Sockin, M. and Xiong, W. (2015). Informational frictions and commodity markets. *The Journal of Finance*, 70(5):2063–2098.

Szymanowska, M., De Roon, F., Nijman, T., and Van Den Goorbergh, R. (2014). An anatomy of commodity futures risk premia. *The Journal of Finance*, 69(1):453–482.

Tang, K. and Xiong, W. (2012). Index investment and the financialization of commodities. *Financial Analysts Journal*, 68(6):54–74.

Trolle, A. B. (2014). Efficient pricing of energy derivatives. In Prokopczuk, M., editor, *Energy pricing models: recent advances, methods, and tools*. Palgrave Macmillan.

Trolle, A. B. and Schwartz, E. S. (2009). Unspanned stochastic volatility and the pricing of commodity derivatives. *The Review of Financial Studies*, 22(11):4423–4461.

van Huellen, S. (2020). Approaches to price formation in financialized commodity markets. *Journal of Economic Surveys*, 34(1):219–237.

Van Huellen, S. (2020). Too much of a good thing? speculative effects on commodity futures curves. *Journal of Financial Markets*, 47:100480.

Venturi, P., Ferreira, A., Gozluklu, A., and Gong, Y. (2021). Binary uncertainty. Working paper.

Wan, E. A. and Van Der Merwe, R. (2000). The unscented kalman filter for nonlinear estimation. In *Proceedings of the IEEE 2000 Adaptive Systems for Signal Processing, Communications, and Control Symposium*, pages 153–158. IEEE.

Watugala, S. W. (2019). Economic uncertainty, trading activity, and commodity futures volatility. *Journal of Futures Markets*, 39(8):921–945.

Wayne, W. Y., Lui, E. C., and Wang, J. W. (2010). The predictive power of the implied volatility of options traded otc and on exchanges. *Journal of Banking & Finance*, 34(1):1–11.

Wickham, P. (1996). Volatility of oil prices. Working Paper, International Monetary Fund.

Wu, K., Wheatley, S., and Sornette, D. (2021). Inefficiency and predictability in the brexit pound market: a natural experiment. *The European Journal of Finance*, 27(3):239–259.

Yang, F. (2013). Investment shocks and the commodity basis spread. *Journal of Financial Economics*, 110(1):164–184.